Proinsulin Trafficking through the Secretory Pathway

By

Gautam Rajpal

A dissertation submitted in partial fulfillment
of the requirements for the degree of
Doctor of Philosophy
(Cellular and Molecular Biology)
in The University of Michigan
2012

Doctoral Committee

Professor Peter Arvan
Professor James Bardwell
Professor Randal J. Kaufman
Professor Ram K. Menon
Associate Professor Martin G. Myers Jr.

Acknowledgements

I want to thank Dr. Arvan for his consistent support throughout my formative years in graduate school. My committee members, Dr. James Bardwell, Dr. Cunming Duan, Dr. Randal Kaufman, Dr. Ram Menon, and Dr. Martin Myers for their feedback. Linda Brush and Alice Koshy for their help with insulin analysis. Dr. Ming Liu for my initial training in the lab. And all the lab members past and present for their continued support and encouragement.

Table of Contents

‘

List of Figures

List of Tables

ABSTRACT

Proinsulin Trafficking through the Secretory Pathway

By

Gautam Rajpal

Chair: Peter Arvan

Proinsulin, the insulin precursor protein, is synthesized in the Endoplasmic Reticulum (ER) of pancreatic beta cells, where it folds to the native state, involving the formation of three evolutionarily conserved disulfide bonds. Once folded, proinsulin exits the ER, traverses the secretory pathway to the trans-Golgi Network (TGN) and into budding secretory granules. Proinsulin is then processed by endopeptidases that excise the connecting C-peptide that links the

B- and A-chains, leading to the creation of mature, two-chain insulin. Upon secretion to the bloodstream, insulin binds to cell surface insulin receptors on target tissues, resulting in the activation of signaling cascades that promote metabolic homeostasis. This thesis aims to look at two distinct aspects of the proinsulin maturation process. In the first part of my thesis work, I have designed a proinsulin with a shortened linker peptide with the intent to create a bioengineered protein that acts as a single-chain insulin (SCI), i.e., without a requirement for cleavage by endopeptidases. SCIs expressed via gene therapy have been found to be effective in reversing diabetes in rodent models, obviating the need for exogenous insulin injection. However, to date, very little structure-function analysis of SCIs has been performed. In Chapter 2, I have examined the structural features of the linker peptide that would allow for mammalian expression, secretion, and bioactivity of SCIs for development into future diabetes therapeutics. In the second part of my thesis work, I have been attempting to identify the ER oxidoreductase(s) that promote(s) formation of the three disulfide bonds of proinsulin, which heretofore are unknown. In Chapter 3, I present results that point to two key members of the family of PDI-like ER oxidoreductases: Protein Disulfide Isomerase itself, and Endoplasmic Reticulum protein 72 (ERp72), which may both play critical, yet opposing, roles in this

process. As the misfolding of proinsulin is implicated in the progression of various forms of diabetes, understanding the key factors that control the balance of proinsulin folding and misfolding (by regulating proinsulin disulfide bond formation) could also provide potential benefit for designing therapies that increase insulin production.

Chapter 1 INTRODUCTION

Like cancer, diabetes mellitus is a disease of various etiologies, with a final common pathology leading to increased blood glucose levels [35, 68, 87, 110]. Diabetes resulting from autoimmune attack on pancreatic beta cells (leading to elimination of the insulin producing cells) is now known as Type IA diabetes [87]. Diabetes in persons with decreased tissue sensitivity to insulin, resulting in elevated blood glucose, is known as Type II diabetes (Interestingly, this also results in eventual loss of pancreatic beta cells, but triggered by non-immune insults) [68]. Type II diabetes is polygenic, and increasing subgroups of individuals are now recognized with mutations in a variety of critical genes impacting on insulin secretion and beta cell physiology (Including the insulin gene itself)[109, 120, 170]. Some monogenic forms of the disease begin in the neonatal period and can be confused for Type 1A diabetes but are now considered Type 1B (non-autoimmune) diabetes [35, 96, 110]. Gestational diabetes, which occurs in mothers during the third trimester of pregnancy, is yet another form of diabetes commonly associated with the development of type II diabetes in later life[145].

All forms of diabetes, in one form or another, involve the insufficiency or inaction of insulin. In humans, insulin is formed as a precursor known as preproinsulin, a 120 amino acid molecule containing a 24 amino acid signal peptide sequence. The signal peptide binds to a signal recognition particle, which brings preproinsulin to the Endoplasmic Reticulum (ER) [97]. During translation on the ribosomes of the rough ER, the signal peptide is recognized and translocated, via the Sec61 channel, across the ER membrane into the ER lumen for folding [10, 55]. The continued translation and translocation into the ER (so-called co-translational translocation) occur simultaneously. In this process, the signal peptide is cleaved by signal peptidase to form proinsulin, which interacts with enzymes and chaperones within the ER lumen [55]. Proinsulin then begins to fold, forming three evolutionarily conserved disulfide bonds, allowing proinsulin to assume its native three dimensional conformation [98]. After achieving its native conformation, proinsulin exits the ER and transits to the Golgi complex, where it enters the Trans Golgi Network (TGN) and is packaged into immature secretory granules [10]. As these granules begin to mature, an acidification process (driven via the action of an ATP driven proton pump) allows for enzymatic activity of endoproteases that cleave residues 31-65, a region otherwise known as the C-peptide [10, 45, 55]. These enzymes include proprotein convertases PC1 and PC2, and carboxypeptidase E. The endopeptidase PC1 recognize cleaves the dibasic motif -RR within proinsulin (near the B-chain) and endopeptidase PC2 cleaves the dibasic motif -KR (near the A-chain); these dibasic residues are then

removed by the action of carboxypeptidase E [45]. Excision of this 31 amino acid C-peptide leaves a two-chain structure, (B- and A-chains, respectively) linked by the two of the three disulfide bonds, resulting in the formation of the mature molecule known as insulin. Once endoptoteolytically processed, insulin hexamers proceed to form higher-order multimers, and ultimately crystallize in the secretory granules in the presence of zinc and calcium [10, 55]. It is estimated a single insulin secretory granule can contain up to a million molecules of insulin[10]. Insulin remains stored in these granules until activation of nutrient mediated signaling cascades, whereupon granules fuse with the plasma membrane by exocytosis, releasing insulin into the extracellular space. The insulin crystals immediately dissolve into monomeric (active) forms (each B-chain/A-chain pair is a monomer), circulating in the bloodstream with insulin exerting its effects on target tissues by binding and activating insulin receptors [55].

Binding of insulin causes dimeric insulin receptors to trans-phosphorylate, via an internal kinase domain, on tyrosines found within the cytoplasmic domain of the insulin receptor [135]. This promotes the recruitment of the IRS (Insulin Receptor Substrate) adapter proteins, which further recruit factors that activate the insulin signaling cascade [135]. Eventually, such signaling in fat and muscle cells results in the translocation of the GLUT4 glucose transporter from the perinuclear membranes to the plasma membrane, which allows for regulated glucose entry into these cells [135].

In Type IA diabetes, autoimmune destruction of pancreatic beta cells leaves the body with little or no insulin and C-peptide. Existing treatment therefore requires daily injections of exogenous, recombinantly-produced insulin. Currently, recombinant insulin is manufactured in two ways. Humulin ® and its analog Humalog ®, produced by Eli Lilly and Company, are formed by separately expressing the cDNA sequences of the insulin B- and A- chains in E. coli [2]. The chains are then combined in a reaction under conditions that allow for the formation of appropriate disulfide linkages between the two chains. Alternatively, insulin produced by Novo-Nordisk is created in yeast, where a single chain insulin precursor is synthesized and recombinant secreted protein is subsequently endoproteolytically cleaved in vitro [1].

Mutations have been engineered into insulin that affect the properties of the injected product, in particular with regards to its half-life in the bloodstream. According to a 2005 New England Journal of Medicine article," the proper use of insulin analogs allows people with diabetes greater flexibility in the timing of meals, snacks, and exercise, which in turn enhances their ability to lead normal lives" [52]. 'Lispro ®', the first insulin analog sold, is a fast acting insulin in which the lysine and proinsulin residues on the C-terminal end of the B-chain are placed in reverse order [56]. The residue swap inhibits formation of insulin dimers and hexamers, which allows for more rapid absorption and bioavailability of monomeric insulin. Lispro® is able to interact with the insulin receptor at similar binding affinities to that of native insulin. In the Novo-Nordisk product

known as “Aspart ®”, the same insulin-B28 residue that is normally a proline is mutated to aspartic acid [72]. This too prevents hexamer formation and allows for a more rapidly absorbed, faster-acting insulin. On the other hand, Glargine ® insulin and Detemir insulin (trade names: Lantus ® and Levemir ®, respectively) are examples of bioactive insulin analogs that are unusually long-lasting [112, 160]. These analogs are able to survive in the bloodstream much longer than normal insulin by shifting their isolelectric points (the pH at which the overall molecule carries no net electrical charge). In the case of Glargine ® insulin, this was done by adding two positively charged arginine residues to the C-terminus of the B-chain (the acid-sensitive asparagine at position 21 in the A-chain to glycine was also changed in order to avoid deamination and dimerization) [160]. Detemir on the other hand was modified so that it could be fatty acylated and thus carried for extended periods in the circulation bound to serum albumin[112].

In Type II diabetes, muscle and fat tissues, the main targets of insulin action, tend to lose their sensitivity to insulin so that the signaling response activated upon insulin binding is attenuated [68, 135]. As a result, pancreatic beta cells must produce more insulin to compensate for the insulin insensitivity [139]. Over time, however, if the insulin insensitivity is not improved (or worsens still), then beta cells may eventually fail to keep up with insulin production as they become overwhelmed by glucose [18, 24, 164]. Under conditions of glucotoxicity, beta cells are predisposed to undergo apoptosis [165]. The mechanism of this pathology is unclear and currently under investigation in many labs. Among the

popular theories, a favored view is that oxidative stress and ER stress may lead to beta cell failure [33, 54, 116, 134, 139, 144]. Oxidative stress (which can also be triggered by ER Stress) occurs when there is an accumulation of reactive oxygen species (ROS), which includes superoxide, hydrogen peroxide, hydroxyl radical, and peroxynitrite molecules [33, 134, 144]. ROS are normally neutralized by antioxidant gene products (enzymes) that can be expressed in cells[144]. Inexplicably, pancreatic beta cells that produce massive amounts of oxidized proinsulin have low levels of expression of antioxidant enzymes, which limits their ability to deal with such insults [89]. ROS production that remains unquenched can cause damage to cellular components and even lead to apoptosis [105]. Evidence for oxidative stress as a potential culprit for pancreatic beta cell failures does exist, both from rodent models and human data. Autopsy of diabetic islets suggested an increase in ROS, while tissue damage has been found to be increased in the pancreas of diabetic subjects when subject to oxidative stress [18, 134].

ER stress occurs when misfolded or unfolded proteins accumulate in the ER [54]. Three ER stress sensor proteins in the ER membrane: Ire1, PERK, and ATF6, activate the unfolded protein response (UPR), which respectively serves three primary functions within the cell: inhibition of general protein translation, increased protein folding capacity of the ER, and degradation of misfolded proteins in the ER [113]. Initially, UPR activation is an adaptive response to reduce ER stress and can serve to improve cell function [11, 113, 140]. In

contrast, prolonged UPR leads to apoptosis via expression of the transcription factor CHOP, among others [54, 147]. ER stress and UPR induction are both increased in islets of human diabetic patients and animal models of diabetes [46, 54, 61, 82, 104]. CHOP in particular may have an important role to play in mediating ER stress-induced beta cell failure, since CHOP deletion ameliorates the diabetic phenotype in genetic and diet-induced models of diabetes [147].

The source of potential ER Stress in pancreatic beta cells may be linked to proinsulin folding [96-98]. To be precise, proinsulin misfolding may elicit a toxic ER Stress response, supported by findings in the *Akita* mouse, which expresses a terminally misfolded proinsulin — the expression of which is ultimately associated with a loss of pancreatic beta cells [161]. Recent studies have revealed that additional coding sequence mutations in the *INS* gene itself — one of the causes of monogenic Type 1B diabetes in humans— also leads to the demise of pancreatic beta cells [96, 110]. While some of these mutations specifically alter the key cysteine residues involved in the formation of proinsulin's three disulfide bonds, other mutations appear to indirectly impact on the ability of proinsulin to create its disulfide bonds and thus to form its native conformation. This even includes mutations in the preproinsulin signal peptide sequence which can result in aberrant proinsulin oxidation [97, 106]. Thus, by affecting the cotranslational transolocation of (pre)proinsulin, this appears to impact on its oxidation. These mutations are also purported to exhibit dominant-

negative effects, perturbing the folding of “bystander” wild-type proinsulin, further exacerbating the toxic phenotype.

In people with Type II diabetes, elevated blood lipid and glucose levels can also become toxic to beta cells [165]. Current treatment has focused on increasing the sensitivity of insulin target tissues as well increasing the amount of insulin secreted from pancreatic beta cells [120]. However clinical data indicate that treatments designed to promote increased insulin synthesis and secretion ultimately lead to more rapid progression of the disease with earlier dependence upon exogenous insulin injection (e.g., the DREAM study) [3, 83]. The data suggest that accelerated loss of beta cells may occur by forcing diabetic beta cells to produce more proinsulin than they are genetically programmed to handle. At the present time, no pharmacological treatments are currently commercially available that are designed to directly reduce ER Stress or failure of pancreatic beta cells.

My Ph.D. thesis research highlights attempts to look at potential treatments for both Type I and Type II diabetes. For my first project, dealing with Single-Chain Insulins (SCIs), I created insulin analogs that might be utilized in a gene therapy approach, obviating the need for daily insulin injections. These analogs do not require endoproteolytic processing for insulin bioactivity. To date, no SCI has come to market, and only a few studies have examined the features that would

be necessary to make a bioactive SCI. Such a treatment was shown to be successful in “curing” diabetes in streptozotocin-treated diabetic rodents [84].

My second project, which represents the larger portion of my thesis work, was designed to understand more about proinsulin folding and its link to insulin production. Specifically, I attempted to identify ER oxidoreductase activities that help or hinder proinsulin disulfide bond formation in the ER. If proinsulin misfolding is a source of ER Stress in pancreatic beta cells, then understanding the mechanism of folding, and using that understanding to potentially improve folding, would be of the upmost importance. Although each project has therapeutic aims and implications, both were set out with the intention of understanding basic mechanisms in proinsulin biology.

Note: each chapter will begin with an introduction that contains a more specific background of the field related to that chapter.

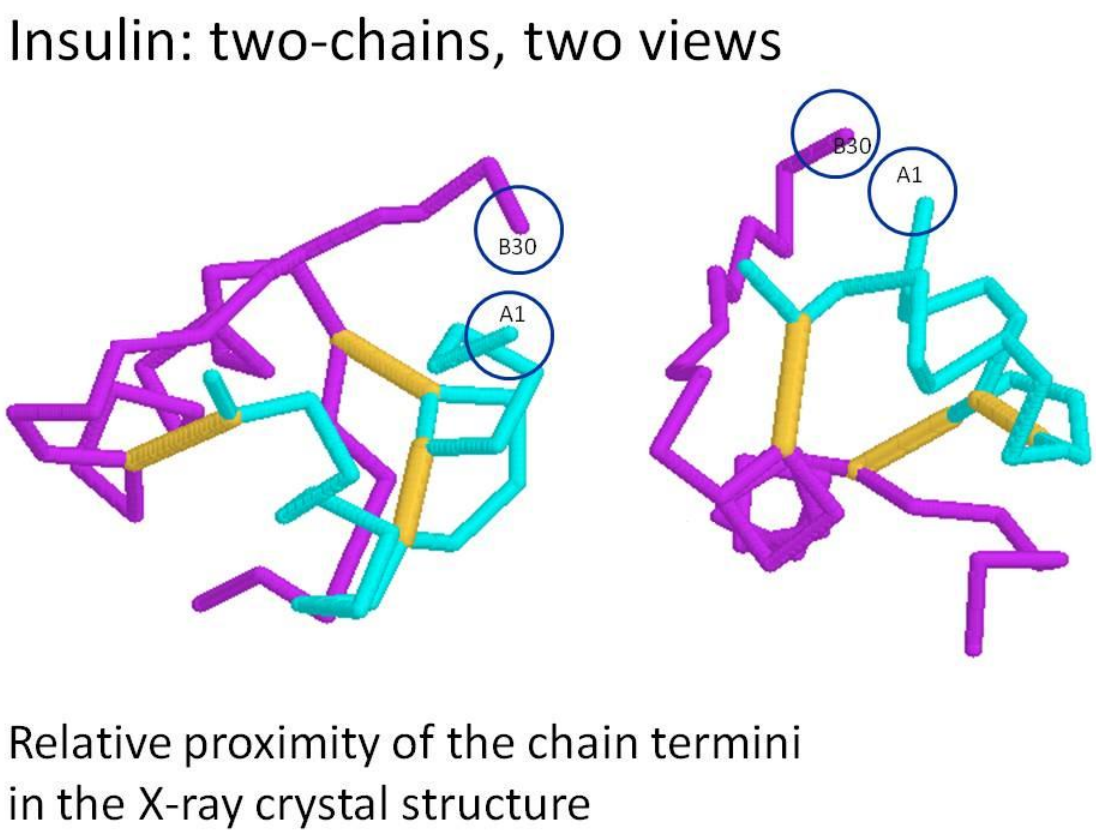

Figure 1-1. Crystal structure of insulin.

B-chain in dark. A-chain in light. Disulfide bonds shown in medium. For proinsulin, the C-peptide region is located between end of the B-chain (B30) and the beginning of the A-chain (A1).

Source: Hidehiko Nakano. http://www.sccj.net/CSSJ/jcs/v4n1/a1/text.html.

Chapter 2 SINGLE-CHAIN INSULINS AS RECEPTOR AGONISTS

Gautam Rajpal, Ming Liu, Yi Zhang, and Peter Arvan. Molecular Endocrinology May 1, 2009 vol. 23 no. 5 679-688.

2.1 Abstract

Single-chain insulins (SCIs) are single polypeptide chains in which the insulin B-chain links contiguously with the insulin A-chain via an uncleaved connecting peptide. While direct linkage of insulin B- and A-chains produces SCIs with little insulin receptor binding, biologists have been interested in bioengineering linker peptides that form a flexible reverse turn, allowing SCIs to activate insulin receptors. In this report, I have investigated a series of cDNAs intended to explore the significance of linker length, cleavability, and the impact of certain site-dependent residues for the expression and bioactivity of recombinant SCIs on insulin receptors. SCI concentration is readily measured by radioimmunoassay with a (proinsulin + insulin)-specific polyclonal antibody. While dibasic flanking residues may result in potential endoproteolytic

susceptibility, a linker with -Gln-Arg- flanking sequences resisted cleavage even in secretory granules, ensuring single-chain behavior. Effective SCIs exhibit favorable and specific binding with insulin receptors. SCIs with linkers bearing an Arg residue immediately preceding the A-chain were most bioactive, although efficient receptor interaction was inhibited as SCI linker length increased, approaching that observed for proinsulin. SCIs activate downstream metabolic signaling — stimulating glucose uptake into adipocytes and suppressing gluconeogenic enzyme biosynthesis in hepatocytes — with only limited cross-reactivity on IGF1 receptors. SCIs might theoretically have utility either in immunotherapy or gene therapy in insulin-deficient diabetes.

Significance: Currently there are very few publications on the efficacy of SCIs [60, 84], and none on the properties that confer biological activity. The significance is that such agents may have potential use in the treatment of diabetes mellitus.

2.2 Introduction

Absolute or relative insulin deficiency is a major factor underlying the inability of diabetic patients to maintain normal blood glucose levels. For both type 1 and type 2 diabetic patients, injection of purified insulin is a major therapy although

alternative products [34] and routes, such as insulin inhalation [131], have been considered. In recent years, insulin gene therapy (especially for type 1 diabetes caused by autoimmune-mediated destruction of pancreatic beta cells) has also been in development, with the intention that hyperglycemia could trigger production and secretion of bioactive insulin from genetically-targeted non-beta cells.

In beta cells, insulin is derived from the proinsulin precursor [62, 78] which is endoproteolytically processed via the combined actions of PC1, PC2, and carboxypeptidase E [174]. These enzymes are optimally active within the intraluminal environment of secretory granules, but they are generally not expressed in cells other than neuroendocrine cells [25]. However, using biotechnology, expression of modified insulin cDNAs in non-beta cells may allow for the synthesis and secretion of products with strong specificity for insulin receptors [155]. For example, mutagenesis to alter endoproteolytic processing sites in proinsulin has been employed to enhance cleavability in non-beta cells. Nevertheless, endoproteolytic processing efficiency of such constructs remains variable [8, 143], limiting production of bioactive insulin from heterologous cells.

As an alternative, single-chain insulin (SCI) constructs [59] may have utility. SCIs require no endoproteolytic processing for activation. Lee at al. described an SCI bearing a heptameric peptide linking insulin B- and A-chains with 20 - 30% binding efficiency to insulin receptors compared to authentic insulin; this

does not preclude favorable *in vivo* effects to lower blood glucose in diabetic rodent models [85] and potentially, in humans [130]. Lee at al. inserted this construct into a plasmid hepatocyte-specific Liver-type pyruvate kinase (LPK) promoter. It has been shown that glucose-induced transcription of the LPK gene is mediated by a carbohydrate response elements (ChRE) located within its promoter [167]. The authors used this to their advantage, selecting a promoter that would be activated by glucose, thereby mimicking the beta cell response, to release insulin on demand. Using a retrovirus to deliver this construct into the hepatocytes of mice, the authors were able to lower blood glucose levels in non-obsese diabetic (NOD) mice (which undergo autoimmune destruction of beta cells) as well as in streptozotocin-induced diabetic rodents (streptozotocin is a drug selectively toxic to pancreatic beta cells). The authors demonstrated remission of diabetes over a fifteen week observation period. Thus, this single chain insulin, despite not being processed nor displaying the full bioactivity of insulin, was nevertheless an effective treatment in treating diabetes, without the need for insulin injections. However, Lee et al did not provide information on the development of the SCI and why certain attributes (linker length, amino acid content) were chosen over other possibilities.

The apparent bioactivity of this heptameric peptide linked SCI calls attention to the function of the C-Peptide. The mammalian proinsulin C-peptide is typically 35 amino acids in length, including the two dibasic motifs found at the ends of the linker, and contains 4 or 5 acidic residues, with at most a single basic residue in

a limited number of species [149]. The conservation in length is fairly consistent across species, including invertebrates such as mollusks and arthropods. [80, 146, 149]. Work done by Liu et al have shown that reducing the length of the C-peptide to less than five amino acids residues results in proinsulin misfolding with improper disulfide bonds [100]. However, above five amino acids, the folding fidelity of proinsulin appears to remain intact. The requirement above five amino acids may also involve additional evolutionary pressures beyond folding. Approximately 95% of proinsulin in secretory granules is converted into mature insulin. In order to maintain this high efficiency, the C-peptide needs to display characteristics that allow its efficient endoproteolytic excision to occur. For instance, at least 8 or 9 residues (6 upstream, 2- 3 downstream) at the two proinsulin processing sites must fit into the catalytic grooves on the convertases for efficient excision [95, 149] . The C-peptide must also allow for proper hexamerization of proinsulin that occurs during its export from the ER to the TGN. Furthermore, the C-peptide is purported to display some biological activity(ies) on its own, which may impose a further evolutionary constraint [51].

Interestingly, a subset of evolutionarily-related proteins to insulin, the Insulin-like Growth Factors IGF-1 and IGF-2, exhibit single chain insulin-like characteristics [90]. The IGFs share similarities in both structure and function, and work through an IGF1 receptor with functional homology to the insulin receptor. Like proinsulin and insulin, they posses three disulfide bonds, connecting regions that correspond to the “B” and “A” chains. However, unlike insulin, the C-peptide

region is never excised and thus remains intact. Furthermore, the C-peptides of IGFs are much shorter than the C-peptide found in insulin, and they appear to contribute to IGF1 receptor binding [19]. This is an important distinction as some Single-Chain Insulins may exhibit greater crossover agonist activity on IGF1 receptors than does two-chain insulin. If the intention is to use the SCI in gene therapy for treatment in diabetes, then minimizing crossover bioactivity with the IGF-1 receptors is of the upmost importance as activation of growth signaling cascades can lead to undesirable clinical side effects [42].

In this work, I have endeavored to further characterize sequences comprising the flexible linker peptide that might improve the biological properties of SCIs. I also tested SCIs for crossover bioactivity on IGF-1 receptors. From my studies, a list has been generated of suitable SCIs that exhibit comparable bioactivity to that studied by Lee et al.[84], including an SCI with no potential to be cleaved by any known endoprotease of the secretory pathway.

2.3 Results

Measuring SCI levels

A list of SCI constructs engineered for this study, varying only by their linker sequences, is summarized in Table 2-1. My screening strategy for this study has been to 1) measure the amount of each recombinant SCI secreted from transiently transfected 239T cells; 2) screen for the potential for endoproteolytic cleavage of recombinant SCIs that would inadvertently convert them from single-chain to two-chain insulins; and 3) compare recombinant SCIs secreted from 293T cells for insulin receptor interaction using a screening assay that obviates the need for protein purification.

To normalize the amounts of secreted SCI protein, I exploited a radioimmunoassay (RIA) kit (based upon a polyclonal antibody intended to detect rat pro/insulin, but with extensive cross-reaction to proinsulin+insulin of all species) in order to measure the relative concentrations of secreted recombinant SCIs. Using this assay in transfected 293T cells, all constructs tested (Table 2-1) yielded in the range of 20 - 200 ng of recombinant SCI protein secreted per well. The stock concentrations of each SCI were then diluted to equalize their concentrations in subsequent bioassays. I verified the validity of the RIA measurements for several SCIs by continuous metabolic labeling of transfected

293T cells for 24 h with ^{35}S-cysteine at a fixed specific radioactivity in complete culture medium, to approach steady state labeling. Because each construct has the same number of Cys residues (six) per SCI molecule, I could directly examine the abundance in these SCIs, and in parallel, quantify SCI levels by RIA. Quantitative recovery of secreted SCIs was achieved by an immunoprecipitation protocol with a vast excess of anti-insulin antibody (see *Methods*), before tris-tricine-urea-SDS-PAGE and autoradiography. In Fig. 2-1, small differences in band mobilities for the distinct constructs can be explained by the presence of 4, 7, 8, and 9 amino acid linker sequences (consistent with previous reports [100]). Importantly, because of precise identity of the insulin B-chain and A-chain sequences in all constructs, immunoreactivity of the SCIs appeared proportionate to the chemical mass of SCI protein detected after steady-state labeling (Fig. 2-1).

Stringent Assay of Cleavability

When considering potential future therapeutic uses, I wished to generate a recombinant SCI that was "effectively uncleavable", yielding a single product with defined biological characteristics. However, most SCI sequences reported to date have one or two sets of flanking dibasic amino acids contiguous with either the B- or A-chain [59, 85]. Many of the SCIs produced also have dibasic residues within the linker sequence (Table 2-1), with at least theoretical potential

for cleavage. To directly test cleavability, I exploited the subtilisin-like proteinases found in secretory granules [148]; specifically, those found in AtT20/PC2 cells that do not synthesize proinsulin yet express PC1 and PC2 and possess a microenvironment conducive to endoproteolytic processing of peptide hormone precursors [25]. I therefore transfected AtT20/PC2 cells with cDNAs encoding SCIs bearing the following linkers: -QRGGGGGQR- (Table 2-1 line 27), -GGGPGKR- (Table 2-1 line 15), -RRGGGGGKR- (Table 2-1 line 20), -RRYLGGGGGGGDVKR- (Table 2-1 line 34), -C-peptide- (ie, proinsulin, Table 2-1 line 36), or Direct Linkage of Thr(B30)-G(A1) with no potential cleavage site between the chains (Table 2-1 line 2). The cells were pulse-labeled with ^{35}S-amino acids and after the first 3 h chase, two further sequential 30 min chase incubations were collected for analysis of media under unstimulated and secretagogue-stimulated conditions, respectively. Anti-insulin immunoprecipitates from media were examined by nonreducing tris-tricine-urea SDS-PAGE and fluorography in order to observe band mobility, which reflects both disulfide bonding as well as potential endoproteolysis [63]. Nearly all bands immunoprecipitable with anti-insulin exhibited stimulated release upon secretagogue addition (Fig. 2-2), indicating that these peptides had entered secretory granules, which maintain an endoproteolytically active internal environment. As expected, the construct with a -C-peptide- linker (ie, proinsulin, 9.5 kD) was in part cleaved, resulting in authentic insulin production (5.9 kD). With this insulin band as a 'standard', it was apparent that SCIs with linkers -

RRGGGGGKR- or -RRYLGGGGGGGDVKR-, respectively, were also endoproteolytically processed to insulin (Fig. 2-2). As a control, the direct linkage construct (lacking any processing site between the chains) was uncleavable. However, this SCI differs from others in that the band mobility under nonreducing conditions is aberrantly slow, reflecting quantitatively mispaired disulfide bonds despite a molecular mass identical to that of authentic insulin [100]. The SCI with linker -GGGPGKR-, used previously for gene therapy in rodent diabetes [85], showed an as-yet uncharacterized cleavage in AtT20/PC2 cells. By contrast, the SCI with a -QRGGGGGQR- linker appeared uncleavable (Fig. 2-2).

A different RIA that measures only processed human insulin provided an indirect but simpler alternative method to confirm that the SCI bearing a nonapeptide linker with QR flanking sequences remains intact as a SCI even under these protease-rich conditions. By comparing the results from an RIA to detect (proinsulin+insulin) to those of an RIA detecting only human insulin, I examined AtT20/PC2 cells transfected to express an SCI bearing a linker with a set of two flanking dibasic sites (Table 2-1 line 19), or a linker with only one dibasic site at the A-chain junction (Table 2-1 line 15), or the -QRGGGGGQR- linker lacking any dibasic sites (Table 2-1 line 27). The ratio of total (proinsulin+insulin)-specific immunoreactivity [ie, total expression] to human insulin-specific immunoreactivity [ie, processed protein] for the SCI with a bilateral set of flanking dibasic sites was 1.94 : 1, indicating significant cleavage. The ratio for the SCI with only one dibasic site at the A-chain junction was 2.65 : 1, and for that with no

dibasic sites the ratio was 20.8 : 1. These data indicate progressive resistance to cleavage and support the contention that an SCI with a -QRGGGGGQR- linker is likely to remain intact as a single-chain protein, even in an endoprotease-rich microenvironment.

Screening of SCI interaction with cell surface insulin receptors

Metabolic responsiveness in insulin-sensitive tissues in the body has long been reported to be reflected by efficiency of insulin extraction from the bloodstream [14, 50, 108] or from the perfusate of isolated organs [150] or the medium bathing cultured cells — in which insulin extraction is linked to (and preceded by) binding to cell surface insulin receptors. Indeed the amount of insulin extracted from the medium and entering intracellular trafficking pathways in cultured cells (eg., hepatocytes) is proportional to the amount that binds to cell surface insulin receptors [92]. With these observations in mind, I devised an assay in which the ability of various recombinant SCIs, secreted from 293T cells, could be screened for interaction with insulin receptors by virtue of their extraction from media bathing Chinese Hamster Ovary cells stably overexpressing human insulin receptors (CHO-IR cells). Following overnight serum starvation, I exposed CHO-IR cells to recombinant SCIs that had been secreted from 293T cells and diluted to a concentration of 5 ng/mL in fresh media. The diluted SCIs were placed upon confluent cells and the incubations cooled to 4°C for 6 h to allow for SCI

extraction from the media via iteraction with cell surface insulin receptors. Extraction was directly measurable by loss of SCIs from the media was directly measured (by RIA) – compared to that observed for chemically purified human insulin (this positive control set to 100%). The technical simplicity of the assay resulted in a highly reproducible means to order the relative extraction efficiency between different SCI constructs. Moreover, our positive control (human insulin) as well as our "negative" controls (Direct Linkage of B- to A-chain, Table 2-1 lines 1 and 2) yielded results reflecting their status as being the strongest and weakest ligands, respectively (although there was inter-assay variability with regards to nonspecific background [93] as measured by constructs known to have little specific receptor interaction [29]). I therefore used this extraction assay as a screening tool to suggest features for effective design of recombinant SCI proteins that were expressed and secreted from transiently transfected 293T cells.

An SCI with a nonapeptide linker (-RRYPGDVKR-), which includes residues that allow bending the linker into a reverse turn, has been described to exhibit 50% of the insulin receptor binding efficiency of that observed for two-chain insulin [22] yet significantly higher than that of proinsulin [59]. I used this linker as my basis for designing further constructs. I observed that substitution of the central Pro by Leu had no adverse (and indeed slightly beneficial) effects on secretory recovery of the recombinant SCI, as well its extraction by CHO-IR cells (Table 2-1, lines 18 and 19).

I then varied the c-peptide length to determine the ability of the SCI to bind to the receptor. It was my hypothesis that an excessive linker length might sterically interfere with insulin receptor interaction while, on the other hand, a minimum linker length may be required to allow flexibility for efficient conformational adaptation of SCI contact sites with the receptor. From the data in Fig. 2-3A, both points seemed apparent. At one end of the spectrum, I expressed SCIs bearing a 15-mer linker (Table 2-1 line 34) and a 20-mer linker (Table 2-1 line 35) that exhibited progressive decreases in extraction by CHO-IR cells, which fell further upon expansion of the linker to include the full proinsulin C-peptide (Fig. 2-3A). These data are consistent with steric hindrance to insulin receptor binding [59, 74]. At the other end of the spectrum, none of our recombinant SCIs with a linker size that was < 6 residues showed important extraction by CHO-IR cells (including linkers -MGGM-, -GKR-, -KR-, or our direct linkage negative control, Fig. 3A and see lines 1-11 of Table 2-1). Some of the inability to interact with insulin receptors may include a degree of misfolding of recombinant SCIs with short linkers [100] as well as the inability of SCIs with tightly tethered chains to undergo the motion needed to fit against the insulin receptor [29, 115]. We did observe binding to the insulin receptor with as few as five amino acids, with the linker-RRGKR-. However, this linker is a predicted furin cleavage site and is in fact a miniproinsulin (ie, not an SCI) that is quantitatively converted in Golgi complex of 293T cells to two-chain insulin (see Table 2-1, and data not shown).

Thus, the minimum linker length for optimal binding appeared to be seven amino acids (Table 2-1 line 15).

Next, because an SCI bearing an -RRYPGDVKR- linker is efficiently extracted by CHO-IR cells (Fig. 2-3B), as is the SCI bearing the published linker sequence -GGGPGKR- [85], I became intrigued by the dibasic site found at the linker-A-chain junction, which has also been reported in another newly-described insulin receptor-binding SCI [59]. To test the significance of flanking dibasic residues in the linker sequence, the SCI from Table 1 line 19 was further mutagenized to either convert the amino terminal end of the linker from RR to GG (Table 2-1 line 22) or the carboxyl-terminal end from KR to GG (Table 2-1 line 21). While loss of the amino terminal RR still resulted in excellent extraction by CHO-IR cells, loss of the carboxyl-terminal KR resulted in a dramatic decrease in extraction efficiency (Fig. 2-3B). Substitution at the carboxyl terminal end of the SCI linker with either HH residues (Table 2-1 line 26) or KQ residues (Table 2-1 line 32) also showed inhibition of CHO-IR cell extraction. Because an SCI bearing only a single flanking R residue contiguous with Gly(A1) was effectively extracted (Table 2-1 lines 25, 27 and 29), the data suggest that a single arginyl side chain proximal to the A-chain may be an important feature for SCI interaction with insulin receptors (Fig. 2-3B), in addition to rendering the SCI effectively uncleavable (Fig. 2-2). By contrast, it would appear that amino acid side chains in the mid-region of the linker are not critically important besides providing a flexible reverse turn, based on the efficient extraction of an SCI bearing only Gly

residues in the mid-region (Fig. 2-3B). Moreover, constructs bearing multiple Gly residues in the mid-region also tended to exhibit higher secretory recovery of the recombinant SCI in the medium of transfected cells (Table 2-1).

Cross-validation of SCI interactions with insulin receptors

The ease of the extraction assay was particularly useful for ranking the relative efficiencies of receptor interaction of different SCIs. Nevertheless, significant ligand depletion from the media during the course of this assay risks minimizing apparent differences in ligand affinity, which could be explained by cross-reactivity with non-insulin receptors. Therefore, I cross-validated these results for selected constructs using a standard competitive binding assay with a fixed amount (12.5 fmoles) of ^{125}iodoinsulin in the presence of a large excess of unlabeled ligand in varying concentrations (Fig. 2-4A). CHO-IR cells were incubated at 4°C for six hours, after which the media was removed and cells were washed three times with PBS to remove all traces of unlabeled ^{125}I-Insulin. The cell lysate was assessed for total counts using a gamma counter (Fig. 2-4A). IC_{50} for each construct was normalized as a fraction (%) of that observed for authentic insulin standard (Fig. 2-4B). An SCI construct which directly links K(B29)-G(A1) (Table 2-1 line 1) that is known to lack significant activity on insulin receptors [29] could not compete for iodoinsulin binding (Fig. 2-4A). Proinsulin (Table 2-1 line 36) similarly interacts only weakly with insulin receptors [93] (Fig.

2-4A). By contrast, SCIs bearing the -GGGPGKR- linker [85] and our newly-described -QRGGGGGQR- linker (Table 2-1 line 27) exhibited significant competition with iodoinsulin for insulin receptor binding (Fig. 2-4A), with the uncleavable SCI (-QRGGGGGQR- linker; Table 2-1 line 27) showing a binding affinity that is at least as strong or stronger than the SCI with the -GGGPGKR- linker (Table 2-1 line 15) that has been used in gene therapy of rodent diabetes [84].

SCI activation of insulin receptors

I next examined insulin receptor activation by SCIs in embryonic fibroblasts from mice (MEFs) genetically devoid of IGF1 receptors but stably overexpressing human insulin receptors [28], thereby eliminating any confusion about the source of SCI signaling. Twelve minutes after addition of either chemically purified human insulin, or recombinant proinsulin or SCIs at 5 ng/mL, the MEFs were lysed in the presence of an anti-phosphatase cocktail and were analyzed by Western blotting with anti-phosphotyrosine (Fig. 2-5A, upper panel) or anti-phospho-AKT (Fig. 2-5A, lower panel). [Note again that the construct bearing an -RRGKR- linker (lane 5, and Table 2-1 line 12) is not a single-chain insulin]. The SCI with K(B29) tethered directly to G(A1) [Table 2-1 line 1] is known to exhibit nearly zero bioactivity [29] and yielded background autophosphorylation of insulin receptors (Fig. 2-5A, lane 4) comparable to that seen for proinsulin (lane 3), with

only slightly greater AKT phosphorylation than that observed in MEFs exposed to conditioned medium alone (lane 9). By contrast, three other SCIs with linkers bearing an Arg residue before Gly(A1) each clearly stimulated autophosphorylation of insulin receptors, and each triggered downstream signaling to AKT (lanes 6-8), similar to that observed for authentic insulin (lane 2).

In additional experiments using an assay in which tracer ^{125}iodoinsulin was pre-bound to MEFs at 4°C prior to the addition of unlabeled ligand, I found that the kinetics of displacement of the tracer ^{125}iodoinsulin into the medium upon addition of unlabeled SCI bearing a -QRGGGGGQR- linker (Table 2-1 line 27) was at least as fast as that observed upon addition of unlabeled insulin, indicating that such an SCI is an effective mimic in ligand-induced dissociation of pre-bound insulin (not shown). Moreover, upon addition of the same SCI to cells that had been serum-starved, the kinetics of insulin receptor autophosphorylation and downstream signaling to AKT also appeared comparably fast to that of insulin, with maximum signaling seen already by 6 minutes after ligand addition (Fig. 2-5C).

SCI-stimulated glucose uptake by adipocytes and suppression of gluconeogenic enyzme synthesis in hepatocytes

To test whether SCI-mediated signaling resulted in standard metabolic effects of insulin, I first pre-incubated 3T3L1 adipocytes with various SCIs and then tested for ^{3}H-2-deoxyglucose uptake over a 5 min test period (see *Methods*). A negative control employed cells exposed to medium in which no recombinant SCI had been added (with uptake of ~120 pmoles deoxyglucose per minute per well of confluent 3T3L1 adipocytes). An SCI directly linking K(B29)-G(A1) (Table 2-1 line 1) in a largely inactive conformation [29], and proinsulin (Table 2-1 line 26) which has very low receptor activation [123] each exhibited minimal stimulation of 2-deoxyglucose uptake (Fig. 2-6). Authentic insulin (positive control, last bar) exhibited a > 4-fold increase in ^{3}H-deoxyglucose uptake (slightly greater than that observed for the construct bearing an -RRGKR- linker which is cleaved to a two-chain protein). Two SCIs bearing a nonapeptide linker (-RRGGGGGQR- and the uncleavable -QRGGGGGQR-, Table 2-1 lines 29 and 27, respectively) exhibited comparably strong stimulation of deoxyglucose uptake (Fig. 2-6), exceeding that observed for the SCI (-GGGPGKR-, Table 2-1 line 15) that had been reported to be effective in lowering blood glucose in diabetic rodent models [85].

Next, serum-starved primary rat hepatocytes were incubated for one day in media containing various recombinant SCIs and then were analyzed by quantitative PCR for mRNA encoding PEPCK, a key enzyme in gluconeogenesis

(Fig. 2-7A). [Once again, addition of authentic insulin served as a positive control while the construct bearing an -RRGKR- linker is processed to a two-chain insulin molecule.] Proinsulin was ineffective in suppressing mRNA levels for this gluconeogenic enzyme, but SCIs bearing linkers of -GGGPGKR-, -RRGGGGGKR-, and -QRGGGGGQR- (Table 2-1 lines 15, 29, and 27) were similarly effective, with the uncleavable linker being perhaps being the best of this latter group. Further, a replication-deficient recombinant adenovirus was engineered to encode this latter SCI, driven by an artificial promoter derived from a small region of the glucose-regulated L-type pyruvate kinase gene (nucleotides -201 to +12). Beginning at 24 h after infection, primary rat hepatocytes were compared to those infected only with a Green Fluorescent Protein (GFP)-expressing control adenovirus. After an additional 24 h exposure to high glucose, glucose-induced expression of the SCI caused an ≥ 85% reduction in hepatocyte PEPCK mRNA compared to control values (Fig. 2-7B). Together, the data in Figs. 2-5, 2-6, and 2-7 support that SCI bioactivity is coupled not only to kinase signaling but also to metabolic regulation in insulin-responsive target cells.

Limited SCI activation of cell surface IGF1 receptors

As IGF1 is a single-chain insulin-like molecule, the potential for cross-activation of IGF1 receptors by SCIs must be considered. To assess cross-activation, I employed NIH-3T3 cells overexpressing IGF1 receptors [69] and examined IGF1

receptor autophosphorylation. Twelve min after addition of either 10 ng/mL authentic IGF1, authentic insulin, or recombinant proinsulin or SCIs, the cells were lysed in the presence of an anti-phosphatase cocktail and were then analyzed by Western blotting with anti-phosphotyrosine. Direct blotting of IGF1 receptors in these lysates (lower panel, Fig. 2-5B) confirmed that gel loading was properly normalized. A low-level phospho-IGF1R band was seen even in cells incubated with no ligand (upper panel of Fig. 2-5B, lane 1) or conditioned media from untransfected 293T cells (lane 3). A strong phospho-IGF1R signal was elicited by authentic IGF ligand (lane 2), while proinsulin and each of the SCIs (lanes 5-8) exhibited low-level cross-activation of IGF1 receptors in a range similar to that observed for authentic insulin (Fig. 2- 5B, lane 4).

2.4 Discussion

In this report, I have been interested to further examine features of SCIs that might affect their potential for future use as insulin receptor agonists. Without altering insulin B-chain or A-chain sequences, I designed several new SCIs (Table 2-1) built around a template design (line 19). Functioning strictly as a single-chain protein, an SCI bearing a -QRGGGGGQR- linker sequence is one that I have been enthusiastic about as a polypeptide that folds with native disulfide bonds (as judged by nonreducing tris-tricine-urea-SDS-PAGE mobility, Fig. 2-2); is cleavage-resistant even in an endoprotease-enriched

microenvironment (Fig.2- 2); is efficiently extracted by cells overexpressing insulin receptors (Fig. 2-3); shows competitive binding with ^{125}iodoinsulin that is at least as efficient as a construct previously used successfully for gene therapy in rodents (Fig. 2-4); stimulates insulin receptor autophosphorylation and downstream signaling to AKT (Fig. 2-5A); drives glucose uptake in adipocytes (Fig. 2- 6); and suppresses gluconeogenic enzyme synthesis in hepatocytes (Fig. 2-7). The only other cleavage-resistant constructs in this study involved direct linkage of insulin B- and A-chains, resulting in disulfide mispairing in the endoplasmic reticulum (Fig. 2) [100]; weak insulin receptor binding (Figs. 2-3A, 2-4A); and little favorable downstream metabolic signaling (Figs. 2-5A, 2-6) [29].

From this study, it appears that the best SCI ligands have an arginyl residue immediately preceding Gly(A1). Replacement of basic residues at the carboxyl-terminus of the linker sequence inhibits insulin receptor interaction (Table 2-1 lines 21, 26, 32) even though the arginyl residue is not required as a cleavage site (Fig. 2-2). One hypothesis would be that a basic residue can mimic a free amino group that would ordinarily be provided by the free amino group of Gly(A1) [91, 94] which is an important residue for receptor contact [124]. In future, this should be tested by engineering a lysyl residue in this position of the linker sequence.

Excessive length of the linker (Table 2-1 lines 34 and 35) is obviously detrimental to insulin receptor interaction (Fig. 2-3A). These findings appear to account for

the low bioactivity of proinsulin itself [59], which was in fact demonstrated herein (Figs. 2-3A, 2-4A, 2-5A, 2-6, and 2-7). Very short linker sequences also appeared unfavorable in their ability to bind insulin receptors (Table 1, Fig. 2-3A). These data are consistent with the idea that a tethered C-terminal portion of the insulin B-chain limits good ligand contact with the receptor [114] while greater mobility in this region may unencumber the N-terminal portion of the insulin A-chain [115]. The presence of a tight turn with a short linker is likely to seriously restrict such movement, while results with a pentapeptide -RRGKR- linker (Fig. 2-5A, 2-6, and 2-7A) are not representative of SCIs with short linkers because this miniproinsulin is quantitatively converted to a 2-chain product as a consequence of its furin-like endoproeolytic cleavage site [168]. Work has not been done to determine to determine if cleavage of this construct occurs on both sides of the linker sequence or only at the A-chain junction.

While SCIs produce many of the same favorable metabolic effects of authentic insulin (Figs. 2-6, 2-7), there are certainly still issues that must be addressed in the further development of SCIs as potential anti-diabetic therapies. No work has yet been performed on the immune response to SCIs bearing foreign linker peptide sequences. I also think it plausible that SCI native structure and immunogenicity might be exploited in vaccine development, since the insulin B-chain 9-23 peptide [15, 23, 36] is thought to contain diabetes-associated epitopes of significance for disease in humans [4] as well as nonobese diabetic (NOD) mice [86, 117, 118, 126, 172].

In conclusion, the results described herein help to establish guidelines for the features of SCI linker sequences that are needed to confer native structure and bioactivity, and provide encouragement for their further development.

2.5 Methods

Directed mutagenesis to generate distinct SCI constructs

67 cDNAs encoding SCIs bearing distinct linker sequences (35 reported in this study) were generated using a 4-primer method using an SCI with direct B-chain-to-A-chain linkage [100] as a template. Briefly, two distinct initial rounds of PCR were employed using primer set 1+2 and primer set 3+4 in which primers 2 and 3 include overlapping, complementary 20-mer oligonucleotide sequences that also contain unique sequence encoding the introduced mutagenized residues, while primer 1 (5'-ggtaccatggccctgtggatgcgcctcctgcc-3') and primer 4 (5'-cctaagctagttgcagtagttctccagctggta-3') amplify the proinsulin signal peptide and the end of the insulin A-chain, respectively. Finally, the purified products of the first two PCR reactions were mixed together as template, and a third round PCR was employed in which amplification used terminal, opposite stranded primer set 1+4. The resultant PCR product was ligated into the mammalian expression vector pTARGET (Promega) and confirmed by DNA sequencing.

Production of recombinant SCI protein

In brief, 293T cells supplemented with Dulbecco's Modified Eagle Medium (DMEM, Gibco 11995) plus 10% FBS were transfected with plasmids encoding various SCIs using Lipofectamine 2000 (Invitrogen). After 24 h, transfection medium was removed and cells were washed twice with PBS. Cell culture media was then replaced with DMEM containing 1% fish-skin gelatin (rather than albumin or other serum constituents that may contain or bind insulin); preliminary studies established that cells transfected with empty vector remained healthy while yielding no background insulin immunoreactivity the media. After a further 48 h in culture, media were recovered and a radioimmunoassay designed to detect rat insulin-plus-proinsulin (ie, cross-reacting with all insulin-containing polypeptides, Linco Diagnostics) was employed to measure recombinant SCI concentration in each sample. The use of SCIs in subsequent studies was then normalized to immuno-assayable levels.

Steady-state, metabolic labeling to compare SCI expression levels

The determination of relative concentration of selected SCI constructs was cross-checked by steady-state radiolabeling, based on the fact that all constructs had an identical number of Cys residues per molecule. In brief, 10 µcCi ^{35}S-Cysteine (without methionine) was added to complete culture medium (to achieve a fixed specific radioactivity) and the cells were labeled continuously in this medium for

24 h to approach steady state. The samples were then split in two aliquots. To one aliquot, RIA was used to measure the relative immuno-assayable SCI levels in comparison to an insulin standard. Note: we confirmed that ^{35}S-cysteine does not in any way interfere with the gamma counting that is used to detect ^{125}I-insulin from the RIA. To the second aliquot, SCIs were immunoprecipitated with a vast excess of polyclonal guinea pig anti-(porcine)-insulin (Linco; pilot re-precipitation experiments confirmed that a saturating quantity of this immunoprecipitating antibody was used). Zysorbin (Zymed) was used to recover the immunoprecipitates, which were washed several times before addition of SDS-gel sample buffer including 100 mM dithiothreitol. Denaturation was completed by boiling each sample for 5 min. Fully reduced SCIs in these samples were analyzed by tris-tricine-urea-SDS-PAGE, fluorography, and the amounts quantified by scanning densitometry.

SCI interaction with insulin receptors

For an estimate of receptor interaction that did not require radioiodination of the ligand(s), recombinant SCIs synthesized in 293T cells were diluted to a stock concentration of 50 ng/ml and then further diluted 10-fold to a final concentration of 5 ng/mL in conditioned media from untransfected 293T cells that had been incubated (in batch) in DMEM plus 1% fish skin gelatin. Standards were also diluted in this medium. CHO-IR cells that overexpress human insulin receptors

were grown to confluency in Ham's F12 medium (GIBCO #11765) plus 10% FBS in 12-well plates. CHO-IR cells were then serum starved overnight in F12 containing 11 mM glucose, and then 500 µL of SCI or standard was applied to the cells for 6 h at 4°C. After incubation, media was removed and the remaining soluble SCI was re-measured by RIA; the calculated difference value reflected the amount extracted by binding to CHO-IR cells.

In competitive binding experiments, CHO-IR cells were incubated for 6 h at 4°C with varying concentrations of unlabeled SCI or human insulin in the presence of a fixed amount (12.5 femtomoles) of ^{125}I-labeled human insulin (Amersham Biosciences cat. #IM166). After incubation, the media were removed and cells washed three times with PBS to remove unbound ^{125}I-insulin. The cells were then lysed and counted in a gamma counter, in triplicate. At each concentration of cold competitor, the data were plotted as a percent of total counts bound when unlabeled ligand concentration was zero. IC_{50} values were determined using GraphPad Prism software by curve-fitting with a one-site competition model.

Phosphorylation of insulin receptors, IGF1 receptors, and AKT

Mouse embryonic fibroblasts lacking IGF1 receptors and overexpressing human insulin receptor B-isoform ("R$^-$IR-B cells" [28], kindly provided by Dr. C. T. Roberts at Oregon Health and Science University, Portland OR) or NIH-3T3 cells overexpressing IGF1 receptors ([69], kindly provided by Dr. D. LeRoith, Mount

Sinai School of Medicine, New York NY) were serum-starved overnight. The R^- IR-B cells were washed and then incubated with 500 µL of media containing 5 ng/mL of each SCI [in conditioned media from untransfected 293T cells that had been incubated (in batch) in DMEM plus 1% fish skin gelatin; standards were also diluted in this medium] in a cell culture incubator for 12 min at 37°C. The NIH-3T3 cells overexpressing IGF1 receptors were washed and similarly incubated with IGF1 or SCIs. Media was then removed and the cells washed twice with ice-cold PBS. Cells were lysed in 150 mM NaCl, 1% NP-40, 0.1% SDS, 2 mM EDTA, 10 mM Tris-HCl pH 7.4 plus 1% protease inhibitor cocktail (Roche #11836153001) and 1% phosphatase inhibitor cocktail (Sigma #P2850 plus #P5726). The samples (40 µg cell protein) were then analyzed by SDS 10%-PAGE and Western blotting with mouse mAb anti-phosphotyrosine (clone 4G10, Millipore #05-321) followed by a peroxidase-conjugated goat anti-mouse IgG (Bio-Rad #170-6516). As a control to confirm band identity, samples were also Western blotted with rabbit polyclonal antibodies against insulin receptor (Santa Cruz #C-19) or IGF1 receptor Santa Cruz #C-20), each followed by a peroxidase-conjugated goat anti-rabbit IgG (Jackson ImmunoResearch #111-035-003). Phospho-Ser473 of AKT (referred to as phospho-AKT) was blotted with a mouse mAb (Cell Signaling #9271). As a control to confirm band identify, samples were also Western blotted with rabbit polyclonal anti-AKT (Millipore #9272) and appropriate peroxidase-conjugated secondary antibody. All primary antibodies were used at a dilution of 1:1000, anti-mouse IgG secondary

antibodies were used at 1:3,000 and anti-rabbit IgG secondary antibodies were used at 1:10,000.

SCI-stimulated glucose uptake

Mouse 3T3L1 preadipocytes were maintained in DMEM plus 10% calf serum, and were induced to differentiate into adipocytes 3 d after achieving confluency in 12-well plates by addition of 100 µg/ml insulin, 1 µM dexamethasone, and 0.5 mM isobutyl-1-methylzanthine for 3 d and followed further by 100 µg/ml insulin for 2 d as previously described [16]. SCIs synthesized as recombinant proteins expressed in 293T cells were diluted to a stock concentration of 50 ng/ml in DMEM plus 1% fish-skin gelatin and then further diluted 10-fold in Hepes-buffered Krebs-Ringers-Bicarbonate (KRBH: 10 mM $NaHCO_3$, 120 mM NaCl, 4 mM KH_2PO_4, 1 mM $MgSO_4$, $CaCl_2$, 30 mM Hepes pH 7.4) to a final concentration of 5 ng/mL plus a final (nonradioactive) glucose concentration of 4 mg/100 mL. The differentiated 3T3L1 adipocytes were then preincubated for 3 h in DMEM containing 5.5 mM glucose plus 0.2% FBS. The cells were then washed once, and 500 µL of KRBH containing each SCI was added to cells in a cell culture incubator at 37°C. After 30 min, 1 µCi ^{3}H-deoxy-D-glucose (~45 nmoles, MPBio cat. #27088S) was added to each well for a further incubation of 5 min. The reaction was stopped by addition of 50 µL of 200 mM nonradiactive glucose per

well, rapidly washing three times with ice-cold PBS, and then lysis in 0.1% SDS (500 µL) for scintillation counting.

The potential for SCI endoproteolysis as measured in AtT20 cells

The potential for cleavage of SCIs was assessed after transient transfection in AtT20/PC2 cells (a kind gift of Dr. R. Mains. U. of Connecticut, Farmington CT). The cells were pulse-labeled for 30 min with ^{35}S-Cys/Met mixture and chased for 3 h under unstimulated conditions. At that time media was replaced with fresh chase media ± 5 mM $BaCl_2$ and the cells chased for an additional 30 min. The stimulated or unstimulated secretion was collected and immunoprecipitated with polyclonal guinea pig anti-(porcine)-insulin. SCI immunoprecipitates were analyzed by tris-tricine-urea-SDS-PAGE and fluorography.

Preparation of primary rat hepatocytes

Hepatocytes were obtained from livers of male Sprague-Dawley rats (Harlan) by collagenase perfusion as previously described [27]. Rat primary hepatocytes were plated in RPMI 1640 media containing 11 mM glucose, 10 % FBS, 100 nM dexamethasone, and 100 nM insulin. At 4 h after plating, nonadherent cells were aspirated and adherent cells were further incubated for adenoviral infection.

Adenoviral infection of primary rat hepatocytes

The pGL3-basic vector (Promega) was used to construct different promoter-driven versions of the SCI #3 construct. PCR of rat genomic DNA was used to generate promoter sequences from the rat liver pyruvate kinase (L-PK) from nucleotide -201 to +12 (forward primer with SacI site: 5'-TCCGAGCTCTGCAGACAGGCCAAAGG-3'; reverse primer with BglII site: 5'-CATAGATCT ACGTTGCTTACCTGCTG-3') which was inserted between the SacI and BglII sites of pGL3-basic. The SCI with a -QRGGGGGQR- linker sequence was engineered to be inserted between NcoI and XbaI sites within the above shuttle vectors. After DNA sequence confirmation, the different glucose-inducible promoter-driven versions of this SCI were inserted between the KpnI and SalI sites of the promoterless pAdTrack (www.coloncancer.org). The pAdTrack-promoter-SCI constructs were digested with PmeI and cotransformed by electroporation in BJ5183 cells with the pAdEasy-1 adenoviral gene backbone, with positive clones selected and diagnostically confirmed by plasmid miniprep and PacI digestion (as well as direct sequence confirmation). After maxi-prep purification, PacI linearized adenoviral DNA was used for transfection to produce virions in 293 cells used as the viral packaging cell line. Adenoviruses expressing green fluorescent protein (GFP) as well as the glucose-inducible regulatory element driven SCI were purified on cesium chloride gradients. After adenovirus plaque assay, primary rat hepatocytes were infected at a multiplicity of infection of 50. After viral addition, the medium was changed

to RPMI 1640 with 5.5 mM glucose, and the cells incubated overnight before another medium change to RPMI 1640 containing 25 mM glucose for 24 h. At this time, RNA was isolated from the hepatocytes using the RNeasy kit (Qiagen) as per the manufacturer's instructions.

Real-time PCR

Isolated RNA was initially treated with DNase I at 37°C for 1 h before quenching with DNase inactivation reagent (Ambion). 1 µg of DNA-free RNA from each sample was used for first-strand cDNA synthesis in the presence of 10 mM dNTP mix and 1 µL of random hexamers (50 ng/µl). Each sample was incubated at 70°C for 10 min and then placed on ice. Next, 2 µL of 10x reverse transcription buffer, 4.5 µL of 25 mM $MgCl_2$, 2 µL of 0.1 M dithiothreitol, and 1 µL of RNaseOUT recombinant ribonuclease inhibitor was added to each tube. After incubation at 25°C for 2 min, each tube was loaded with 1 µL of SuperScript III reverse transcriptase. The tubes were incubated at 25°C for 10 min, 42 °C for 1 h, and 85 °C for 15 min. RNase H was added to each to each tube and incubated at 37°C for 20 min. The parameters for real-time PCR were as follows: 95°C for 11 min followed by 40 cycles of 95°C for 30 s and 60°C for 1 min and, for the melt curve, 100 cycles of 10 s from 60 to 100°C in 0.4°C increments. The final concentration of primers in each PCR well was 0.1 µM. Oligonucleotide standards were serially diluted from 10^{-5} µM to 10^{-9} µM to be used as template

for a standard curve. The rat PEPCK forward primer was 5'-TGAGGAAGTTTGTGGAAGGCA-3' and reverse primer was 5'-GCCGTCGCAGATGTGAATATACT-3'. An 18S rRNA primer set was also employed (forward primer 5'-CGGCTACCACATCCAAGGAA-3' and reverse primer 5'-TTTTCGTCACTACCTCCCCG-3' [102]. 1 µL of a 1:50 dilution of each cDNA was used as a template to assess either PEPCK mRNA or 18S rRNA (which was used to normalize the PEPCK mRNA measurements).

2.6 Figures

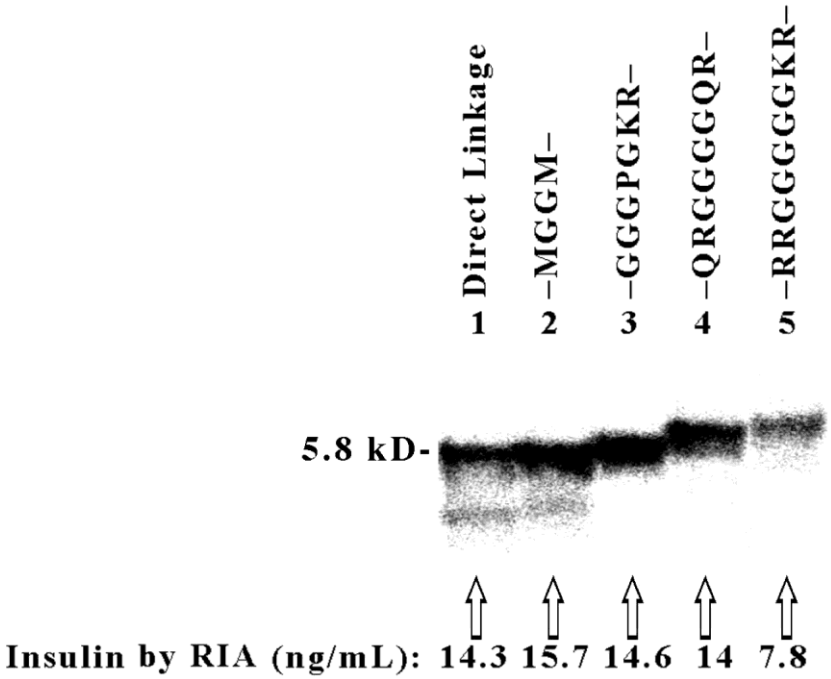

Figure 2-1. Comparison of SCI levels measured by RIA to that measured by steady state metabolic labeling.

293T cells were transiently transfected with cDNAs encoding SCIs containing the linker sequences shown at the top of the Figure. The 'Direct Linkage' construct (lane 1; also Table 1 line 2) fuses the insulin B-chain Thr(B30) to the A-chain Gly(A1) with no intervening sequence. The other constructs expressed contained the following linkers: -MGGM- (lane 2, also Table 1 line 11); -GGGPGKR- (lane 3, also Table 1 line 15); -QRGGGGGQR- (lane 4, also Table 1 line 27); and -RRGGGGGKR- (lane 5, also Table 1 line 20). Transfected 293T cells were labeled continuously for 24 h with ^{35}S-Cysteine at a fixed specific radioactivity to approach steady state. Media were analyzed both by RIA (values for each sample shown at bottom) and by immunoprecipitation with a saturating amount of antibody (see *Methods*) followed by reducing tris-tricine-urea-SDS-PAGE and fluorography. A representative experiment (of three) is shown. The relative gel band densities for each construct were within 10% of the RIA readings when the smaller fragments shown in lanes 1 and 2 (not seen in all experiments) were included in the densitometry. Note that the Direct Linkage construct has a molecular mass of 5.8 kD, identical to that of human insulin.

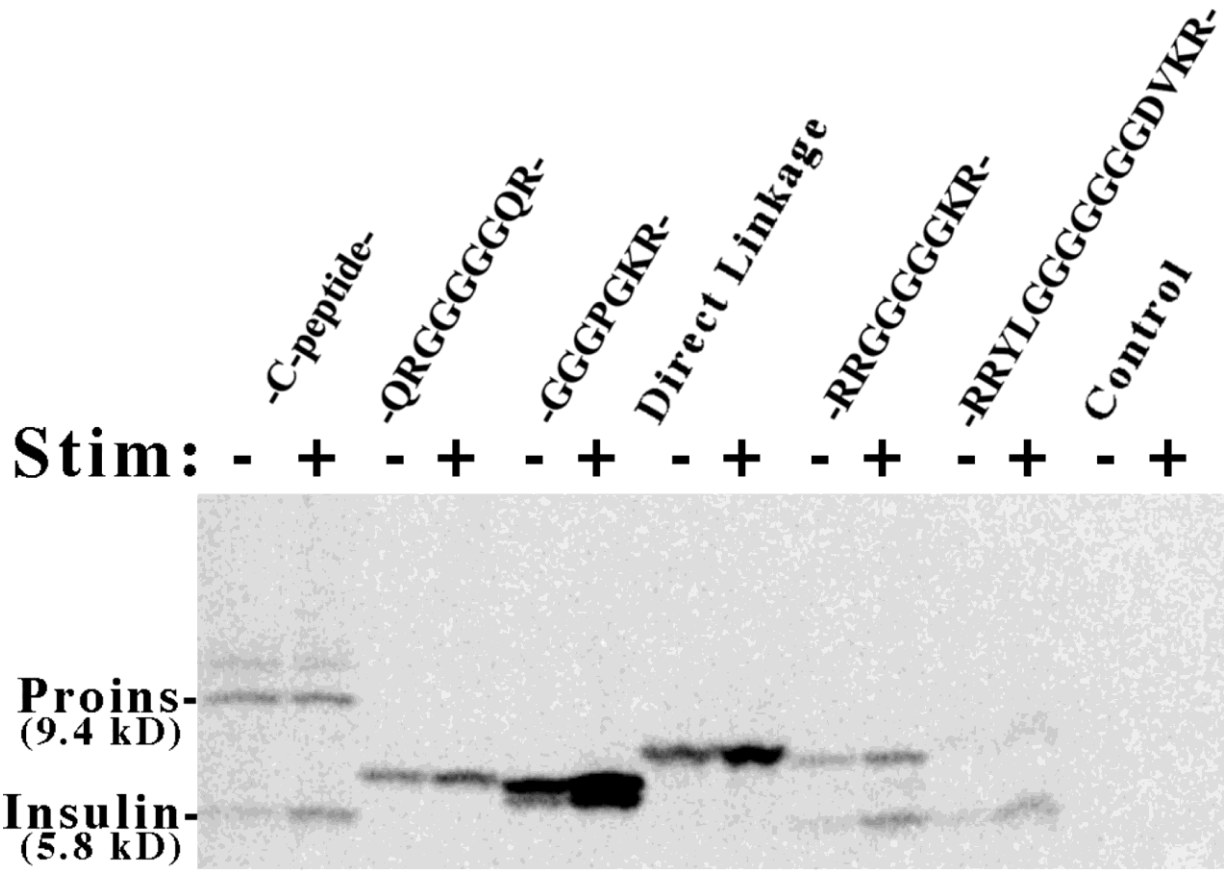

Figure 2-2. Cleavage of SCIs in the secretory granule environment of AtT20/PC2 cells.

Cells were either untransfected ("Control") or transiently transfected with the constructs bearing the linkers shown. For proinsulin (molecular mass = 9.4 kD) the linker is C-peptide. The other linkers are -QRGGGGGQR- (Table 1 line 27 -GGGPGKR- (Table 1 line 15), Direct Linkage (Table 1 line 2), -RRGGGGGKR- (Table 1 line 20), and -RRYLGGGGGGGDVKR- (Table 1 line 34). The cells were pulse-labeled for 30 min with ^{35}S-amino acids. After the first 3 h of chase, fresh chase media was added for 30 min in the absence of secretagogues ("Stim –"), and then for an additional 30 min in the presence of 1 mM $BaCl_2$ ("Stim +"). Media were immunoprecipitated with anti-insulin, which was analyzed by tris-tricine-urea-SDS-PAGE under nonreducing conditions. Mature insulin has a molecular mass 5.8 kD.

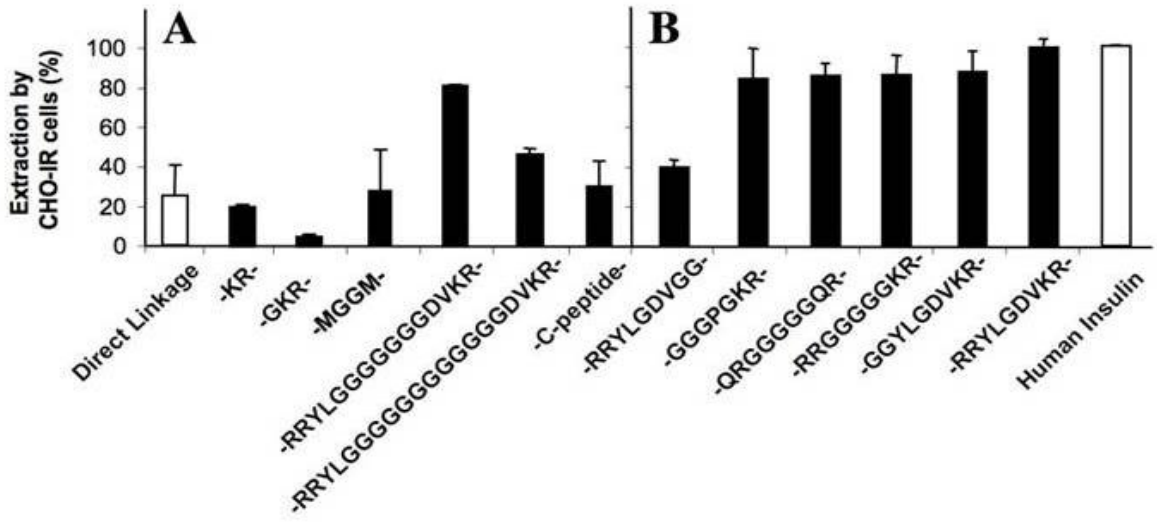

Figure 2-3. Extraction of SCIs, or insulin standard, from media bathing CHO-IR cells (overexpressing human insulin receptors).

First, the recombinant proteins were produced in transfected 293T cells. Then, confluent CHO-IR cells that had been serum starved overnight in 12-well plates underwent a medium change to contain 500 µL conditioned media containing recombinant SCI that had been diluted to 5 ng/mL in fresh medium. The samples were cooled to 4°C and incubated for 6 h at 4°C. SCI extraction from the media was measured using an RIA for (proinsulin+insulin) that cross-reacts with unprocessed and processed products of multiple species. The 'Direct Linkage' construct, in which the insulin B-chain Thr(B30) is directly linked to the A-chain Gly(A1), served as a negative control (white bar, panel A, *left*). Purified human insulin served as a positive control (white bar, panel B, *right*), and all extraction data were normalized to that observed for this standard (set at 100%; actual human insulin extraction in this assay was 85%). The mean +/- standard deviations of three independent experiments are shown. (**A**) SCI extraction as a function of unusually short or extended linker length. The 'C-peptide' linker represents native recombinant proinsulin. (**B**) Mutation of dibasic sites at the amino and carboxyl-terminal ends of the linker sequence.

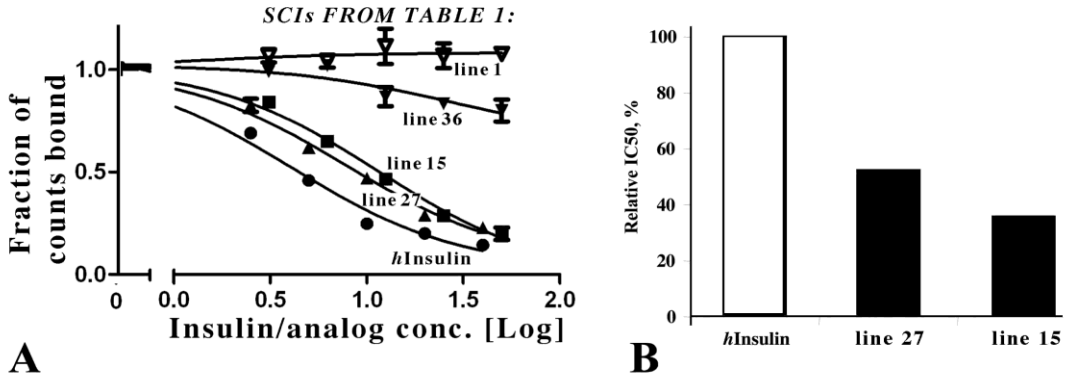

Figure 2-4. Competitive binding of recombinant SCIs (produced in transfected 293T cells) with ^{125}iodoinsulin.

Representative experiment (of three) of CHO-IR cells co-incubated with a fixed concentration of ^{125}iodoinsulin and varying concentrations of authentic human insulin or SCIs bearing the following linkers: [C-peptide (proinsulin, Table 1 line 36); -QRGGGGGQR-, Table 1 line 27); -GGGPGKR- (Table 1 line 15); or B29-A1 (Table 1 line 1) for 6 h at 4°C. (A) The media were removed and the cells washed once with ice cold PBS before counting the cell lysates in a gamma counter. Standard deviations in these measurements are ~15% of mean values. (B) From curve-fitting of the data plotted in panel A, IC50 values for the SCI with a linker sequence -QRGGGGGQR- is compared against that of the published SCI from Table 1 line 15 [85], normalized as a fraction (%) of that observed for authentic human insulin standard (white bar).

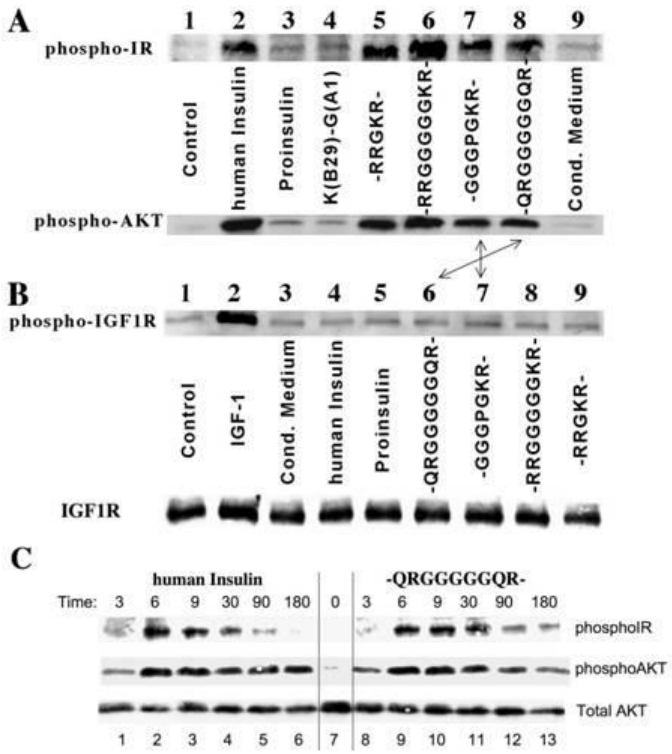

Figure 2-5. Kinase activation of insulin receptors and IGF1 receptors by recombinant SCIs (produced in transfected 293T cells).

(A) Confluent serum starved mouse embryonic fibroblasts (MEFs, from IGF1 receptor null mice, overexpressing human insulin receptors) in 12-well plates were incubated in 500 µl of media containing 5 ng/mL of each SCI or insulin standard for 12 min at 37°C. Cells were washed and lysed in the presence of phosphatase inhibitors as described in *Methods*. The samples were resolved by SDS-PAGE, electrotransferred to nitrocellulose, and Western blotted with anti-phosphotyrosine (upper panel) or anti-phosphoAKT (lower panel) as described in *Methods*. The "Control" sample had no medium change from serum starved medium. *Lane 2* is a positive control incubated with chemically purified human insulin; *lane 9* is a negative control incubated with conditioned medium from untransfected 293T cells. Separate Western blotting of these samples were also performed with antibodies against insulin receptor (not shown) to confirm the identify of the bands shown in the upper panel and to serve as a loading control. **(B)** Confluent serum starved NIH3T3 cells overexpressing IGF1 receptors in 12-well plates were incubated in 500 µl of media containing 10 ng/mL of each SCI or insulin standard for 12 min at 37°C, exactly as in (A). Cells were washed and lysed in the presence of phosphatase inhibitors as described in *Methods* and the samples analyzed by SDS-PAGE with Western blotting using with anti-phosphotyrosine (upper panel) or anti-IGF1 receptor (lower panel, which serves as a loading control). Note that the SCI bearing a -QRGGGGGQR- linker is run in lane 8 in panel A and lane 6 in panel B (see double headed arrow in Figure).

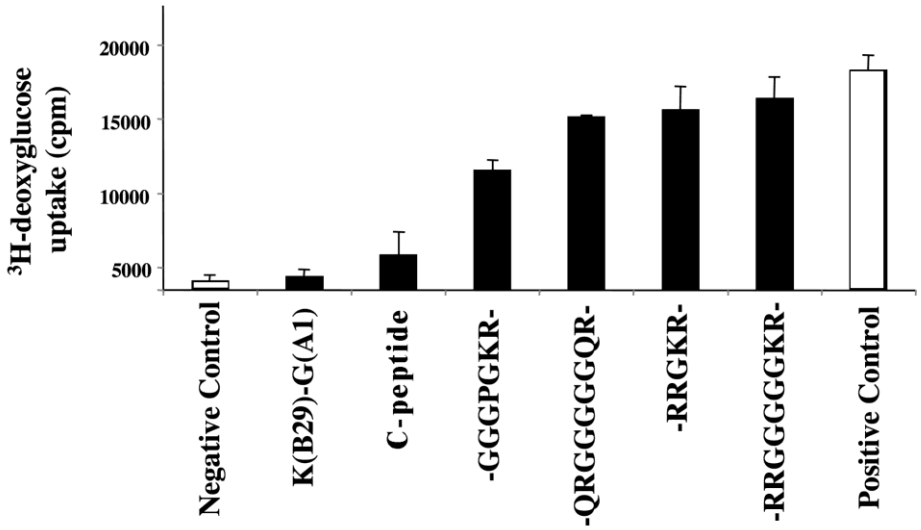

Figure 2-6. ^{3}H-deoxyglucose uptake in 3T3L1 adipocytes.

Differentiated 3T3L1 adipocytes were serum starved in DMEM containing 5.5mM glucose, 0.02% FBS for 3 h. Recombinant SCIs (produced in transfected 293T cells) were diluted into KRBH buffer (containing 4 mg/100 mL nonradioactive glucose) to a final concentration of 5 ng/mL. After a 30 min incubation at 37°C, ^{3}H-deoxyglucose uptake was performed for 5 min as described in *Methods*, followed by scintillation counting. The linker sequences for each SCI construct are listed beneath each bar. A negative control (white bar, *left*) includes conditioned medium bearing no SCI and a positive control (white bar, *right*) contains authentic human insulin; the linker called "Cpeptide" represents recombinant proinsulin.

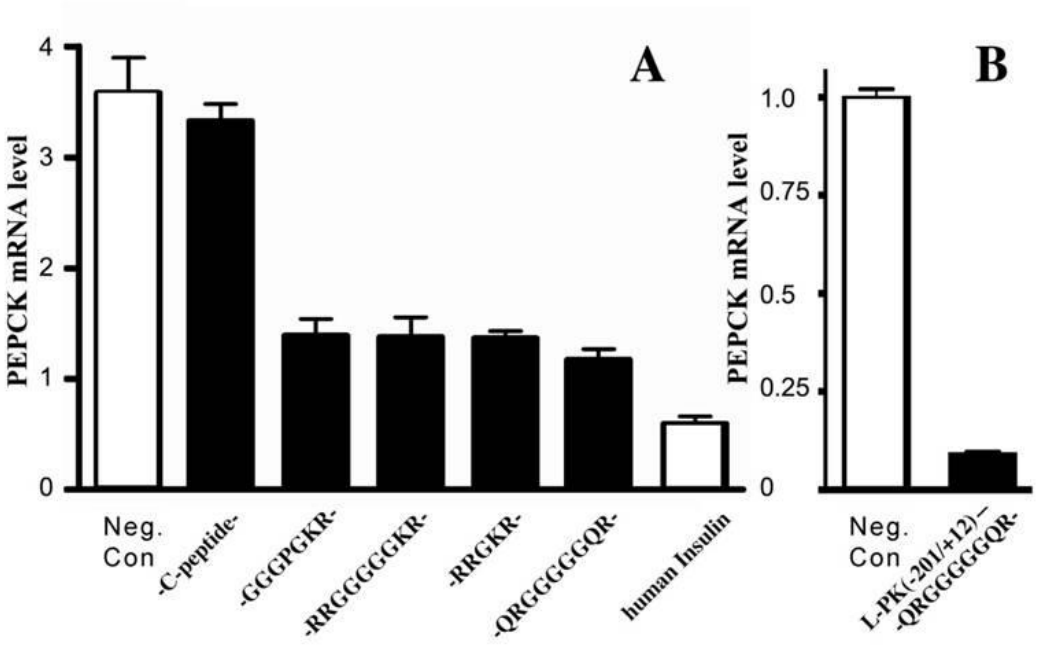

Figure 2-7. A single-chain insulin bearing a -QRGGGGGQR- linker (Table 1 line 27) suppresses gluconeogenesis in primary rat hepatocytes.
Primary rat hepatocytes were prepared as described in *Methods*. (**A**) Cells were first serum starved in RPMI-1640 medium containing 5.5 mM glucose, and then incubated in the same media containing 5 ng/mL of proinsulin ("Pro"), insulin, or the SCIs shown. A negative control ("Neg. Con", white bar, *left*) had no SCI added, a positive control (white bar, *right*) included authentic human insulin. After 2 h of incubation, cells were lysed and PEPCK mRNA was measured by real-time PCR. (**B**) Cells were infected by replication-deficient adenoviral vectors expressing either GFP alone ("Neg. Con", white bar) or the SCI bearing a -QRGGGGGQR- linker, driven by nucleotides –201/+12 of rat liver pyruvate kinase ("L-PK"). At 24 h after infection, the cells were incubated in RPMI-1640 media containing 25 mM glucose for a further 24 h before RNA was purified and analyzed for PEPCK mRNA abundance by real-time PCR. The data shown in both panels are the mean ± S.E. from three independent preparations of hepatocytes.

	Linker Sequence	Length	Dibasic?	Secretory Recovery	Extraction Screen
1	*B29-A1*	*-1*	*N*	*L*	*NS*
2	*Direct Linkage*	*0*	*N*	*H*	*NS*
3	M	1	N	H	NS
4	GG	2	N	M	NS
5	RR	2	Y	M	NS
6	*KR*	*2*	*Y*	*M*	NS
7	MM	2	N	M	NS
8	GGG	3	N	M	NS
9	*GKR*	*3*	*Y*	*M*	NS
10	GGGG	4	N	M	NS
11	*MGGM*	*4*	*N*	*M*	*NS*
12	*RRGKR*	*5*	*Y**	*L*	+++
13	MGGGGM	6	N	M	NS
14	MGGGGGM	7	N	M	NS
15	*GGGPGKR*	*7*	*Y*	*H*	+++
16	RRGPGKR	7	Y	L	+++
17	MGGGGGGM	8	N	M	++
18	RRYPGDVKR	9	Y	L	+++
19	*RRYLGDVKR*	*9*	*Y*	*L*	+++
20	*RRGGGGGKR*	*9*	*Y*	*M*	+++
21	*RRYLGDVGG*	*9*	*Y*	*L*	+
22	*GGYLGDVKR*	*9*	*Y*	*L*	+++
23	RQYLGDVKR	9	Y	L	+++
24	FFYLGVDKR	9	Y	L	NS
25	RRYLGDVGR	9	Y	L	+++
26	RRYLGDVHH	9	Y	L	NS
27	***QRGGGGGQR***	***9***	***N***	***M***	**+++**
28	QRGGGGGKR	9	Y	L	+++
29	RRGGGGGQR	9	Y	L	+++
30	MGGGGGGGM	9	N	M	NS
31	GGGGGGGGG	9	N	M	NS
32	RQYLGDVKQ	9	N	L	+
33	RRYLGGGDVKR	11	Y	L	+++
34	*RRYLGGGGGGGDVKR*	*15*	*Y*	*L*	++
35	*RRYLGGGGGGGGGGGDVKR*	*20*	*Y*	*L*	+
36	*Full C-peptide*	*35*	*Y*	*L*	+

Table 1. SCI constructs prepared for this study.

Except for the first construct shown, cDNAs encoding SCIs bear fixed B-chain/A-chain sequences, ie, varying only by the sequences (shown in Table) that link B-chain to A-chain. The linkers vary in specific sequence and in length. The presence or absence of dibasic sequences in any portion of the linker is indicated as a Yes (Y) or No (N), with one construct (line 12) yielding a predicted furin-type cleavage sequence (this construct on line 12, is indicated with asterisk because it is not a single-chain protein, being quantitatively cleaved in the secretory pathway of 293T cells). Immunoassayed SCI recovery in the conditioned media bathing transfected 293T cells (a measure of both protein expression and secretability) was characterized as: **Low** (L, < 20 ng/mL recovered), **Medium** (M,

20 – 50 ng/mL recovered), or **High** (H, 50 – 100 ng/mL recovered). A screening assay of the ability of various SCIs to be extracted from conditioned media by CHO-IR cells overexpressing insulin receptors, which correlates with receptor binding (see text), was characterized as: **NS** (≤ 25 % extracted), **+** (25 – 50 % extracted), **++** (50 – 75 %), **+++** (> 75 % extracted). Constructs from this with data explicitly shown in the Figures are designated in italics. Work presented in this manuscript highlights the SCI with a –QRGGGGGQR- linker (line 27 in bold) because of a balance of favorable properties.

CHAPTER 3 ENDOPLASMIC RETICULUM OXIDOREDUCTASES AND PROINSULIN FOLDING

3.1 Abstract:

Disulfide bond formation is critically dependent upon the local environment; intracellularly, multiple host-cell gene products provide the environmental and compartment-specific control in which these reactions take place. Indeed, in the secretory pathway of cells, rather than being spontaneous, disulfide bond formation in biologically active peptides is primarily catalyzed, by PDI-like oxidoreductases. *In vitro* studies provide a solid understanding of the spectrum of enzymatic capabilities of PDI and related family members. However, these *in vitro* studies cannot replicate the complexity of the oxidoreductase working environment within the secretory pathway. In the yeast ER — which may be more a more oxidizing environment than the ER of mammalian cells — there is strong evidence that PDI facilitates disulfide bond formation in exportable protein substrates, with evidence also supporting a role for PDI in disulfide isomerization and possibly reduction. In mammalian cells, past literature has tended to group

PDI-like family members as if they were a single protein, but more recent evidence points to the idea that distinct PDI-like family members are subspecialized for somewhat different (albeit overlapping) *in vivo* functions. This probably reflects differences in their relative redox setpoints, alterations/modifications of their catalytic CXXC sequences and neighboring residues, differences in their hydrophobic pockets for substrate binding and chaperone function, and differences in their ER resident partners that provide substrate specificity and function. A case in point is for proinsulin folding in pancreatic beta cells: *in vitro* results support a role for PDI in proinsulin disulfide bond formation while thus far limited results in beta cells provide limited support for this view. In this Chapter, I attempted to characterize the action of PDI on proinsulin in pancreatic beta cells. I provide evidence that PDI directly interacts with proinsulin, and that PDI-knockdown actually increases proinsulin export as well as insulin production. As opposed to widely held assumptions, my results are consistent with a model in which PDI exhibits unfoldase activity for proinsulin, increasing the retention of proinsulin within the ER of pancreatic β-cells, which decreases insulin production. Interestingly, my results point to another ER oxidoreductase, ERp72, as a candidate oxidase (foldase) for proinsulin in the ER of pancreatic β-cells.

Significance: Currently only one paper has been published attempting to ascertain the role of PDI in insulin production in the context of pancreatic beta cells[171]. The previous report employed an overexpression system for PDI to ascertain a role in pancreatic beta cells, and thus may have limitations because of an unphysiological expression level of PDI not observed in normal beta cells. The previous paper also did not look at a direct role of PDI in proinsulin folding, using secretion of insulin and intracellular content as a surrogate measure of folding. My research looks at the role of PDI using physiologically relevant knockdown studies. In addition to looking at the secretion of insulin, my research also looks directly at the folding of newly synthesized proinsulin. The maturation of proinsulin to insulin, employed as a barometer of ER Exit and as an indirect measurement of proinsulin folding, is also measured. During the course of the research work, data pointed to another PDI family member, ERp72, potentially involved in the oxidation and formation of proinsulin disulfide bonds. The role of ERp72, among the most abundant ER oxidoreductases expressed in pancreatic beta cells, also has not been studied in mammalian cell culture systems. This thesis work provides insight into the role ER oxidoreductases in proinsulin egress through the secretory pathway.

3.2 Introduction

Disulfide bonds are made in nearly one-third (7000) of the proteins in the eukaryotic proteome [48], many of which are destined for contact with the relatively non-reducing extracellular environment as secretory or cell surface proteins. Disulfide bond formation involves a reaction between the sulfhydryl (SH) side chains of two cysteine residues: an S^- anion from one sulfhydryl group acts as a nucleophile, attacking the side chain of a second cysteine to create a disulfide bond, and in the process releases two electrons (reducing equivalents) for transfer. Proper disulfide bonds provide stability to a protein, decreasing further entropic choice, which facilitates folding progression towards the native state by limiting unfolded or improperly folded conformations. An increase in stability of the native structure resulting from the formation of a particular disulfide bond is roughly proportional to the number of residues between the linked cysteines; i.e., the larger the number of residues in the 'disulfide loop', the greater the stability provided to the native structure [103, 121].

The chemistry of protein disulfide bond formation is directly influenced by three key factors: *1)* the spatial accessibility/physical proximity of the partner cysteine residues forming the disulfide bond; *2)* the difference between the pKa of the involved thiol groups and the pH of the local environment (with lower pH limiting

reactivity and higher pH favoring increased reactivity); and *3)* the redox environment (with lesser reactivity under more reducing conditions and greater reactivity under more oxidizing conditions) [9, 103, 138, 163]. As the latter two factors are environmentally controlled, specific cellular compartments have evolved within cells to facilitate disulfide bond formation. In bacteria, disulfide bonds in bioactive peptides and polypeptides of the secretory pathway are formed in the periplasm; in eukaryotes, such (poly)peptides tend to acquire their disulfide bonds in the endoplasmic reticulum (ER) . The ER is a vastly more common site than the cytosol for disulfide formation (which is very rarely the site of disulfide bond formation) because the ER intralumenal environment is more oxidizing than that of the cytosol [5]. The redox environment is at least in part reflected by the ratio of oxidized glutathione (GSSG) to reduced glutathione (GSH), which in the case of the ER (and periplasm), is shifted in favor of GSSG [5].

3.2.1 The Concept of Secretory Pathway Catalysis of Disulfide Bond Formation

Although disulfide bonds can form spontaneously (albeit very slowly) via molecular oxygen or directly via oxidized glutathione as an electron acceptor, the main mechanism of disulfide bond formation in the secretory pathway involves enzymatic catalysis, via oxidoreductase proteins bearing a catalytically active

thioredoxin domain motif: CXXC (where ‘X’ residues tend to be hydrophobic amino acids) that is responsible for disulfide bond transfer from oxidoreductase to substrate [48]. In secretory proteins that contain more than one disulfide bond in their final structure, the formation of these bonds is typically not a linear process, insofar as their order of formation may vary *en route* to the native state. In general, newly-synthesized secretory proteins have preferred folding intermediates (such as has been become well known from *in vitro* folding studies of ribonuclease and bovine pancreatic trypsin inhibitor [26, 103, 138]). Oxidoreductases may help to promote a particular folding pathway both by selective disulfide catalysis and by acting as molecular chaperones that limit off-pathway folding choices. Once a transient intramolecular disulfide bond has formed within the CXXC motif of the oxidoreductase, the catalytic event proceeds via a transient mixed disulfide bond between the amino-terminal cysteine of the CXXC and the substrate protein, which is then resolved by completion of an intramolecular disulfide bond formed within the substrate protein (Fig. 3-1) in a process facilitated by both the carboxyl-terminal cysteine of the CXXC motif and neighboring residues that influence the CXXC redox potential. Catalyzed disulfide bond formation occurs very rapidly, with dynamic sampling and release of substrate proteins by oxidoreductase enzymes [6, 47]. The reaction catalyzing disulfide transfer to the substrate protein does not result in a net loss or gain of disulfide bonds, as a reduced CXXC motif is regenerated in the disulfide transfer process; i.e., the transfer reaction involves oxidation of the substrate protein

concomitant with reduction of the thioredoxin motif in the oxidoreductase. Thus, within the ER, there is a net flow of electrons from substrate proteins to oxidoreductases that catalyze disulfide bond formation. In the ER of eukaroyotes, Protein Disulfide Isomerase (PDI) is the most prominent and most evolutionarily conserved of these oxidoreductases — but there are at least 21 PDI-like family members in mammalian cells [48, 128] — several of which shall be touched upon in this Introduction (Table 3-1).

The secretory pathway operates as a protein manufacturing and export factory. Once properly folded, the most recent cohort of oxidized secretory proteins is exported, only to be immediately followed by a new cohort of incoming (newly-synthesized) secretory proteins — and these new polypeptides begin their 'life' with a full complement of reduced cysteine thiols. In order to bring about another round of substrate protein oxidation, the catalytic oxidoreductases must again form a transient intramolecular disulfide bond within their CXXC motif(s); thus, they must become re-oxidized. In bacteria, secretory protein oxidation by the Disulfide Bond Formation (DSB) family of proteins begins with DsbA catalyzing initial disulfide bond formation in substrates, with DsbA being re-oxidized by electron transfer to the periplasmic membrane-bound DsbB (from which electrons are subsequently ‘unloaded’ to ubiquinone that is finally reoxidized by the respiratory chain involving molecular oxygen as the terminal electron acceptor [12, 65, 103]). In the secretory pathway of eukaryotes, the various ER oxidoreductases also must become re-oxidized, and the identity of the reoxidant

is still somewhat unclear, however, this is an extremely active area of ongoing investigation. PDI (encoded by the P4HB gene) can be specifically re-oxidized by Endoplasmic Reticulum Oxidoreductin-1 (ERO1), an ER membrane-associated protein that serves as the functional analog of bacterial DsbB [6, 7, 39, 40]. In yeast, ERO1 was first identified because its genetic deletion resulted in a phenotype in which exportable proteins lacked disulfide bonds [39]. Indeed, ERO1 was found to form a transient mixed disulfide with PDI and yet ERO1 appeared unable to interact directly with exportable protein substrates [40]. Moreover, overexpression of ERO1 itself cannot rescue perturbation of disulfide bond formation resulting from PDI knockout, strongly suggesting that, at least in *S. cerevisiae*, oxidized PDI is required for ongoing disulfide bond formation in secretory proteins and ERO1 is required for the catalytic re-oxidation of PDI [40]. From these and additional studies performed in higher eukaryotic cells and animals [5][5-7, 142, 175], ERO1 proteins are now considered to be one of the major catalysts of disulfide bond formation in the ER lumen [142] — although still under active investigation are possible important roles for other oxidizers of lumenal ER oxidoreductases and substrate proteins — including oxidized glutathione (discussed above) plus additional enzymes including but not limited to Peroxiredoxin 4 (PRDX4) , Vitamin K-dependent OxidoReductase (VKOR), and Quiescin–Sulfhydryl OXidase (QSOX), (discussed below) [5].

3.2.2 *Transfer of Reducing Equivalents from the ER Lumen to the Cytosol*

ERO1, containing a variant of the thioredoxin motif known as a cysteine triad, provides a mechanism for delivery of reducing equivalents back to the cytosol, leading ultimately to molecular O_2 [142]. In the case of the mammalian gene product, whereas the last two cysteines of the amino-terminal cysteine triad (residues C94 and C99) of ERO1 catalytically transfer a disulfide bond to the active site of PDI, the last two cysteines of the carboxyl-terminal triad (residues C394 and C397) of ERO1 are used to transfer reducing equivalents to FAD^+ [13]. Reducing equivalents are internally shuttled within ERO1 from C94/C99 to C394/397, in order to ready C94/C99 for another round of disulfide bond formation. The reduction of FAD^+ to $FADH_2$ (which, in the cytosol, can transfer these reducing equivalents to molecular oxygen as the terminal electron acceptor) is accompanied by formation of hydrogen peroxide (H_2O_2) in the ER, as a byproduct [142]. The stoichiometry is such that for every ERO1-catalyzed disulfide bond, one molecule of hydrogen peroxide is generated.

As H_2O_2 is one form of Reactive Oxygen Species (ROS), the catalytic activity of ERO1 has been considered a contributor to cellular oxidative stress that is seen an undesirable outcome [142], although this has been debated [5]. New studies

indicate that Peroxiredoxin 4 (PRDX4) links the reduction of cytoplasmic hydrogen peroxide to additional disulfide bond formation in PDI-like oxidoreductases of the ER lumen [17, 176]. In the process of reducing H_2O_2, PRDX4 becomes chemically oxidized at the carboxyl-terminal cysteine of its CXXC motif, followed by formation of a mixed disulfide bond that is transferred to PDI or other PDI-like oxidoreductase. Notably, mice bearing a double knockout of ERO1α and ERO1β (the two mammalian ERO1 genes) are still able to generate disulfide bonds in secretory proteins with only a minor delay [175], but a triple knockout of ERO1α, ERO1β, and PRDX4 displays a more severe oxidative folding defect [176]**.** In addition to PRDX4, PDI peroxidases GPX7 and GPX8 also reduce cytoplasmic H_2O_2 and may promote disulfide bond formation in the ER lumen, although these molecules are relatively under-studied [17, 119].

Vitamin K-dependent OxidoReductase (VKOR) is another protein that can receive reducing equivalents from PDI-like family members. VKOR is an ER transmembrane protein that catalyzes reduction of Vitamin K epoxide to hydroquinone (a cytoplasmic co-factor needed for gamma-glutamyl carboxylation of newly-synthesized blood clotting factors in the ER (of hepatocytes) [158]), allowing the CXXC motif in VKOR itself to become oxidized. VKOR can then in turn receive reducing equivalents from PDI-like oxidoreductases, as shown by ‘disulfide trap mutants’ of oxidoreductases bearing the active site cysteine mutation CXXA that allows for creation/capture of a stable mixed disulfide complex with VKOR [141].

Quiescin–Sulfhydryl OXidase (QSOX), another source of direct disulfide bond oxidation in substrate proteins (in a manner entirely independent of PDI-like oxidoreductases), uses molecular oxygen as its terminal electron acceptor to very potently generate disulfide bonds directly in substrate proteins (preferentially over those in PDI-like family members) and produces H_2O_2 as a byproduct [49, 53]. In yeast, the overexpression of QSOX, a monomeric flavoprotein, can rescue mutant phenotypes of *ero1* null mutants[21]. Yet the physiological role of QSOX in mammalian cells remains unknown because of its low expression level and its apparent localization in the Golgi complex rather than the ER where most secretory protein disulfide bonds are thought to form [20].

3.2.3 Proper Disulfide Bond Formation in the Secretory Pathway may also Include Disulfide Reduction and Isomerization

Even after disulfide bond formation in the secretory pathway, there are times when existing disulfide bonds must be broken within the ER (or periplasmic space of bacteria). For example, initial disulfide bond formation may involve cysteine mispairing, leading an exportable protein into a non-native 'off-pathway' conformation. Such mispaired disulfide bonds need either to be broken (reduced) or isomerized to native pairings. In higher eukaryotes, the large number of distinct PDI-like oxidoreductases makes it all the more likely that subspecialization exists among family members to function more as oxidases or

more as reductases for specific substrates — even as all members must cycle their catalytic CXXC motifs between oxidized and reduced states. While this is largely unproven in higher eukaryotes, it is plausible that evolution may have divided catalysts of disulfide bond formation *versus* disulfide reduction or isomerization into distinct gene products, since such specialization might allow for greater functionality. Even in bacteria, isomerization activity is carried out by DsbC and DsbD, which tend not to assist in initial disulfide bond formation within substrates [107, 129].

PDI — which is certainly associated with disulfide bond formation in yeast as well as ER reoxidation after reductive stress in higher eukaryotic cells [5] — can also be clearly shown to exhibit disulfide isomerase activity. Indeed, disulfide isomerization catalyzed by PDI was one of the observed activities reported by Anfinsen in his Nobel prize-winning studies of the *in vitro* refolding of denatured ribonuclease [44]. By contrast, there are other agents, like QSOX (and others described below) that do not appear capable of reduction or isomerization of disulfide bonds in secretory proteins [53, 127] — providing support for the notion of specialization of enzymes in the secretory pathway primarily dedicated to substrate oxidation rather than isomerization or reduction.

3.2.4 The Family of PDI-like ER Oxidoreductases

As PDI is a prototypic ER oxidoreductase, it is worth briefly reviewing its structure-function relationships. A 55 kDa protein containing two catalytic thioredoxin (a and a') domains, PDI also contains two non-catalytic (b and b') domains arranged as a-b-b'-a' (**Figure 2*c***) [41, 77, 152]. The non-catalytic b and b' domain (and its following linker region) tend to contain hydrophobic pockets that contribute importantly to low affinity binding of a wide variety of substrates [47]. The low affinity allows PDI to "sample" many potential substrates and thereby to potentially direct rapid catalysis — within the ER, the apparent K_m of the enzyme for a given substrate is at least as much about protein sampling as it is about catalytic activity. The a and a' domains may also contribute to substrate recognition [47, 152]. PDI and many other members of the PDI-like family of ER oxidoreductases also contain the 4 amino acid carboxyl-terminal KDEL-like sequence that functions as a Golgi retrieval signal to enrich these proteins within the ER. With the combination of its four domains, PDI can also function as a molecular chaperone — preventing aggregation of proteins — in addition to its function as an enzyme. In yeast, catalytically-dead PDI rescues the lethal PDI null phenotype, suggesting that PDI's essential role in the ER goes beyond its role in disulfide bond formation [81]. Thus, it is thought that through both its catalytic and non-catalytic activities, PDI can minimize kinetic traps — helping to eliminate 'dead-end' folding intermediates[103, 159].

Other PDI-like family members differ in length and activity, but share the common thioredoxin-like fold, being grouped on the basis of their content of a, a', b or b' homology domains. The non-catalytic b and b' domains are often not well defined; moreover, some PDI-like family members are entirely non-catalytic as they contain no "a-domain" bearing a CXXC motif (a Ser residue is often found to be substituted in place of Cys) — nevertheless, these family members assist in protein folding of substrates [136]. For a list of PDI-like ER oxidoreductases, please see Table I. This broad family of PDI-like ER oxidoreductases displays a diversity of functions that continues to be discovered. As a complete review of all family members and their putative functions is beyond the scope of this thesis, I will cite only a few limited examples. ERp57, like PDI, has structural units that include two redox-active a and a' domains [48]. However for ERp57, the non-catalytic b domain contains no substrate-binding hydrophobic pocket [76]. Instead, the positively-charged non-catalytic domain of ERp57 appears to be specialized for interaction with the negatively-charged tip of the P-domain of lectin-like chaperones calreticulin and calnexin — it is for this reason that ERp57 substrates are almost exclusively comprised of glycoproteins [66, 76]. ERdj5 has been shown to function mainly as a reductase, breaking disulfide bonds in misfolded proteins [154]. ERp72 can act on the same protein substrates as PDI, yet ERp72 does not have an identified hydrophobic domain, and its phenotypic effects tend to be opposite to those of PDI. In one such example, PDI has been found to act as an unfoldase that enhances the retrotranslocation of cholera toxin

from the ER lumen to the cytosol, whereas ERp72 limits cholera toxin retrotranslocation [38]. ERp72 and another PDI-like oxidoreductase, P5, have been found to complex with the molecular chaperone BiP (GRP78) and may also be involved in recognition of misfolded protein cargo [67]. PDILT (PDI-Like Testis, restricted to testis) and PDIp (PDI Pancreas, restricted to pancreas) interact with endogenous substrates specific to those tissues [31, 48, 156]. Overall, existing results tend to support the view that different ER oxidoreductases are selective about their choice of substrates — the central issues (besides cell type-specific gene expression) include their relative abundance in the ER, the molecular organization and structure of their catalytic and non-catalytic domains, their redox potential (relative ease of reduction vs. oxidation of the catalytic CXXC), and the availability of ER resident partner proteins for the oxidoreductase that may bring it into close proximity with selective substrate proteins.

3.2.5 Selective Activities of Oxidoreductases within the ER Environment

While PDI-catalyzed substrate (re-)folding has been extensively characterized *in vitro*, there remains little data on the role(s) of PDI-like oxidoreductases *in vivo*. It has been reported that siRNA-mediated knockdown of PDI in the HepG2 hepatocyte cell line results in a modest retardation in oxidative folding of various

substrates[133]. The effect is enhanced when combined with simultaneous knockdown of other oxidoreductases such as ERp57, resulting in delayed substrate exit from the ER — with the authors suggesting functional redundancy among members of the PDI-like family of ER oxidoreductases [133]. Conversely, it has previously been shown that siRNA-mediated depletion of ERp57 in mouse L cells causes a delay in the oxidative folding of MHC class I heavy chain and a delay in the export of class I molecules from the ER [173] — and ERp57 knockout mice die *in utero*, thought primarily to represent a B cell defect in the formation of MHC class I peptide-loading complexes [43]. Thus, it would appear that other ER oxidoreductases cannot adequately replace this essential physiologic function of ERp57. Likewise, neither ERp72 nor ERp57 can support normal retrotranslocation of cholera toxin A1 polypeptide from the ER to the cytosol — a function that appears to be facilitated selectively by PDI [38]. Indeed, PDI overexpression stimulates ER-Associated Degradation (ERAD, a process involving retrotranslocation for proteolysis via the ubiquitin-proteasome pathway) of mutant thyroglobulin, while ERp72 overexpression decreases ERAD rate for the same mutant [38]. Taken together, these examples suggest that ER oxidoreductases exhibit distinct behaviors within the ER. Nevertheless, multiple ER oxidoreductases are induced by ER stress (also known as the Unfolded Protein Response, or UPR), and deficiency of a variety of different ER oxidoreductases (including ERdj5) can sensitize cells to ER stress-mediated

apoptosis [151] — at least in part resulting from deficiency of disulfide reductase activity that is needed for the ERAD process [32, 154].

3.2.6 Oxidation of Proinsulin Within the ER

PDI has been well studied with regard to disulfide bond formation within proinsulin/insulin, both *in vivo* and *in vitro*. Insulin is comprised of two peptide chains (B and A), linked by two disulfide bonds [C(B7)-C(A7), and C(B19)-C(A20)] (For schematic, please turn to Fig. 1-1). Proinsulin, the secretory polypeptide precursor to biologically active insulin, is a single-chain molecule in which the two insulin chains are contiguous because of the presence of the 35 amino acid connecting peptide plus flanking cleavage sites that is proteolytically excised in the final processing events leading to the synthesis of active insulin [45]. Thus after cleavage of the signal peptide, the proinsulin primary sequence, beginning from the amino-terminus of the molecule, sequentially encodes B-chain, C-peptide, and A-chain.

Human proinsulin, produced as an 86 residue peptide (along with a 24 residue signal peptide that is cleaved), contains three intramolecular disulfide bonds: the two noted above interlink the B- and A-chains while a third is contained entirely within the A-chain [C(A6)-C(A11)] [97]. Each of the three bonds is ultimately essential to the biological activity of insulin. In pancreatic beta cells, upon folding

to the native state (that includes of course the proper disulfide pairings), proinsulin exits the ER and is delivered to the Golgi complex from which newly-made secretory granules are first formed — the compartment in which processing from proinsulin to insulin takes place [55]. Ultimately, the insulin granules migrate to the periphery of beta cells to ready themselves for exocytosis in response to secretory stimuli such as elevated blood glucose[10].

The proinsulin gene product is just one member of the large insulin/IGF superfamily, each sharing the 3-disulfide structure[90]. Multiple members of this family, including both IGF-I and IGF-II, have a branched protein folding pathway that can lead to distinct disulfide-linked final structures — including structures with fairly similar thermodynamic stability — although only one of these disulfide isomers (the native form) has optimal bioactivity [57].

Quality control in the endoplasmic reticulum, mediated via recognition of non-native structures by ER chaperones (and oxidoreductases), is designed to limit ER export of secretory protein substrates that are biologically inactive due to conformational immaturity (i.e., ‘unfolded’) or from having formed inappropriate ‘dead-end’ folding products (i.e., ‘misfolded’). In this regard, the three disulfide bonds of proinsulin are not equal in importance. Specifically, without the C(B19)-C(A20) interchain disulfide bond, proinsulin is incompetent for export from the ER, indicating recognition and retention of the “open structure” by ER quality control mechanisms [162]. Likewise, absence of the C(B7)-C(A7) interchain

disulfide bond both impairs thermodynamic stability and dramatically decreases secretability[98, 125]. However, selective absence of the intrachain C(A6)-C(A11) disulfide bond creates only a modest structural perturbation of proinsulin (or insulin) and does not impair secretion [99].

Not only does improper disulfide bond formation critically perturb insulin function, it also appears linked to a chain of events that leads to full-blown diabetes with loss of pancreatic beta cell survival. This is quite a curious situation, as complete deletion of up to three of the four wild-type proinsulin-encoding alleles from the mouse genome (or loss of expression of one of the two wild-type alleles from the human genome) does not cause diabetes or beta cell death [97]. However, the presence of mutant proinsulins bearing cysteine substitutions inexorably leads to this autosomal-dominant phenotype. An interesting structural feature of wildtype proinsulin is that the C(B7)-C(A7) disulfide bond is nearly exposed at the surface of the molecule [58, 169] potentially rendering it susceptible to persistent thiol attack. In fact, recent evidence suggests that the presence of "*Akita* proinsulin", a mouse mutant bearing the C(A7)Y substitution, blocks the secretion of co-expressed wild-type proinsulin and results in the production of aberrant disulfide-linked protein complexes in the ER that contain both wild-type and mutant gene products [97]. Moreover, studies of certain additional proinsulin coding sequence mutations (including those altering residues other than the cysteines themselves), leading to the syndrome of "Mutant INS-gene induced Diabetes of Youth" (MIDY), also result in improper disulfide bond formation that triggers the

same diabetes phenotype as that seen in the *Akita* mouse [96]. These findings validate a sensitive role of proper disulfide bond formation not only for the substrate itself, but also for innocent bystander proteins that may come under attack by co-expressed proteins that bear reactive cysteine thiols [97]. It is believed that proinsulin dimerizes in the ER [64]; what remains to be established is whether misfolded proinsulin triggering dominant negative blockade of innocent bystander substrates is restricted exclusively to bystander proinsulin or may also impact — either through inappropriate mixed-disulfide bonds or via a generalized ER stress response — on any other cysteine-bearing secretory proteins that happen to be co-expressed in the same ER.

PDI can catalyze the formation of proinsulin disulfide bonds *in vitro* [166], yet the physiological role of PDI in the ER of pancreatic beta cells remains unknown. There are data that do not support the notion of PDI as a facilitator of the oxidative maturation of proinsulin in pancreatic beta cells. Specifically, overexpression of PDI in beta cell lines results in a decrease in insulin content and secretion, while proinsulin accumulates intracellularly (presumably in the ER) [171]. While it is possible that PDI overexpression can result in non-specific effects, the results imply an apparent PDI-mediated inhibition of proinsulin export from the ER, which in turn suggests a probable defect in the proinsulin folding process. ERO1-Beta has been reported to function as the primary oxidoreductin in pancreatic beta cells [175], and, as described in detail above, ERO1 accepts reducing equivalents from PDI (and some other PDI-like family members [5]) to

allow the ER oxidoreductases to form a catalytic disulfide bond that can be transferred to exportable protein substrates. Impaired expression of the ERO1-Beta gene produces a phenotype — both in mouse islets and in cultured pancreatic beta cells — similar to that seen upon PDI *overexpression*, i.e., there is a delay in ER exit of proinsulin with lower beta cell insulin content and lower insulin secretion [70, 175]. Unlike in yeast, knockdown or deletion of PDI gene expression is not lethal in higher eukaryotic cells — undoubtedly because of the presence of many other PDI-like family members that can partially or fully replace its function [133]. Thus, based on the foregoing discussion, PDI knockdown in pancreatic beta cells is perfectly feasible, and can be used to directly examine PDI effects on proinsulin disulfide bond formation.

3.3 Results

3.3.1 PDI & WT-Proinsulin interaction

In the case of genetic deficiency of ERO1-Beta — at least in part as a consequence of incomplete proinsulin thiol oxidation — insulin production and consequent insulin secretion is diminished [70, 175]. If proinsulin oxidation from ERO1-Beta is mediated by PDI, then loss of PDI expression would be expected to phenocopy ERO1-Beta knockdown. I therefore examined the effect of ERO1-Beta or PDI knockdown (PDI-KD) in Ins-1 (mouse) beta-cells. I monitored the

recovery of newly-synthesized native proinsulin (nonreducing conditions) relative to total proinsulin (reducing conditions) as analyzed by Tris-tricine-urea-SDS-PAGE after pulse-labeling cells for 15 min. As expected (15), ERO1-Beta knockdown decreased initial oxidation of proinsulin to the native monomer (Fig. 3-3 left) by about 20%. In contrast, PDI-KD did not perturb proinsulin oxidation but actually augmented native proinsulin (Fig. 3-3 right). Importantly, PDI-KD did not result in upregulation of other beta cell ER oxidoreductases (Fig. 3-4) Moreover, PDI-KD in INS1 cells did not upregulate levels of ER molecular chaperones BiP and GRP94, nor activate net phosphorylation of eIF2alpha (Fig. 3-4) or activate splicing of XBP1 (unlike thapsigargin treatment, Fig. 3-4) extra lane). Thus, there was no discernible evidence that PDI-KD triggers ER stress in β-cells. Furthermore, overexpression of PDI in Min6, a mouse derived pancreatic beta cell line, lead to reduction of the recovery of newly-synthesized native proinsulin, consistent with results seen with knockdown (Fig. 3-5).

The perturbation of proinsulin oxidation upon ERO-1Beta knockdown (Fig. 3-3) is accompanied by inefficient proinsulin transport through the secretory pathway with decreased insulin production [70, 175]. However, by pulse-chase analysis after PDI-KD, I actually observed faster maturation of newly-synthesized proinsulin (Fig. 3-6, left) with an increased insulin:proinsulin ratio at 1 h chase (Fig. 3-6, right). To estimate the consequences of this acceleration on the steady state distribution of proinsulin+insulin in INS cells incubated at either 11 or 25 mM glucose, I found by RIA that PDI-KD shifted the distribution from cells to

media (Fig. 3-7). Upon steady-state radiolabeling, I found that most of the insulin immunoreactivity secreted from PDI-KD cells was mature insulin, i.e., molecules that had exited the ER and were processed in secretory granules (Data not shown). This was further observed in Ins832/13 cell that are engineered to stably expresses human proinsulin, which becomes processed into human insulin (Fig. 3-8). To exclude that enhanced secretion was mediated by PDI-KD altering prohormone convertase activity, I examined effects of PDI-KD on recombinant proinsulin trafficking in 293 cells that have no secretory granules or processing enzymes. By pulse-chase, PDI-KD still led to accelerated secretion (Fig. 3-9, top), and shifted the steady-state distribution of proinsulin from cells to media (Fig. 3-10, top).

The experiments were repeated in HepG2 cells (in which PDI knockdown *perturbs* the oxidation and ER exit of several proteins, including albumin, transferrin, α-fetoprotein, and α_2-HS glycoprotein [133].) with similar *positive* effects for proinsulin to those observed in INS1 and 293 cells (Fig. 3-9, bottom, Fig. 3-10, bottom). In INS1 cells, PDI-KD did not accelerate acquisition of Golgi glycosylation of recombinant alpha1-antitrypsin (AAT) (Fig. 3-11). Moreover, PDI-KD did not affect the steady-state levels of processed versus unprocessed IAPP (Fig. 3-12, left) nor IAPP secretion over 72 h at low or high glucose (Fig. 3-12 right). Thus PDI exhibits selective retention activity for endogenous proinsulin in the ER of pancreatic beta-cells and recombinant proinsulin in the ER of heterologous cell types.

Given the specificity of PDI effects on proinsulin, a possible direct effect of PDI on proinsulin was investigated. Mutations in both A and A' thioredoxin domains (CHGC to SHGS) were found to eliminate the ability of overexpressed PDI to prolong the intracellular retention of proinsulin in pancreatic beta cells [171], and I obtained similar results for recombinant proinsulin in 293 cells (Fig. 3-13). (Interestingly, mutations in key residues of the peptide binding region of PDI (B', F258W, I272A) [73, 122] did *not* impair the ability of PDI to retain proinsulin in the ER). I also attempted siRNA-mediated knockdown of PDI in 293 cells with "rescue" using expression of a siRNA-resistant (mouse) PDI. Catalytically-dead PDI (A and A' mutant) was unable to restore proinsulin intracellular retention, while the WT PDI was able to do so (Fig.3-14). This indicates that the catalytic activity of PDI, even at physiologic levels of expression, is likely to be important for retaining proinsulin within the ER.

The catalytic interaction of PDI for proinsulin appeared more consistent with a model in which PDI displayed unfoldase activity, as the knockdown of PDI appeared to accelerate, as opposed to perturbing, the oxidation of proinsulin. In order to further investigate this, I decided to test the ability of individual domains of PDI to retain proinsulin. Kulp et al have described the A' domain as the oxidase domain of PDI, and the A domain as the reductase domain [79]. This is consistent with a model in which the A' domain that receives oxidative equivalents from ERO-1[6, 7, 79] In my experiments, the PDI A' domain mutant, in which the A' CXXC motif is mutated to AXXA (while the A domain remains

intact) was able to retain proinsulin at similar levels to the wild-type PDI (Fig. 3-15, top right). Mutating the A domain, on the other hand, eliminated the ability of PDI to cause efficient retention of proinsulin in the secretory pathway (Fig. 3-15, bottom right). Although it is unclear whether these mutations impact on the physical structure of PDI, these findings appear to be supportive of a mechanism in which a reduced (domain) of PDI facilitates its retention, slowing its oxidative folding and ER exit.

As my data indicated a potential PDI/proinsulin interaction occurred via the A domain of PDI, a PDI "Trap" mutant, in which the C-terminal cysteine in the CXXC motif of the A domain was mutated to alanine, was used to probe a direct PDI –proinsulin interaction in pancreatic beta cells. A flag-tagged PDI bearing an A domain Trap mutation was expressed in Min6 cells. At 72 hours post-transfection, cells were labeled with 500 uCi ^{35}S-cysteine/ methionine in a 60 cm dish for 20 minutes. The cells were then washed once with ice cold Hanks Buffer solution supplemented with 20 mM NEM, lysed, and then split into two samples. One half was immunoprecipitated with anti-insulin antibodies, while the other half was Immunoprecipitated with anti-FLAG antibody overnight. The samples were analyzed under both reducing and non-reducing conditions using 4-12% gradient SDS-PAGE, followed by autoradiography.

PDI-TRAP was found to co-precipitate endogenous proinsulin, whereas the PDI catalytically-dead mutant could not (Fig. 3-16). WT-PDI also co-precipitated

proinsulin, but to a lesser extent than PDI-TRAP, suggesting a more transient interaction between WT-PDI and proinsulin. Under nonreducing conditions, the co-precipitated proinsulin monomer band could not be detected upon FLAG IP, but instead a higher molecular weight adduct appeared above the PDI-TRAP band, consistent with a mixed disulfide between PDI-TRAP and proinsulin (Proinsulin is approximately 8 KD, and PDI-TRAP is 56 KD; thus the adduct band appears to be the correct molecular mass of one proinsulin bound to one PDI-TRAP). This adduct band is also formed by WT-PDI, but to a lesser extent than for PDI-TRAP —although the band was not at all observed in the presence of catalytically dead PDI, or in untransfected controls. By insulin IP, I confirmed that proinsulin synthesis was the same in all samples; thus the interaction seen between newly-synthesized proinsulin and PDI-TRAP was not due to differences in proinsulin synthesis in the different samples. The conclusion from this experiment is that proinsulin in-vivo has the potential to interact with PDI via its catalytic domain. This is the first time in a mammalian cell culture based system such a potential interaction has been demonstrated.

3.3.2 ERp72 & WT-Proinsulin Interaction

To look for other potential ER oxidoreductases that may assist in the oxidation of proinsulin, I set out to quantify mRNA levels for all currently known ER

oxidoreductases expressed in pancreatic beta cells. I did this by designing qPCR primers for each of the ER oxidoreductases (http://www.roche-applied science.com/sis/rtpcr/upl/index.jsp?id=UP030000). The primers were then validated by performing serial dilutions of 1x, 10x, and 100x cDNAs (in this case, from Min 6 cells) and plotting cycle threshold values (CT) against the amount of input cDNA, with primer efficiency measured as the slope of the line. Primers used for each of the ER oxidoreductases had a primer efficiency ≥95%. (Several had to be redesigned in order to achieve this). I then explored two methods and found that the second, widely-reported method [70] comparing relative mRNA expression levels between genes calculated from CT values obtained with validated primers yielded results equivalent to those found in public databases (Fig. 3-17A, 3-17B). Using this method, the data indicated that PDI is among the most abundant beta cell oxidoreductase-related mRNA (Fig 3-17B). P5, ERp57, ERP72, represent the next three most abundant oxidoreductase-related mRNAs in beta cells. PDIp, Agr2, Agr3, PDILT, and ERp27 are not expressed. ERO1-Alpha is also expressed in beta cells, but its mRNA are found at lower levels, consistent with published results [70]. The transmembrane proteins (TMXs), appear to be expressed at low levels as well except for TMX2.

Responsiveness to high glucose was also used as a parameter for suggesting oxidoreductases that might be involved in proinsulin folding. Proinsulin translation (and later, transcription) increase under high glucose conditions which may require a commensurate increase in the synthesis of folding factor(s) that assist

in the formation of proinsulin's three disulfide bonds. Min6 cells were grown at 11 mM glucose for 24 hours. The media were then changed and cells were grown further for 48 hours at 11 mM glucose or 25 mM glucose. cDNA was then obtained from replicates under each condition.

The results indicate that the mRNAs of ERO-1Beta, PDI, ERp72, P5, ER72, (five of the most abundant ER oxidoreductase-related mRNAs found in beta cells) are upregulated by glucose (Fig. 3-18). PDIr mRNA was also upregulated with glucose (and this mRNA has also been reported to be found at relatively high levels according to the Unigene database). The mRNAs of ERdj5, TMX3, ERp44, and ERO-1alpha, which happen to be at the low end of the expression spectrum, appear to decrease in response to glucose. The high abundance of ERO-1Beta, PDI, ERp72, P5, ER72, and PDIr, and their upregulation with glucose, may be indication of their importance to proinsulin biology, possibly in the assistance of creating proinsulin's three disulfide bonds.

To explore this observation further, the experiment was repeated once with cDNA isolated from islets (in this case, 2.8 mM glucose was chosen for low glucose, 11 mM for high glucose) and a few selected genes were chosen to be examined. The data were generally consistent with what was seen from Min6 cells: the mRNAs of PDI, ERP72, P5, and ERp57 all increase upon incubation in high glucose (Fig. 3-18). ERO-1Beta mRNA also increases, to an even greater

degree than that observed in Min6 cells (300% in islets vs 35% in Min 6 Cells). ERO-1Alpha mRNA levels decreased, as in Min6 cells.

Due to limited amount of time and resources, I decided to focus on one particular ER oxidoreductase to further characterize, specifically targeting an enzyme involved in the oxidation of proinsulin's disulfide bonds. Data from our collaborator, Dr. D. Stoffers (U. Pennsylvania), indicated that ERp72 was positively regulated by the transcription factor PDX-1 (Pancreatic and duodenal homeobox-1), a master regulator of key genes involved in the differentiation of pancreatic beta cells (including ERO-1Beta). In human islets, they found that ERp72 was the only ER lumenal oxidoreductase upregulated by PDX-1 (Table 2). Given that ERp72 is among the most abundant oxidoreductases, upregulated by glucose and by PDX-1, I chose to study it further. ERp72 has also previously been shown to interact with proinsulin in-vitro, but in a context that facilitates reduction of proinsulin disulfide bonds rather than oxidation [101, 132, 137, 157].

To investigate the effects of ERp72 on the folding of proinsulin, I used the same assay comparing native proinsulin recovered under nonreducing conditions to total proinsulin recovered under reduced conditions, at 48 hours after siRNA transfection to obtain ERp72-knockdown. As with ERO-1Beta knockdown, in ERp72-KD cells, there was decreased recovery of the native proinsulin band (Fig. 3-19). I then assayed for proinsulin to insulin maturation as a measure of proinsulin export through the secretory pathway. ERp72-KD cells exhibited

slowing of proinsulin to insulin maturation (Fig. 3-20), suggesting impaired transport. This phenotype appeared strikingly similar to that seen with ERO-1Beta knockdown [175]. ERp72-KD displayed no effect on AAT, indicating that the general secretory pathway was unaffected with a reduction in ERp-72 protein. (Fig. 3-21). Finally, using RIA in ERp72-KD cells, I observed a reduction in both intracellular and extracellular total insulin levels (50% and 30%, respectively) (Fig 3-22). These results were further confirmed via Western blotting, which displayed a significant decrease in both proinsulin and insulin levels (Data not shown)

3.4 Discussion

While it is widely assumed that PDI participates in oxidation of proinsulin disulfide bonds, which in turn facilitates proinsulin export, I have found instead that PDI functions as an ER retention factor for proinsulin in pancreatic beta cells. The evidence for this is that in PDI-KD cells, proinsulin transit along the secretory pathway is accelerated as measured by pulse-chase experiment, and with a net increase in efficiency of total insulin secretion as measured by RIA. While it is conceivable that compensatory changes in gene expression — especially that of other ER oxidoreductases — could account for the enhanced proinsulin export,

there are no discernible changes in protein levels of other major ER oxidoreductases (ERp72, P5, or ERp57) in PDI-KD cells.

The argument is compelling that proinsulin egress from the ER is linked to the kinetics and efficiency of proinsulin disulfide bond formation — especially since loss of ERO1-Beta activity is linked not only to decreased efficiency of formation of proinsulin's three native disulfide bonds [[70, 175] and this report] but is also linked to inefficient export of newly-synthesized proinsulin, with delayed and decreased production of newly-synthesized insulin [175]. Given the current finding that in PDI-KD beta cells, native proinsulin disulfide bond formation is not impaired, it seems safe to surmise that PDI is not the primary oxidase responsible for receiving reducing equivalents from proinsulin's cysteine thiols.

My findings do not preclude the possibility that PDI could help to oxidize secretory protein substrates in other cell types [133] or other secretory proteins in beta cells under certain environmental conditions. Even proinsulin can be oxidized by PDI, based on reconstitution in vitro [166] . Nevertheless, it seems plausible that in the ER of beta-cells, the net effect of PDI activity may act as an unfoldase for proinsulin, thereby lengthening its ER residence time. Substrate unfolding has been implicated in the activity of PDI to promote polypeptide retrotranslocation for ER-associated degradation of selected substrates [153] , which may include proinsulin [71]. PDI-mediated unfoldase activity for proinsulin could account for diminished insulin production and induction of ER stress upon

increased expression of PDI in beta cells [171]. Data from 293 results have shown that only a small fraction of PDI molecules are fully oxidized, with 80% of PDI molecules at least partially reduced, a majority consisting of the A domain of PDI in a reduced state [111]. My preliminary data has shown a high proportion of reduced/partially reduced PDI in pancreatic beta cells (Data not shown). This can certainly facilitate the ability of PDI to act as unfoldase. Currently, there is no evidence that knockdown of PDI leads to either proinsulin misfolding or generalized protein misfolding in INS1 beta cells. Indeed, there is no net increase in phosphorylation of eIF2-alpha, no increased splicing of XBP1, and no increase of the hsp70 and hsp90 family members of the ER (BiP and GRP94). Thus, all evidence points to the idea that PDI-KD in beta-cells is nontoxic.

On the other hand, in ERp72-KD cells, across several experiments, I observed phenotypes of reduced intracellular insulin content, lower insulin secretion, and slowing of proinsulin to insulin maturation. Thus it appears ERp72-KD faithfully recapitulates the ERO-1Beta-KD phenotype. Additionally, ERp72 is among the most abundant of the ER oxidoreductase-related mRNAs expressed in pancreatic beta cells (like ERO-1Beta), upregulated by glucose (like ERO-1Beta), and upregulated by PDX-1 (like ERO-1Beta). I conclude that, similar to ERO-1Beta, ERp72 is a candidate oxidoreductase in the pathway of formation of proinsulin's three disulfide bonds.

3.5 Methods

Materials — Anti-PDI was from Dr. P. Kim (U. Cincinnati) and from StressGen; anti-IAPP from Dr. B. Verchere (U. British Columbia); anti-KDEL from Stressgen; anti-ERp72 from Enzo Life Sciences; anti-P5 from Thermo Scientific, anti-ERp57 from Dr. D. Williams (U. Toronto), anti-phospho-eIF2 alpha from Cell Signaling; anti-alpha-tubulin from Sigma; guinea pig anti-insulin was from Millipore. Wild-type human AAT cDNA in pCDNA3 was from Dr. R. Sifers (Baylor College of Medicine); rabbit anti-AAT was from DAKO.

Cell Culture and Transfection — Min6 and 293 cells were grown in DMEM (containing 4.5 g/L D-glucose, 2.5 mM L-glutamine, and 110 mg/L sodium pyruvate) plus 10% FBS and Pen/Strep; Min6 medium was supplemented with 140 Beta-M 2-mercaptoethanol. INS1 cells were grown in RPMI-1640 supplemented with 10% FBS, Pen/Strep and 28 Beta-2-mercaptoethanol.

PDI, ERO-1Beta, and ERp72 knockdown in INS1 and 293 cells employed transfection with 40 nM siRNA using RNAiMax lipofectamine reagent (Invitrogen); plasmid transfection in these cells used Lipofectamine 2000 (Invitrogen) — both following the manufacturer's instructions. The sequences of PDI siRNA oligos were as follows: for INS1, AUAGAACUCCACCAGCAGGTT, GCGCAUACUUGAGUUCUUUTT; for 293, GACCUCCCCUUCAAAGUUGUU, CCGACA GGACGGUCAUUGAUUACAA. ERO-1Beta, Ins-1:

GCGCUCAAUUGUUGATCUU, GCAUCUUUCAGGAUACAAA. ERp72: CCAGGACCCAGGAAGAAAU, GCCCUGAAAUAGCCAAGUU. For experiments involving silencing of Ero1-Beta and PDI in Min6, 2 x 106 were nucleofected using program G-016 as per the manufacturer's instructions (AMAXA). Cells were nucleofected with 1 nmol of ON-TARGET plus nontargeting siRNA pool or 1 nmol of Ero1-Beta ON-TARGET plus SMARTpool (Dharmacon). For PDI knockdown, 1 nmol of siRNA was nucleofected into Min6 cells using the same combination of oligos used for PDI knockdown in INS1 Cells. siRNA duplex controls for GFP or Luciferase knockdown were from Invitrogen.

Metabolic Labeling — At 72 h post-transfection, cells were labeled with 100 uCi 35S-Cys/Met (MP Biomedical) in Cys/Met-free DMEM. When indicated, cells were washed and incubated with 10 mM N-ethylmalemide in ice-cold PBS; then lysed in 1% NP-40, 0.1% SDS, 150 mM NaCl, 2 mM EDTA, 10 mM Tris-HCl (pH 7.4) containing 10 mM NEM and a protease inhibitor cocktail. Lysates were immunoprecipitated overnight with anti-insulin, boiled in SDS sample buffer ± 0.1 M DTT, and analyzed by Tris-tricine-urea-SDS-PAGE.

RIA and ELISA — An RIA that detects proinsulin+insulin of all species (Millipore) was used in all experiments. Media were collected for 24 h at which time total insulin levels were assessed in cell lysates and media. Secretion of IAPP was measured by ELISA cross-reacting with rat IAPP (Millipore).

Statistical Analysis — Data are presented as mean value +/- s.d.. Statistical significance was analyzed by the student's T-Test; a p-value < 0.05 was deemed statistically significant.

3.6 Figures

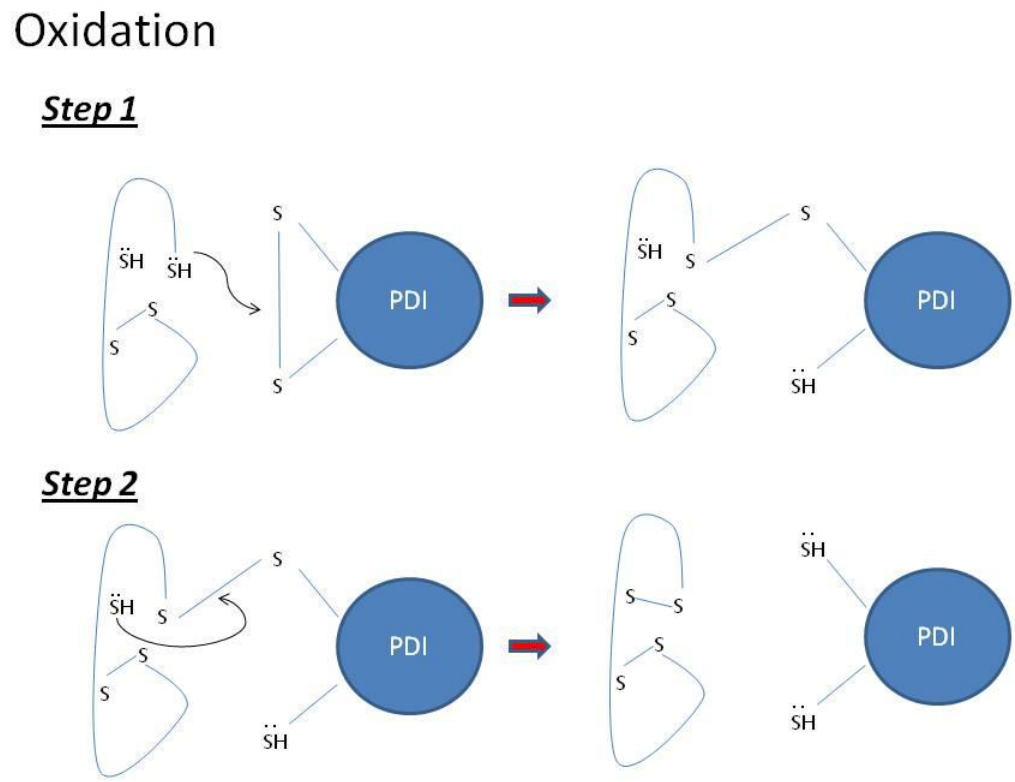

Figure 3-1. Oxidoreductase-catalyzed disulfide bond formation.

In this diagram, the ER oxidoreductase (oval) oxidizes a secretory protein substrate (shown schematically, as a line, at left). In the first step, a sulfhydryl group in the substrate attacks a disulfide bond in the thioredoxin motif (CXXC) within the oxidoreductase, creating a transient mixed disulfide bond between the two proteins. In the second step, folding changes in the substrate bring another cysteine sulfhydryl moiety into proximity with the mixed disulfide. The nucleophilic attack results in the formation of an intramolecular disulfide bond, creating a disulfide loop structure within the substrate, and leaving the CXXC motif of the oxidoreductase as reduced thiols (electrons represented by dots). This will require reoxidation in order that another round of catalyzed disulfide bond formation may proceed.

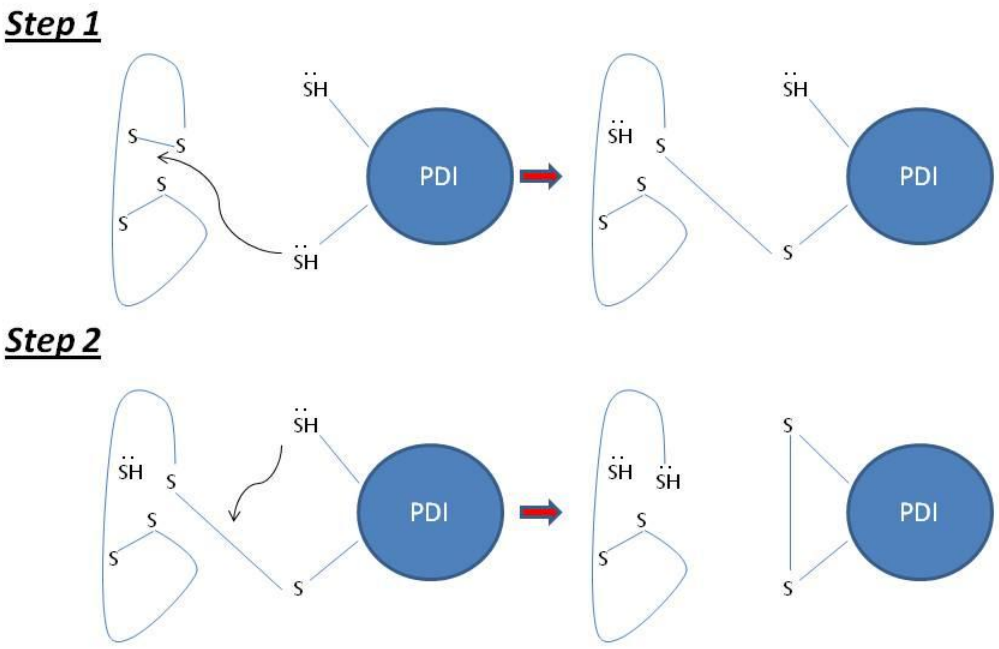

Figure 3-1. Oxidoreductase-catalyzed disulfide bond reduction.

In the first step, the C-terminus cysteine of a sulfhydryl group, in the thioredoxin motif in an oxidoreductase, attacks a disulfide bond in within the substrate, creating a transient mixed disulfide bond between the two proteins. In the second step, nucleophilic attack by a sulfhydryl group the N-terminus cysteine on the mixed disulfide leads to the oxidation and formation of a disulfide within thioredoxin domain of the oxidoreductase. The substrate now is (partially) reduced. Note, mutation of the N-terminus cysteine negates the ability of the mixed disulfide from being resolved, which becomes “trapped” in this conformation.

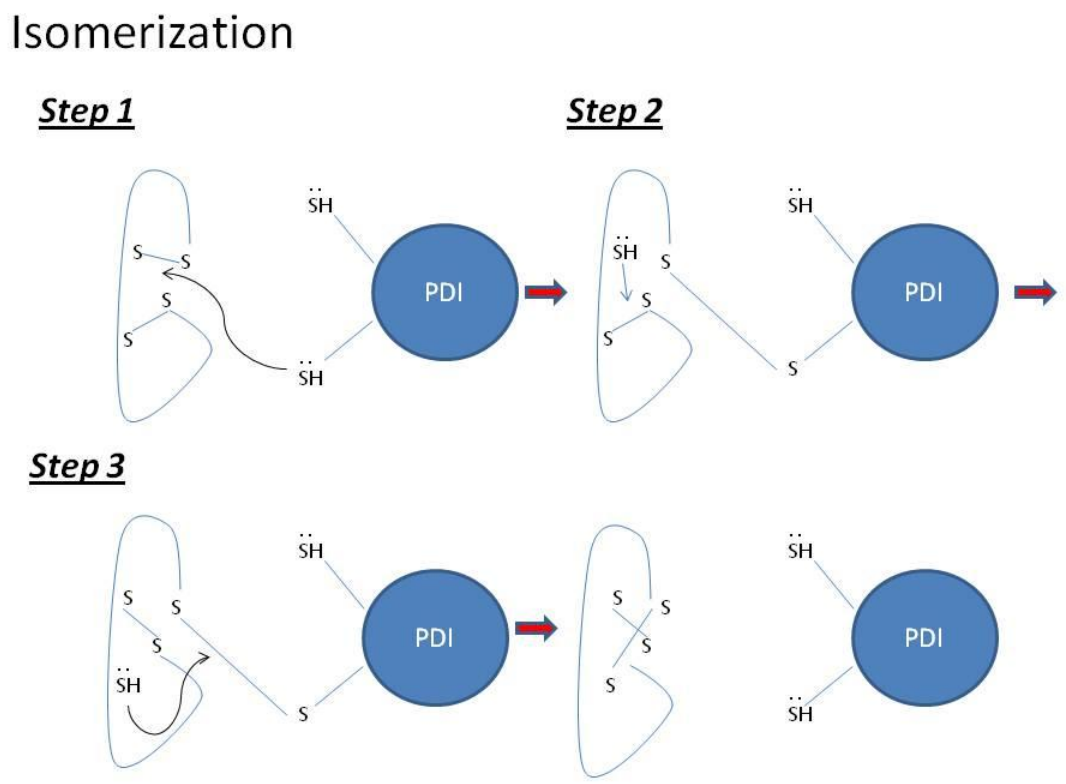

Figure 3-1. Oxidoreductase-catalyzed disulfide bond isomerization.

The process of isomerization begins similar to the process of reduction, with the C-terminus cysteine of a sulfhydryl group in the thioredoxin motif in an oxidoreductase attacking a disulfide bond within the substrate, creating a transient mixed disulfide bond between the two proteins. However unlike in the reduction reaction, where the mixed disulfide is resolved by attack by the sulfhydryl from the N-terminus cysteine in the thioredoxin motif, the now free sulfhydryl group in the substrate attacks another intramolecular disulfide bond within the substrate, leaving the sulfhrdyl group on the remaining unpaired cysteine to attack the mixed disulfide. This results in a rearrangement/isomerization of disulfide bonds within the substrate, with no change in the redox status of the oxidoreductase, which remains in the reduced state.

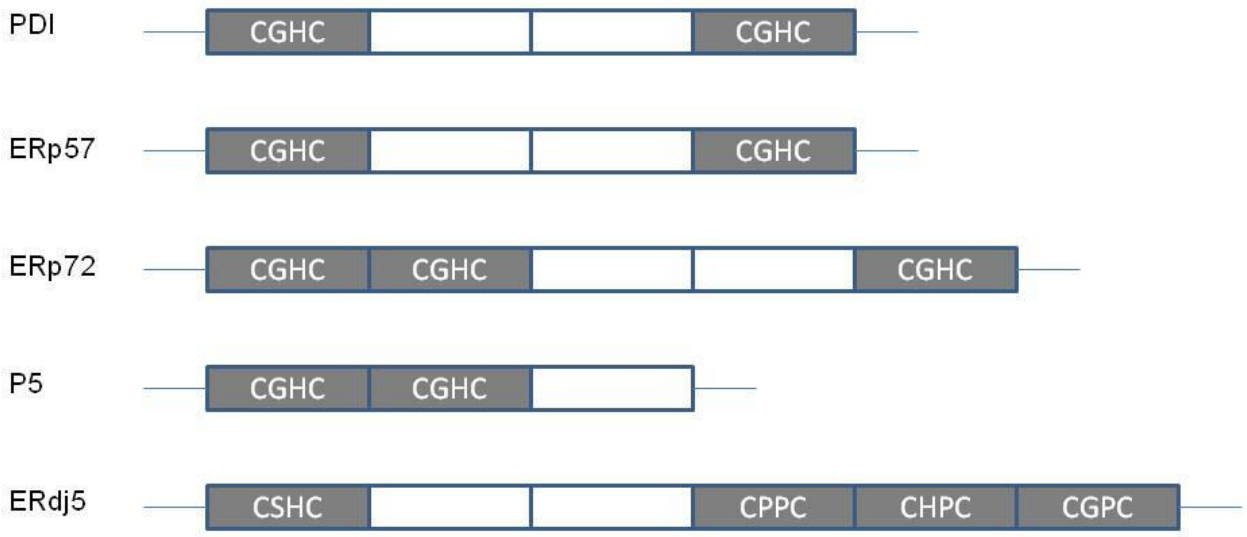

Figure 3-2. Domain structure of selected ER oxidoreductases.

Schematic of PDI-like family members, comprising "A"-type thioredoxin domains that are catalytically active (shown in gray), and "B"-type non-catalytic thioredoxin domains.

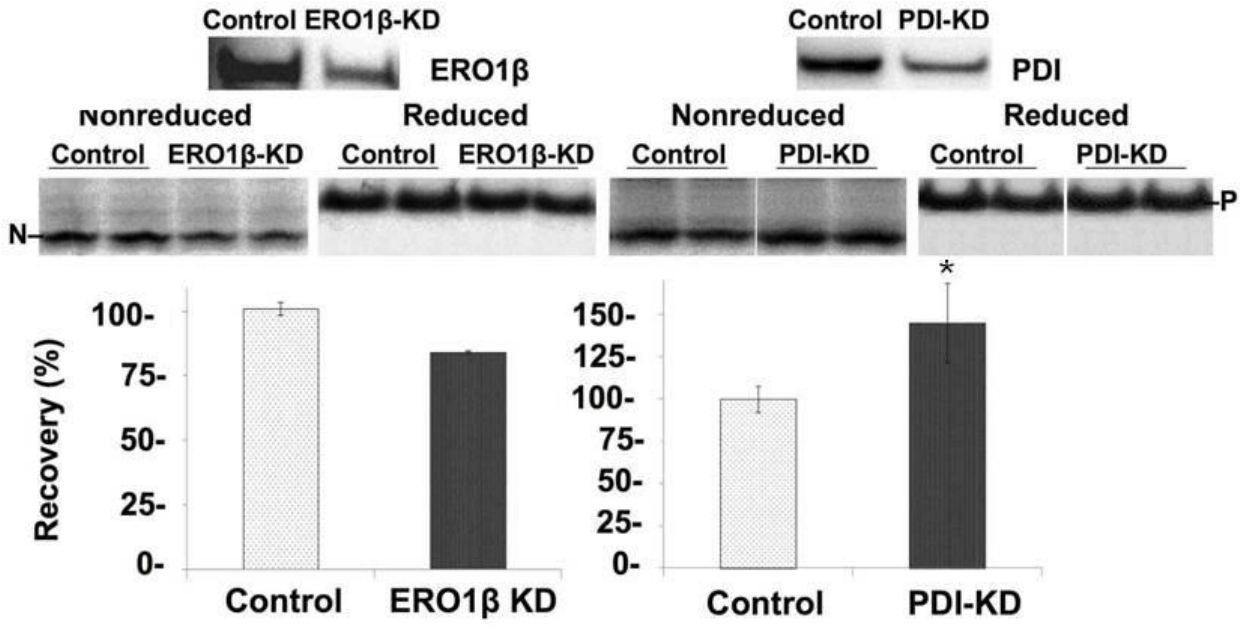

Figure 3-3. Recovery of newly synthesized proinsulin with PDI and ERO1 beta knockdown

Middle panel: At 48 h post-transfection with either scrambled (Con) or ERO1β or PDI siRNA duplexes (20 nM), Ins-1 cells were pulse-labeled for 15 min with ^{35}S-Cys/Met, and lysed in SDS buffer with 10 mM NEM. Lysates were immunoprecipitated in duplicate with anti-insulin and analyzed by Tris tricine-urea-SDS-PAGE under reducing ("P" = 100 mM DTT) or nonreducing ("N") conditions. *Panel above:* Western blotting for PDI and ERO1Beta at 48 hours post-transfection. *Lower panel*: Quantitative band densitometry of the Native proinsulin disulfide isomer (gel at left band "N") was divided by that for total labeled Proinsulin ("P") to calculate the percentage of native form. For ERO-1Beta-KD, the data are from one experiment conducted in triplicate (N=3). For PDI-KD, the data represent five independent experiments (N=10), with an average pulse time of eight minutes. The p-Value for PDI-KD was =0.03.

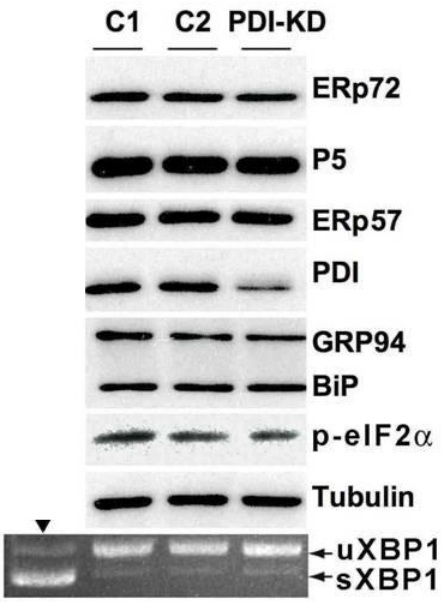

Figure 3-4. Measurement of ER Oxidoreductases and Stress Markers.

INS1 cells treated with siRNA duplexes (100 nM) designed for knockdown of the Luciferase mRNA (a negative control, "C1"), GFP mRNA (negative control "C2"), or PDI-KD were lysed at 72 h post siRNA transfection. *Upper eight set of bands*: Western blotting for the antigens indicated, normalized to protein (10 or 20 μg, depending on antigen), with γ-tubulin serving as a loading control. BiP and GRP94 were identified with anti-KDEL antibodies. *Bottom row*: XBP1 mRNA was measured by RT-PCR using primers that amplify both unspliced ("u") and spliced ("s") forms (22). As a positive control for ER stress, cells were treated with thapsigargin (downward arrowhead first lane: 1 μM for 3 h).

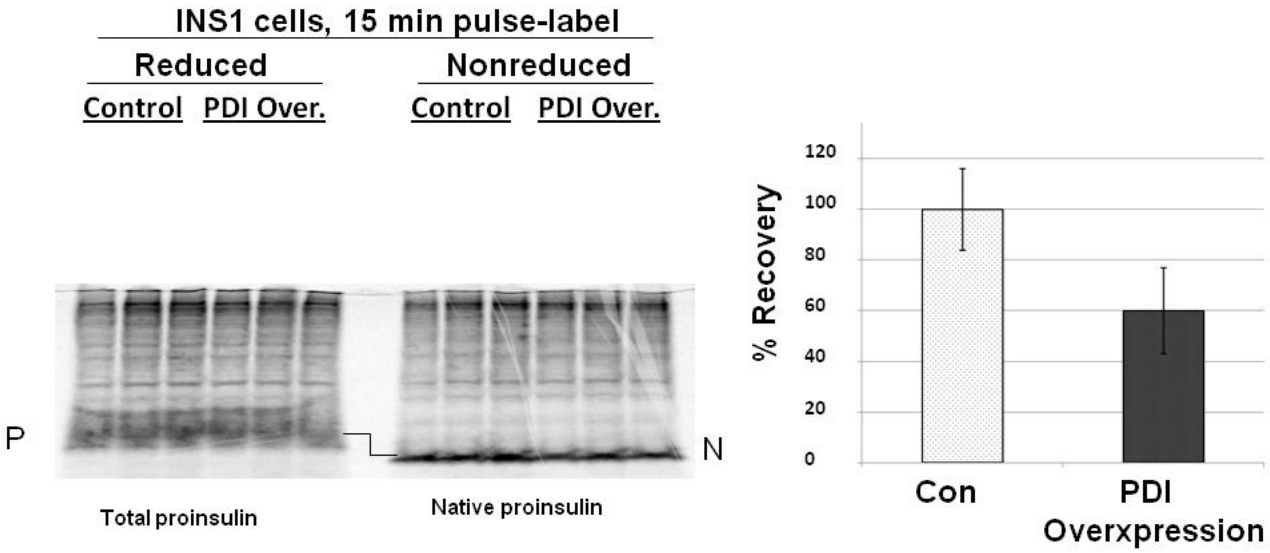

Figure 3-5. Recovery of newly synthesized proinsulin with PDI overexpression.

Left panel: At 48 h post-transfection with PDI plasmid, Ins-1 cells were pulse-labeled for 15 min with ^{35}S-Cys/Met, and lysed in SDS buffer with 10 mM NEM. Lysates were immunoprecipitated in duplicate with anti-insulin and analyzed by Tris tricine-urea-SDS-PAGE under reducing or nonreducing conditions. *Right panel*: Quantitative band densitometry of the native proinsulin disulfide isomer was divided by that for total labeled to calculate the percentage of native form. Data is quantified from panel on the left.

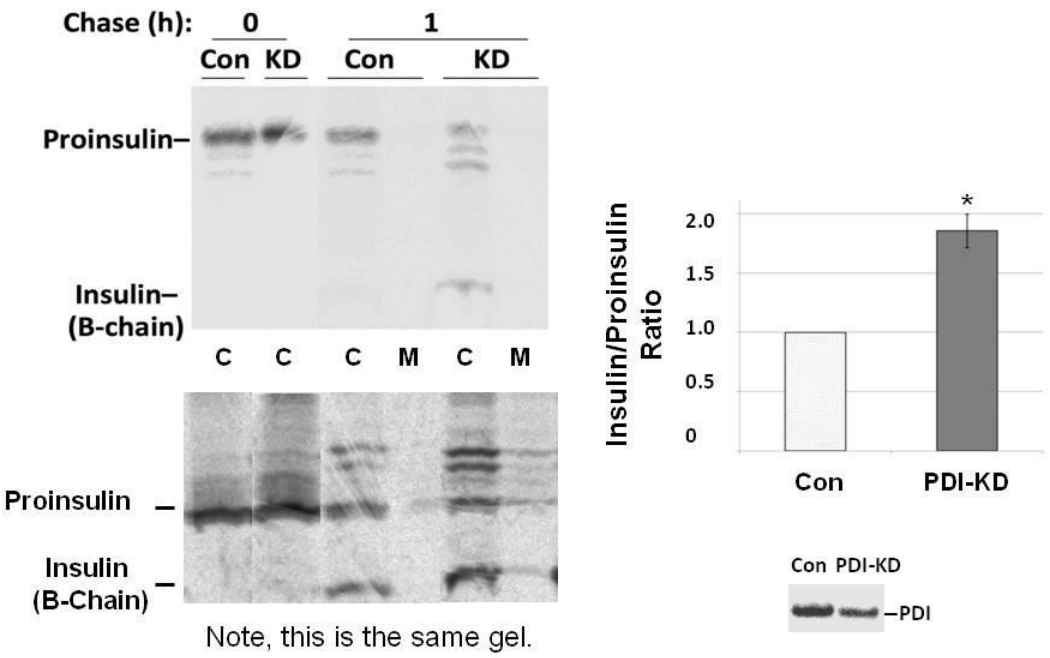

Figure 3-6. ER Exit of proinsulin, PDI-KD (Ins-1 Cells).

At 72 h post transfection with either scrambled (Con) or PDI siRNA ("KD") duplexes (100 nM), INS1 cells were pulse-labeled for 20 min with ^{35}S-Cys/Met and either lysed immediately or chased for 1 h and both media ("M") and cell lysates ("C") collected. Samples were immunoprecipitated with anti-insulin and analyzed by Tris tricine-urea-SDS-PAGE under reducing (100mM DTT) and nonreducing conditions. *Right panel*: Quantitative band densitometry of the labeled insulin at 1 h chase was divided by that for labeled proinsulin; in control cells this ratio was arbitrarily set to 1. The labeled insulin/proinsulin ratio in PDI-KD cells was then compared to that in control cells ($p = 0.001$). N=5 independent experiments.

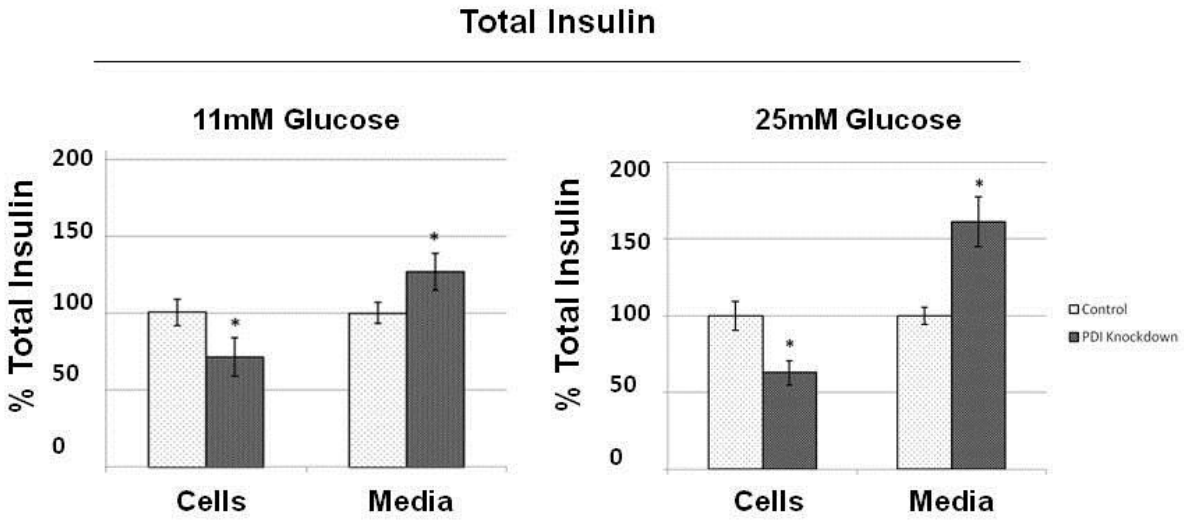

Figure 3-7. Steady-State Measurements of total insulin in Ins-1 cells, PDI-KD.

Left Panel. After 48 h post-transfection with either scrambled (*light bars*) or PDI siRNA duplexes (*dark bars*), the media was changed and fresh media at the indicated glucose concentrations applied, and collected for an additional 24 h. At that time, the cells were lysed and total insulin (i.e., insulin plus proinsulin) in both cell lysates and media was measured by RIA. The data are the mean of two experiments with 5 independent replicates; control values were set to 100%. At 11 mM glucose for cells (control v. PDI-KD) p = 0.001; for media p = 0.01. At 25 mM glucose for cells (control v. PDI-KD) p = 0.001; for media p = 0.002.

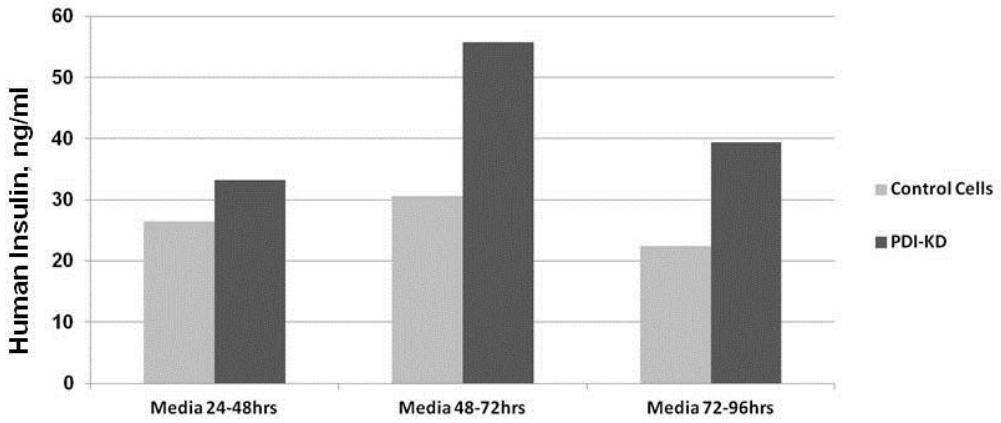

Figure 3-8. Steady-State Measurements of Human Insulin in Ins 832/13 cells.

Ins 832/13 cells were transfected with either scrambled (*light bars*) or PDI siRNA duplexes (*dark bars*). Media was collected for 24 hour period. Each time point represents an individual biological replicate. Processed, human insulin was measured via a human-specific insulin RIA that only recognizes processed human insulin. The experiment is N=1 for each time point. Values are normalized to total protein.

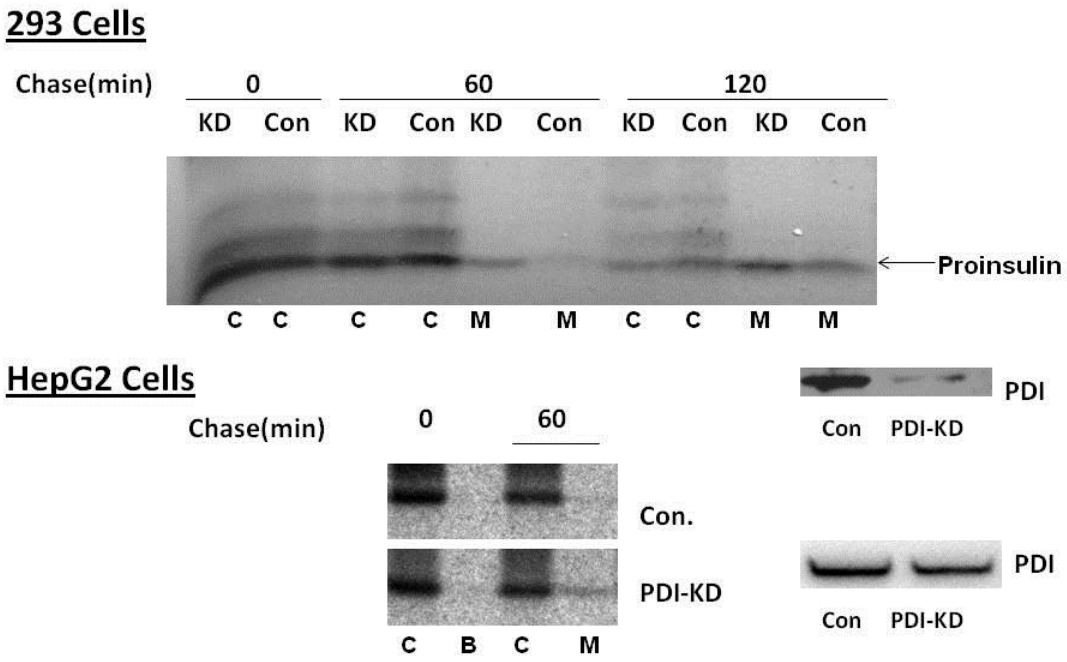

Figure 3-9. PDI-KD effects on enhanced ER export are selective for proinsulin as a substrate

Top panel. At 48 h post-transfection with either scrambled (Con) or PDI siRNA duplexes (100 nM), 293 cells were pulse-labeled for 30 min with ^{35}S-Cys/Met and chased, with media ("M") collected and cells analyzed ("C") Proinsulin ("Proins") was immunoprecipitated with anti-insulin and analyzed by Tris tricine-urea-SDS-PAGE. *Bottom panel*: A similar experiment was performed in HepG2 cells. B=Blank lane.

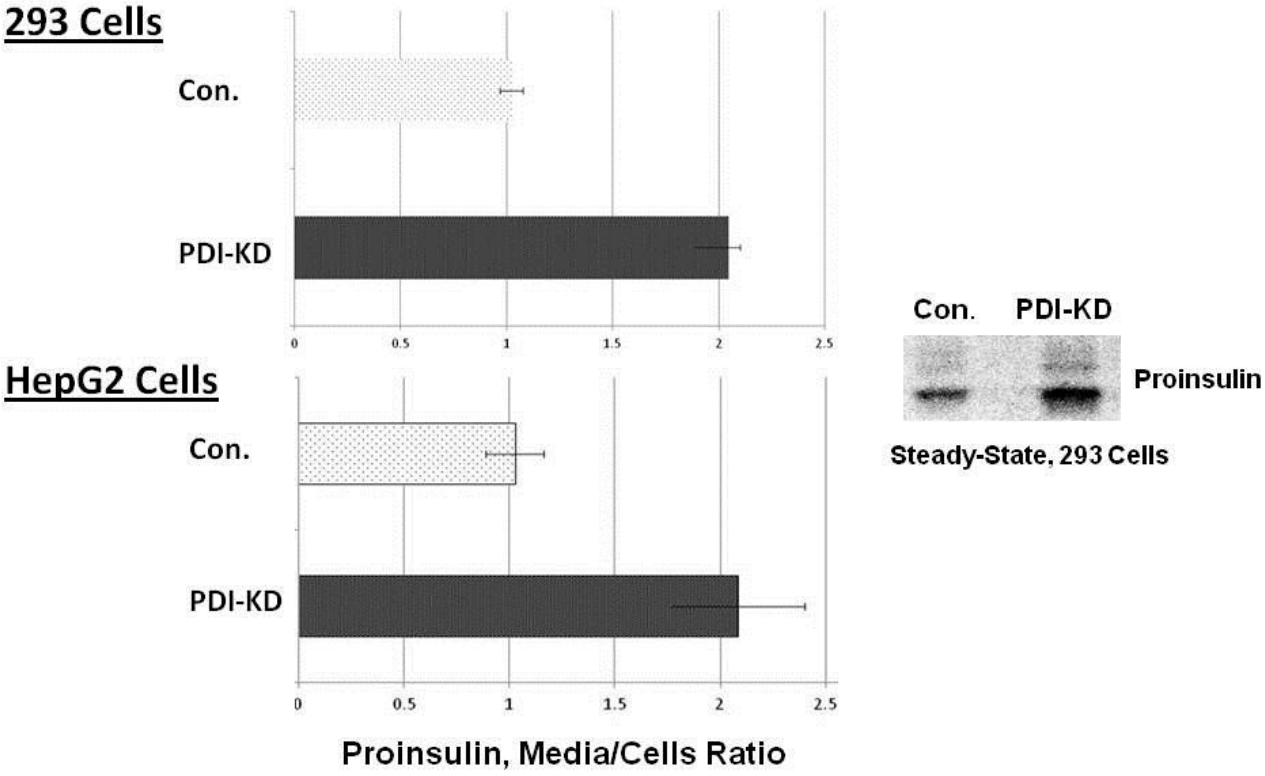

Figure 3-10. Steady-State Levels of Proinsulin, 293 and HepG2 cells.

After 48 h post-transfection with either scrambled (*light bars*) or PDI siRNA duplexes (*dark bars*), the media bathing 293 cells was changed and fresh media collected between 48 - 72 h. At that time the cells were lysed and proinsulin in both cell lysates and media was measured by RIA. For purposes of quantification, the amount of proinsulin recovered in the media was divided by the amount recovered in the cells. The control value was arbitrarily set to one. Control v. PDI-KD cells, p = 0.007. (Four experiments with 9 independent replicates). For HepG2, cells and media was collected 24- 48 post transfection and analyzed as in 293 cells. Control v PDI-KD, p=0.002.

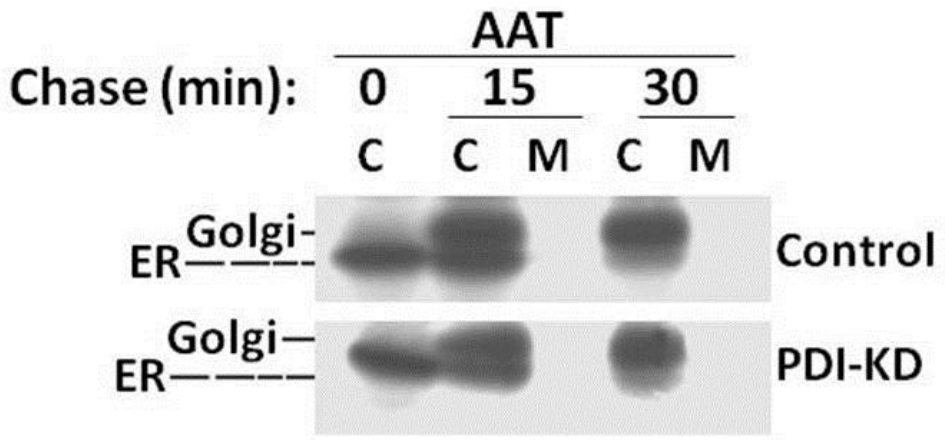

Figure 3-11. ER Exit of AAT, PDI-KD.

INS1 cells were transfected to express α1-antitrypsin (AAT). The cells were then split and treated with either scrambled (Con) or PDI siRNA duplexes (100 nM, PDI knockdown was confirmed by Western blotting, not shown). The cells were pulse-labeled for 20 min with ^{35}S-Cys/Met, chased for the times indicated, and media collected and cells lysed as in Fig. 1C. The samples were immunoprecipitated with anti-AAT and analyzed by SDS-PAGE. ER exit was evaluated by migration from the ER-glycosylated form of AAT to the Golgi-glycosylated form

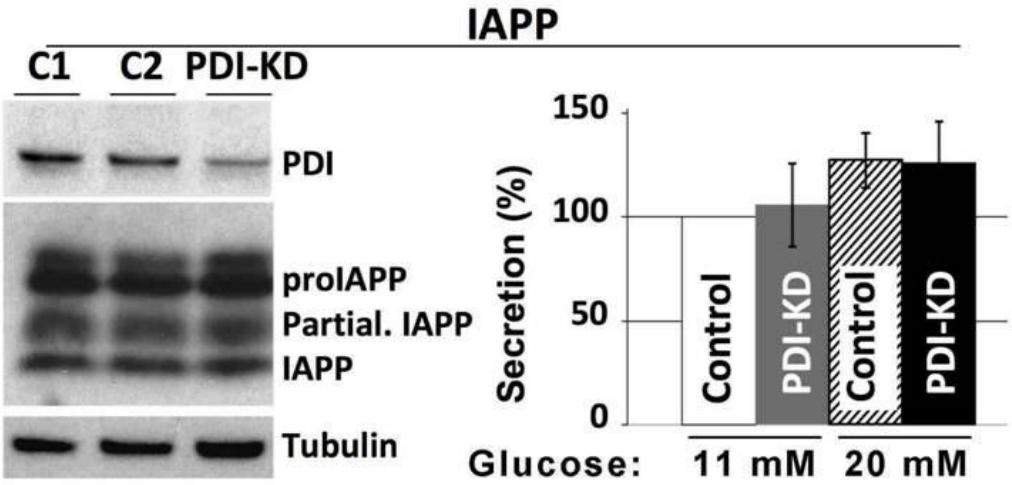

Figure 3-12. IAPP Processing, PDI-KD (Ins-1 Cells).

INS1 cells treated with siRNAs duplexes (100 nM) designed for knockdown of Luciferase mRNA ("C1"), GFP mRNA ("C2"), or PDI-KD exactly as in Fig. 1B, for 72 h. *Left panel*: Western blotting for the antigens indicated, normalized to protein (10 µg), with γ-tubulin serving as a loading control. The result is representative of three independent experiments. *Right panel*: INS1 cells transfected with siRNAs (100 nM) were grown for 3 days in RPMI media at lower (11 mM) or higher (20 mM) glucose. The media were collected, and IAPP secretion was analyzed by ELISA (see *Experimental Procedures*).

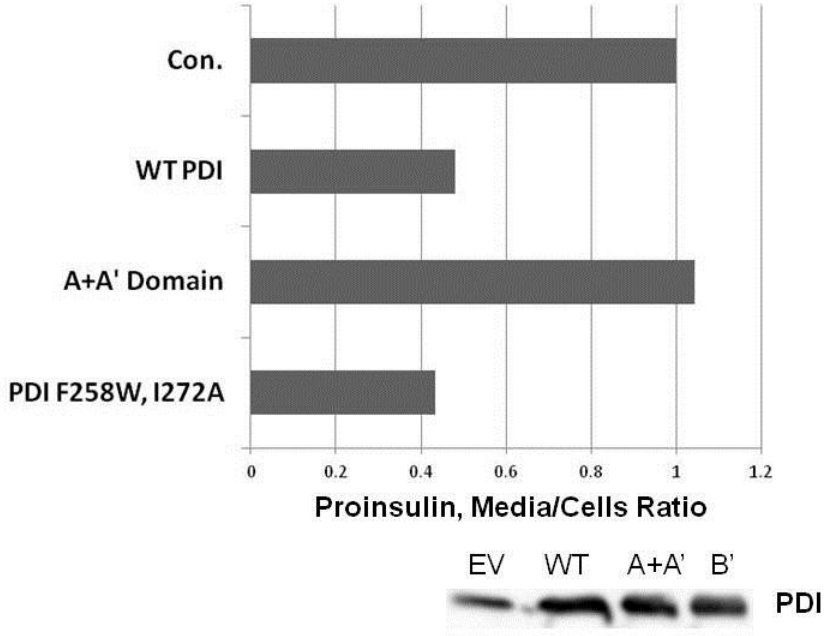

Figure 3-13. Catalytic domain is required for retention of proinsulin when overexpressing PDI.

After 24 h post-transfection with either WT PDI, A + A' , or PDI F258W, I272A (B' mutant) plasmid, the media bathing 293 cells was changed and fresh media collected between 24 - 48 h. At that time the cells were lysed and proinsulin in both cell lysates and media was measured by RIA. For purposes of quantification, the amount of proinsulin recovered in the media was divided by the amount recovered in the cells. The control value was arbitrarily set to one.

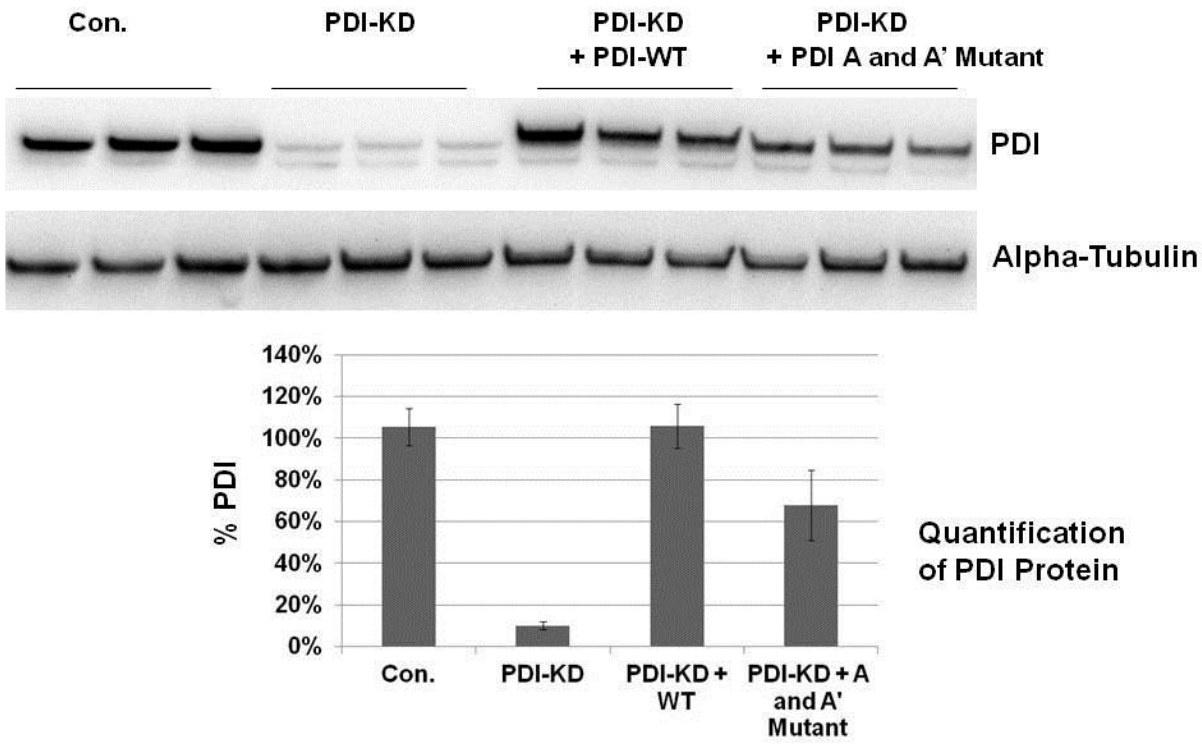

Figure 3-14a. The catalytic domain of PDI is required to restore the retentive function of after knockdown.

PDI Western. 293 cells were transfected with WT Proinsulin, split, and then transfected with PDI or scrambled oligo. Cells were subsequently transfected with a plasmid encoding for WT PDI, PDI A and A' mutant, or in the case of the control GFP.

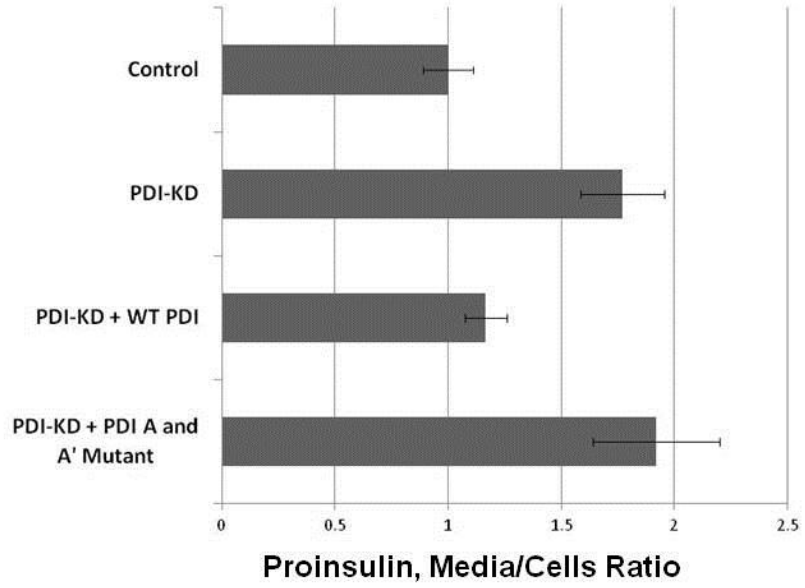

Figure 3-14b. The catalytic domain of PDI is required to restore the retentive function of after knockdown.

Samples were analyzed as previously described. Data is from two independent experiments conducted in triplicate (N=6).

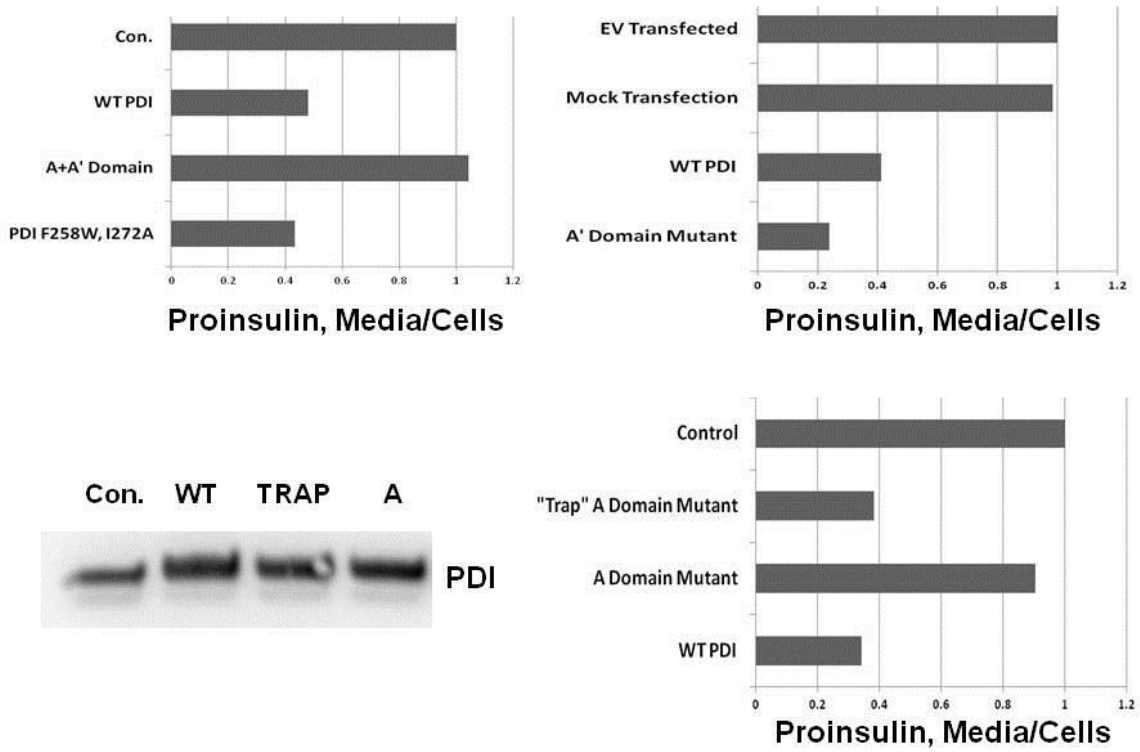

Figure 3-15. The A domain is required for efficient retention of proinsulin by PDI.

Various mutant constructs were transfected into 293 cells and assessed for retention of proinsulin as previously described. Each graph represents one experiment conducted in duplicate.

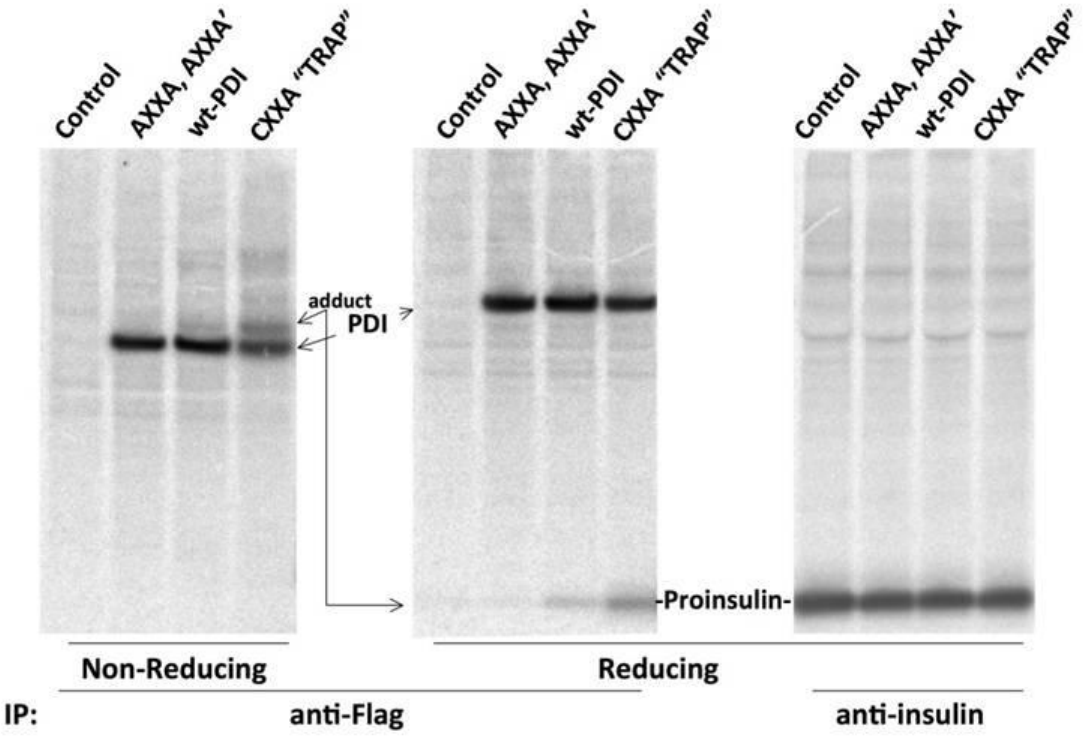

Figure 3-16. PDI directly interacts with proinsulin via its catalytic domain.

Min6 cells were transfected with a plasmid encoding for a WT PDI, A and A' mutant PDI, or a Trap "A (CXXA)" PDI Mutant. Each construct was tagged with a FLAG epitope. GFP was transfected into control cells. At 72 hours post-transfection, cells were labeled with 500 uCi ^{35}S-cysteine/ methionine in a 60 cm dish for 20 minutes. The cells were washed once with ice cold Hanks Buffer solution (with calcium and magnesium chloride) supplemented with 20 mM NEM, lysed, and then split into two samples. One half was immunoprecipitated with anti-insulin antibodies, while the other half was Immunoprecipitated with anti-FLAG antibody overnight. The samples were analyzed under both reducing and non-reducing conditions using 4-12% gradient SDS-PAGE, followed by autoradiography.

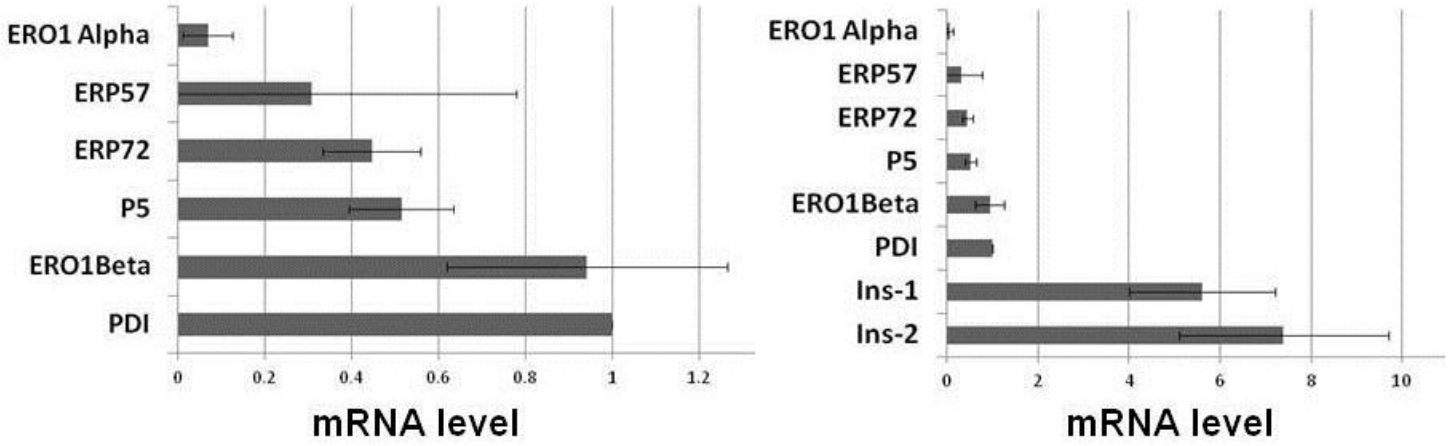

Figure 3-17. Quantification of relative transcription levels of ER Oxidoreductases

Mouse pancreatic islets. The data represent the average of two data sets available from Unigene. (http://www.roche-applied science.com/sis/rtpcr/upl/index.jsp?id=UP030000, libraries 16013 and 5429.) For ER Oxidoreductases not shown, data was unavailable. The value of PDI was arbitrarily set to one.

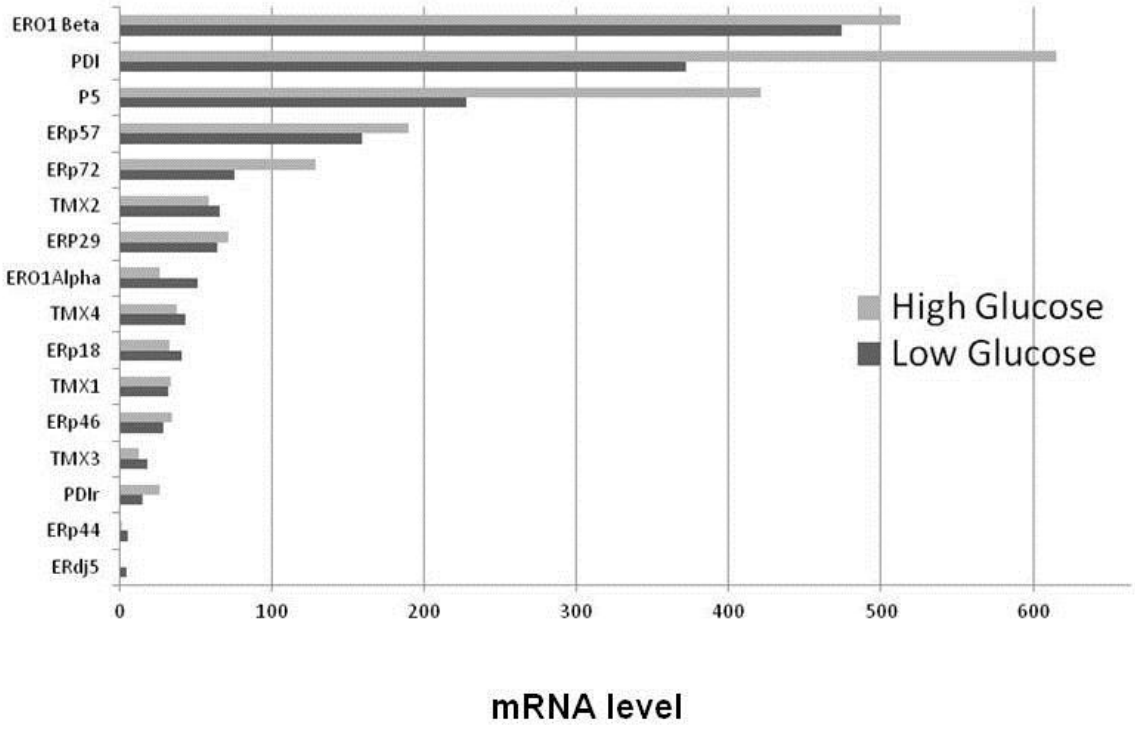

Figure 3-17. Expression levels of ER Oxidoreductases.

Min 6. Reverse transcribed cDNAs were obtained from Min6 cells grown in 11mM or 25mM growth media for 48 hours. qPCR analysis was performed for each ER oxidoreductase. Relative expression levels were obtained using the formula, message Level= 2^CT Value. The expression level of ERdj5, the gene with lowest level of expression, was arbitrarily set to 1. Note data was not assessed for statistical significance.

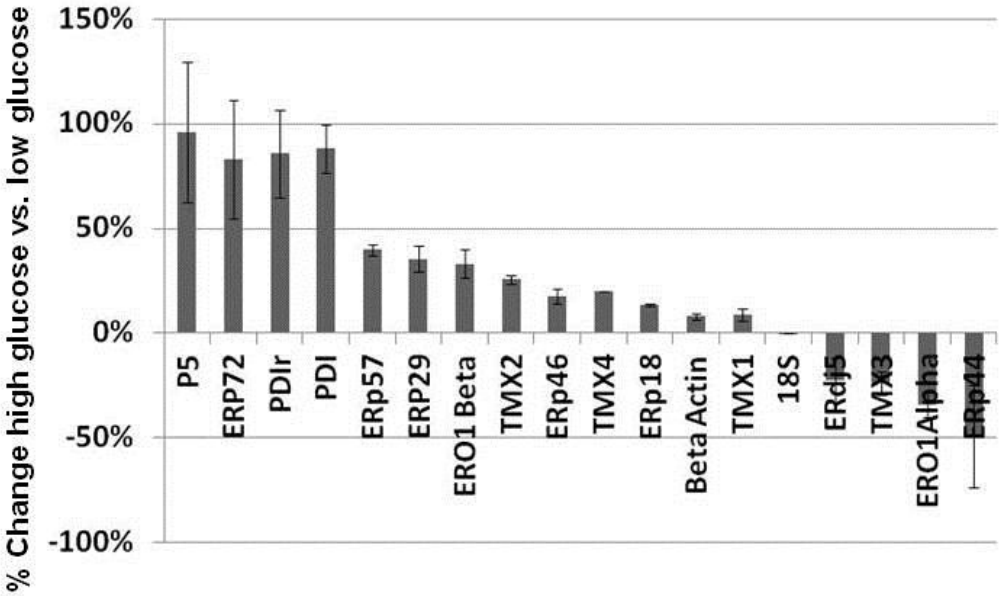

Figure 3-18a. Expression of ER oxidoreductases in response to high glucose.

Min6 cells. Min6 cells were initially grown at 11 mM glucose for 24 hours, then changed to 11 mM glucose or 25 mM glucose for 48 hours. cDNA was then obtained from replicates under each condition. The percentage increase = the relative amount of message in high glucose/low glucose. The data is representative of two experiments, each conducted in duplicate (N=4).

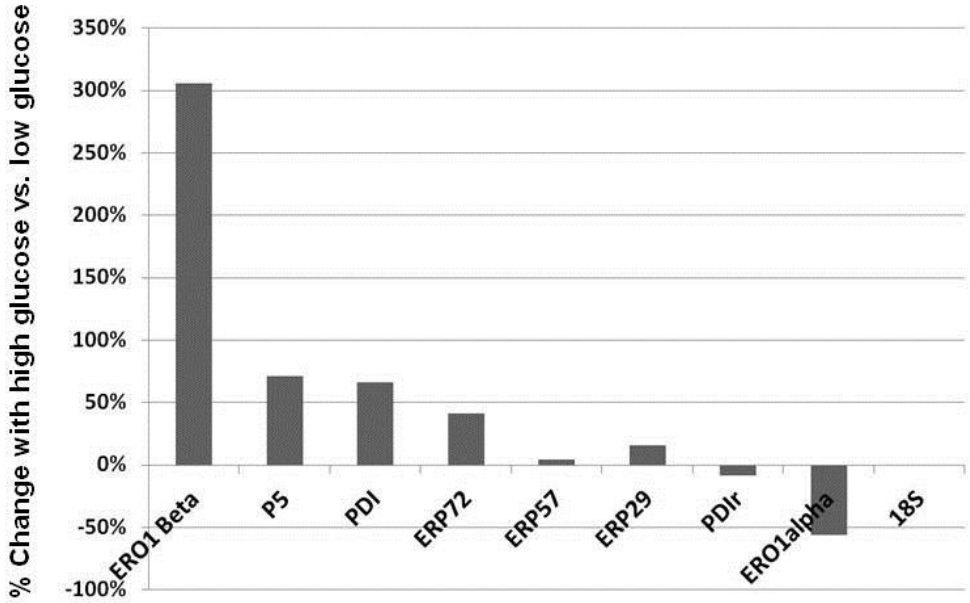

Figure 3-18b. Expression of ER oxidoreductases in response to high glucose.

Pancreatic Islets. Reverse transcribed cDNAs were obtained from freshly isolated pancreatic islets were grown at either 2.8 mM (low) glucose or 11(high) mM glucose for 48 hours. qPCR analysis was performed for each ER oxidoreductase. The data is representative of one experiments. (N=1).

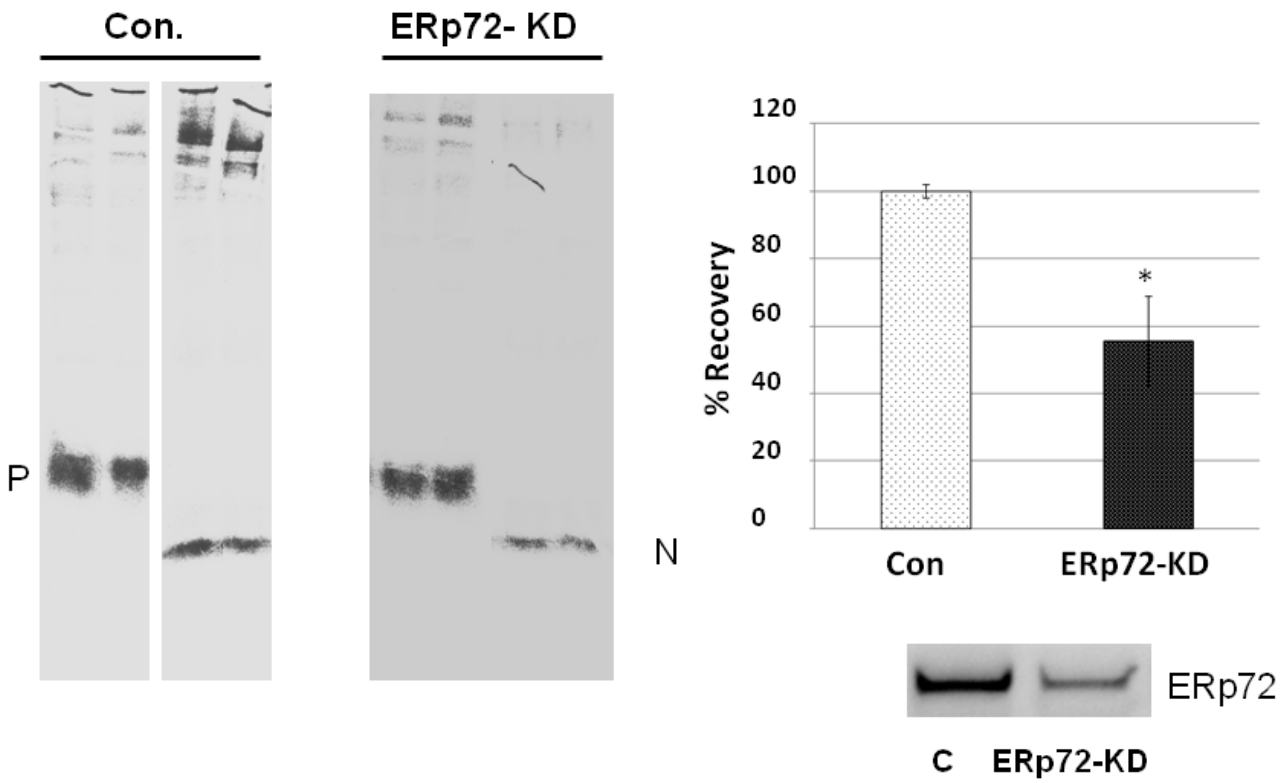

Figure 3-19. Recovery of newly synthesized proinsulin with ERp72 knockdown.

Left panel. At 48 h post-transfection with either scrambled (Con) or ERp72 siRNA duplexes (20 nM), Ins-1 cells were pulse-labeled for 15 min with ^{35}S-Cys/Met, and lysed in SDS buffer with 10 mM NEM. Lysates were immunoprecipitated in duplicate with anti-insulin and analyzed by Tris tricine-urea-SDS-PAGE under reducing or nonreducing ("N") conditions. *Right panel.* : Quantitative band densitometry of the Native proinsulin disulfide isomer (gel at left band "N") was divided by that for total labeled Proinsulin ("P") to calculate the percentage of native form. The data represent three independent experiments (N=6), p=.0048.

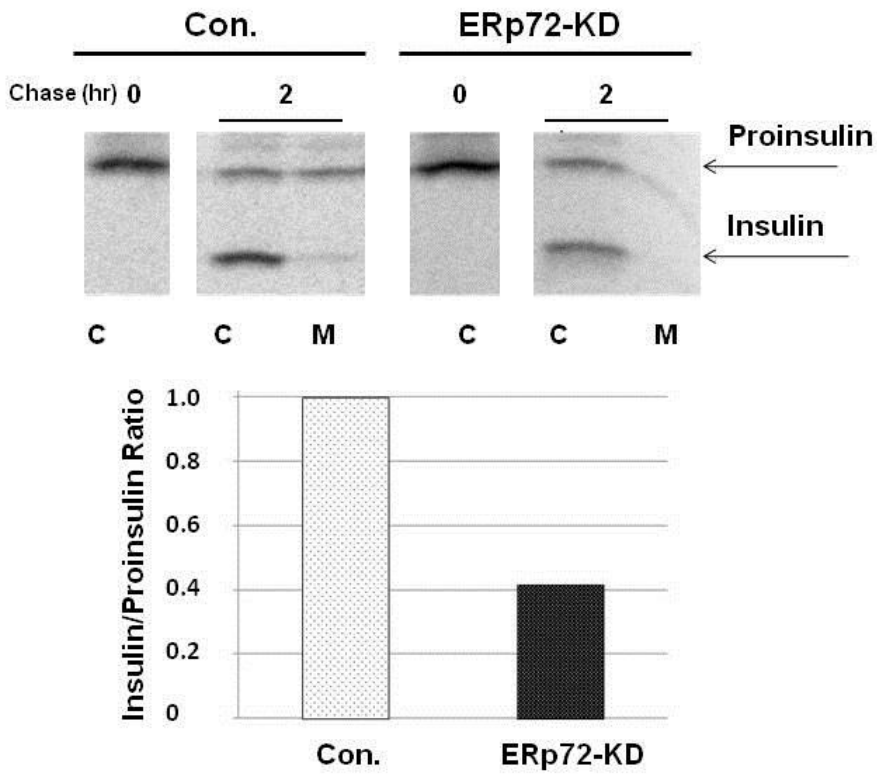

Figure 3-20. ER Exit of newly synthesized proinsulin, ERp72-KD.

At 72 h post transfection with either scrambled (Con) or ERp72 siRNA ("ERp72-KD") duplexes (100 nM), INS1 cells were pulse-labeled for 20 min with ^{35}S-Cys/Met and either lysed immediately or chased for 2 h and both media ("M") and cell lysates ("C") collected. Samples were immunoprecipitated with anti-insulin and analyzed by Tris tricine-urea-SDS-PAGE under nonreducing conditions. *Right panel*: Quantitative band densitometry of the labeled insulin at 2 h chase was divided by that for labeled proinsulin; in control cells this ratio was arbitrarily set to 1. The labeled insulin/proinsulin ratio in ERp72-KD cells was then compared to that in control cells. The calculations are representative of two independent experiments.

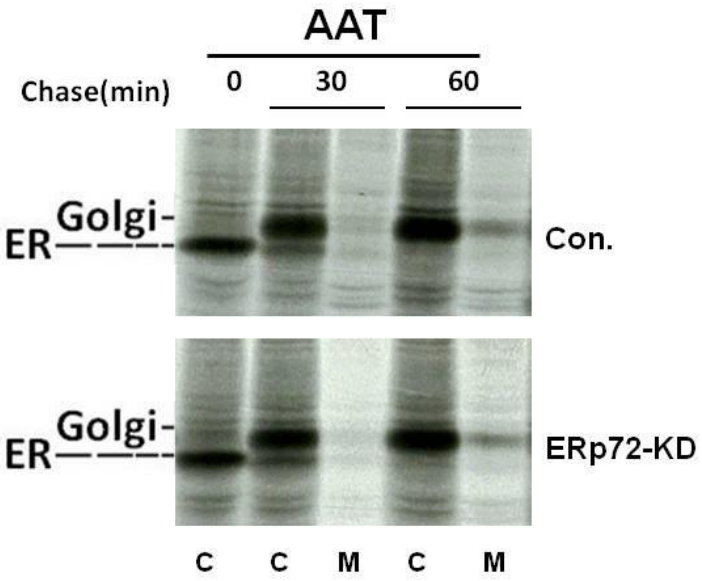

Figure 3-21. ER Exit of AAT, ERp72-KD.

INS1 cells were transfected to express α1-antitrypsin (AAT). The cells were then split and treated with either scrambled (Con) or ERp72 siRNA duplexes (100 nM, ERp72 knockdown was confirmed by Western blotting, not shown). The cells were pulse-labeled for 20 min with ^{35}S-Cys/Met, chased for the times indicated, and media collected and cells lysed as in Fig. 1C. The samples were immunoprecipitated with anti-AAT and analyzed by SDS-PAGE. ER exit was evaluated by migration from the ER-glycosylated form of AAT to the Golgi-glycosylated form.

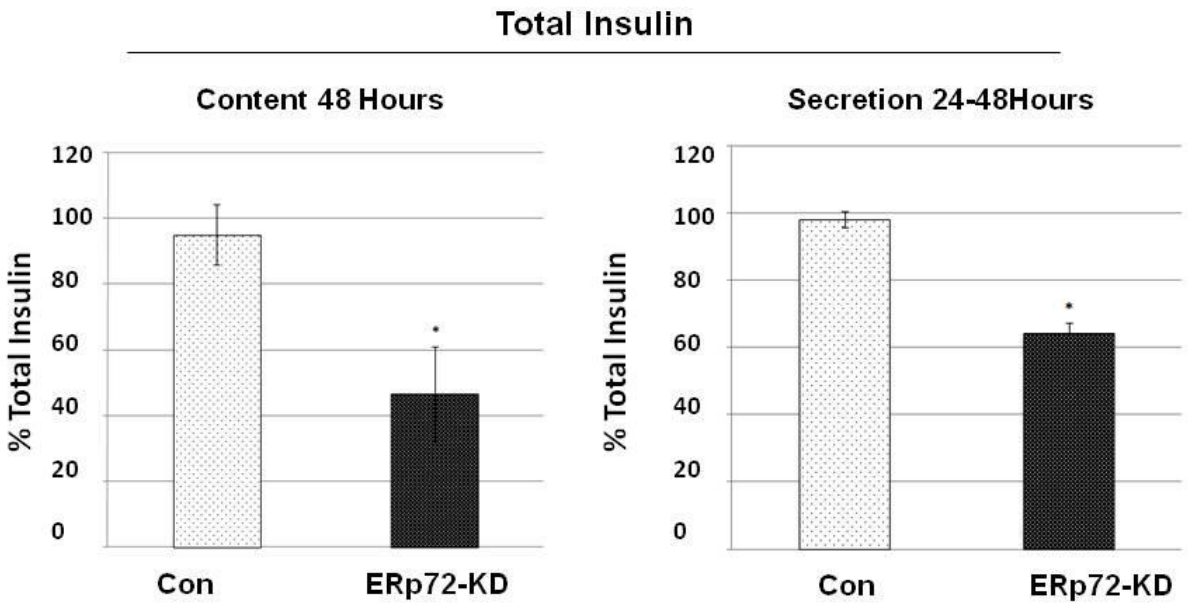

Figure 3-22. Steady-State Measurements of total insulin in Ins-1 cells, ERp72-KD.

After 24 h post-transfection with either scrambled (*light bars*) or ERp72 siRNA duplexes (*dark bars*), the media was changed and fresh media at the indicated glucose concentrations applied, and collected for an additional 24 h. At that time, the cells were lysed and total insulin (i.e., insulin plus proinsulin) in both cell lysates and media was measured by RIA. The data are the mean of three experiments with 9 independent replicates; control values were set to 100%. For cells, p=.0048. Media, p=.0045.

	Gene Name	Protein	Thioredoxin Domains	Catalytic Motif Sequence
1	**P4HB**	**PDI**	**4 (2)**	**CGHC, CGHC**
2	**PDIA3**	**ERp57**	**4 (2)**	**CGHC, CGHC**
3	**PDIA4**	**ERp72**	**5 (3)**	**CGHC, CGHC, CGHC**
4	**PDIA6**	**P5**	**3 (2)**	**CGHC, CGHC**
5	**DNAJC10**	**ERdj5**	**6 (4)**	**CSHC, CPPC, CHPC, CGPC**
6	PDIA2	PDIp	4 (2)	CGHC, CTGC
7	PDIA5	PDIr	4 (3)	CSMC, CGHC, CPHC
8	TXNDC12	ERp18	1 (1)	CGAC
9	ERp27	ERp27	2 (0)	None
10	ERp29	ERp29	2 (0)	None
11	ERp44	ERp44	3 (1)	CRFS
12	ERp90	ERp90	5 (0)	None
13	TXNDC5	ERp46	3 (3)	CGHC, CGHC, CGHC
14	PDILT	PDILT	4 (2)	SKQS*, SKKC
15	Agr-2	Agr-2	1 (1)	CPHS
16	Agr-3	Agr-3	1 (1)	CQYS
17	TMX1	TMX1	1 (1)	CPAC
18	TMX2	TMX2	1 (1)	SDNC
19	TMX3	TMX3	3 (1)	CGHC
20	TMX4	TMX4	1 (1)	CPSC
21	TMX5	TMX5	1 (1)	CRFS

Table 3-2. Mammalian PDI-like family members.

Gene names (first column) as well as protein alias (second column) are shown. The total number of thioredoxin domains in each gene product is indicated, with the number of catalytically-active domains listed in parentheses. The specific CXXC sequences are listed in the last column; note that for PDILT (line 14) the SKQS motif bears strong resemblance to the A domain of PDI and is listed under the catalytic motif sequence, although it does exhibit catalytic activity. Family members highlighted with gray background signify transmembrane proteins, and the first five members in large font denote those whose functions are specifically mentioned within the text.

Gene	Mouse Islets	Human Islets
P4HB	Yes	No
PDIA3	Yes	No
PDIA4	**Yes**	**Yes**
PDIA5	Yes	No
PDIA6	Yes	No
TMX1	Yes	No
TMX2	Yes	No
TMX3	Yes	No
TMX4	Yes	No
TMX5	No	No
Erp29	Yes	No
Erp46	No	No
Erp44	Yes	No
Erp18	No	No
DNAJC10	Yes	No

ERp72 (PDIA4) Peak Occupancy, Human Islets: 60 FOLD

Only Oxidoreductase with PDX-1 Occupancy in both Mouse and Human Islets

Only Oxidoreductase with PDX-1 Occupancy in Human Islets

PDX-1 Upregulates ERp72. (Sachdeva, Stoffers et. Al. PNAS. 2009 Nov 10;106(45):19090-5).

Note: AGR2, AGR3, ERP27, PDILT, and PDIA2 are not expressed in Mouse Beta Cells

Table 3-3. PDX-1 occupancy in Mouse and Human Islets..

CHIPseq data of ER Oxidoreductase occupancy using PDX-1 as input. (Data provided by Dr. Cythnia Khoo).

CHAPTER 4 CONCLUSIONS

Arguably, insulin may be the most important hormone regulator of metabolism. The gene family is ancient, and even in modern, highly-evolved organisms, the continuous production (and secretion) of insulin, every minute of every day, is central to metabolic homeostasis, including actions in the brain, in classical insulin-sensitive peripheral tissues, and in the pancreatic islets themselves [88]. There are few if any cell types in the body that express *no* insulin receptors. Insulin action at a physiological level has major effects not only on blood glucose, but also on redistribution of amino acids, and generalized anabolism.

Insulin is the first protein to be sequenced, and its X-ray crystal structure has been studied again and again. The molecule serves as one of the prototypes in studies of protein structure and function, it is a major pharmacological target, and virtually every residue of the polypeptide has been individually mutagenized in different labs around the world. The amount of attention surrounding insulin comes as no surprise, as its loss leads to devastating metabolic consequences, whether it occurs on the first postnatal day or after 50 years of life. So much is known about insulin, yet there are many questions that remain unanswered in how and why insulin is manufactured in pancreatic beta cells.

Insulin is made as processing intermediates that are consecutively cleaved . First the signal peptide is removed as soon as the preproinsulin is translocated into the ER. Then comes the excision of the C-peptide, endoproteolytically removed from the middle of the proinsulin molecule as the protein exits the Golgi complex and completes its maturation in immature secretory granules. In between these two steps, proinsulin matures into its native conformation. The nascent proinsulin, to become active insulin, needs not only to make three disulfide bonds, but they specifically must be C(B7)-C(A7), C(B19)-C(A20), and C(A6)-C(A11). The overall theme of my thesis project touches on two of these aspects of the insulin manufacturing process – the making of the proinsulin disulfide bonds, and the endoproteolytic cleavage of proinsulin into insulin.

In Chapter 2 of my dissertation, I investigated the requirement of endoproteolytic cleavage for proinsulin of the C-peptide. Proinsulin is purported to display only 2% binding to the insulin receptors as processed insulin [149]. While it is unclear what led the evolution (pro)insulin into a pathway requiring cleavage-dependent activation, I wondered if it were possible to generate a “proinsulin” that might specifically and selectively activate insulin receptors (and not growth factor receptors).The idea of a single chain insulin (like) molecule has already been conjured up by evolution. IGF-1 and IGF-2 are structurally similar to insulin, being secreted from cells and acting on cell surface receptors – and even activating a number of common downstream signaling pathways [90]. Yet IGF-1 and IGF-2,

and many other members of the larger insulin/IGF superfamily – do not undergo endoproteolytic cleavage for purposes of making a bioactive peptide.

My studies in Chapter 2 were influenced by a paper reporting a Single Chain Insulin (SCI) used in gene therapy that was shown to reverse diabetes in rodent models [84]. I wanted to see if I could learn any of the primary structural principles that would lead to a bioactive SCI, and with this in mind, through rational mutagenesis, I created a range of constructs to be tested, in order to understand the rules and guidelines that would allow a SCI to exhibit biological activity. I specifically focused on modifying the C-peptide length and amino acid content without at all altering the primary structure of the insulin B-chain or A-chain. As for specific residues to modify, I focused most of my attention on the two flanking residues on the N- and C-terminal ends of the C-peptide, which normally represent the dibasic cleavage sites of proinsulin.

In regards to the size of the linker, the progressive loss of biological activity of SCIs as their linker sequences grew to ever greater length (>15) most likely reflects an inability of the insulin moiety to make proper contact with insulin receptors, resulting in limited activation. These findings readily explain the low bioactivity of proinsulin itself [59], as the intervening C-peptide sequence sterically interferes with ligand binding. At the other end of the spectrum, I found that a linker length of five amino acid residues was an absolute minimum in order to exhibit biological activity. Although consistent with published results that

demonstrate that a linker length below 5 residues alters the alignment of the B- and A- chains of the polypeptide in such a way that the proper disulfide bonding no longer occurs [99], it also raises some important questions. Does a small linker length limit the ability of the SCI to activate the receptor, or is it the case that the limiting factor is the formation of the proper disulfide bonds during peptide biosynthesis?

Perhaps both these mechanisms factor into the inability of pro(insulin) and the SCIs from activating the insulin receptor. It has been reported that a direct tethering of the B- and A-chains, even with proper disulfide bonds, does not yield a biologically active construct [30]. The presence of a tight turn with a short linker between B- and A-chains is likely to seriously restrict the movement of the distal B-chain to “side-step” [11] so that the N-terminal portion of the A-chain can make proper receptor contact [12].

In addition to these findings, the amino acids immediately adjacent to the B- and A-chain termini appeared to have great impact on the biological activity of SCIs, particularly the C-terminal end of the linker, adjacent to the A-Chain. In all constructs, the presence of a basic residue directly preceding the A-Chain was required for biological activity. My data suggested that a single arginyl side chain proximal to the A-chain may be an important feature for SCI interaction with insulin receptors. Note that the endoproteolytic processing of proinsulin creates a free amino-terminal Gly(A1). This free amino group appears to be required for

receptor activation, and in my SCIs, a preceding Arg residue with a charged amine side chain is likely to mimic this free amino group that presents itself after proinsulin cleavage. Substitutions at this position with a Lys residue would be a useful next step, but in each of my constructs, I worked with Arg because it is the evolutionarily conserved residue at this position in proinsulin.

An additional basic amino acid next the arginyl group adjacent to the A-Chain was used by others working on SCIs. However, dibasic residues raised the possibility of potential cleavage which would eliminate the single-chain structure. In fact, my experiments conducted in AtT20/PC2 cells that expressed the secretory granule endopeptidases (Chapter 2, Figure 2) showed that such dibasic residues are in fact cleavable by naturally-occurring endopeptidases of the secretory pathway. For this reason, I worked to create alternative SCIs that have no potential to be cleaved. The –QRGGGGQR- linker peptide between the B- and A-chains generated a SCI that exhibits comparable bioactivity to the best available, as well as moderately high expression levels (Chapter 2, Table 2). I believe that this construct could have great future utility if gene therapy for diabetes (type 1 or 2) continues to advance.

In the course of my studies, I found that the amino acids in the middle of the linker peptide somehow affects protein expression level. For example, the linker peptides –RRYGLDVKR- and –RRGGGGGKR- (Lines 19, 20 in Chapter 2, Table

1, respectively) result in comparable biological activity on insulin receptors, but very different protein expression levels upon biosynthesis (approximately 5-7 fold difference in favor of the –RRGGGGGKR- linker). Thus, although the specific amino acid content in middle of the linker appear to be less restrictive in comparison to the flanking residues from the vantage point of bioactivity (with the only requirement perhaps being a flexible chain to allow the connecting structure to make a turn), the impact of these amino acids on expression or stability of SCIs warrants further study.

Finally, in addition to gene therapy, SCIs might have utility as analogs. Although not studied, these SCIs might have differences in stability, solubility, and clearance from the bloodstream, which is the pharmacological basis for which analogs already on the market have been selected as treatments for diabetes. From a manufacturing perspective, SCIs also may also be easier to produce recombinantly than two-chain insulins (see Chapter 1).

In Chapter 3 of my dissertation, I turned my attention to the formation of the three disulfide bonds of proinsulin. Each of these three disulfides is absolutely required for the biological activity of insulin — just as is the case for the insulin-like growth factors. For the IGFs, it is famously known that they form two distinct stable disulfide-bonded structures — only one of which is bioactive [57]. Since both these structures can be found secreted from cells, evidently the ER quality control mechanisms do not sensitively recognize the native state from a

conformation that engages all Cys residues in disulfide bonding, but nevertheless exhibits mis-pairing. In my Introduction to Chapter 3, I highlighted that the pathways of disulfide bonding in the ER still remain an area of extensive ongoing investigation. A secretory protein may make its way to the native state via distinct disulfide intermediates, in which the individual native disulfide bonds may form in different sequential order. It would therefore seem that proinsulin and IGFs would be likely substrates both for the actions of ER oxidoreductases acting as 'oxidases', promoting disulfide bond formation, and as 'reductases and isomerases', requiring the breakage of at least one disulfide bond after it has been made.

In Chapter 3, I focused my own experiments primarily on two of the most abundant ER oxidoreductases of pancreatic beta cells, PDI and ERp72. With regards to PDI, I found that this protein does interact with proinsulin in a manner that requires a catalytically active thioredoxin motif in the PDI A-domain. Curiously, however, my results unequivocally do not support PDI as a facilitator of proinsulin disulfide bond formation. My hypothesis is that PDI acts as net reductase for proinsulin, and this clearly warrants further investigation. As mentioned in the Introduction to Chapter 3, proinsulin is believed to have an exposed surface disulfide bond in C(B7)-C(A7). Thus, even after its formation, this disulfide bond may remain susceptible to attack. Using a PDI-TRAP mutant, I was able to recover a mixed disulfide adduct with the endogenous proinsulin of pancreatic beta cells. Moreover, even upon overexpressing WT-PDI, I was still

able to detect this adduct, although it was less abundant than with the TRAP mutant. This may signify that the mixed disulfide with PDI is rapidly resolved, such that steady-state levels of adduct are ordinarily very low. Conceivably, reduced PDI might attack the surface-accessible C(B7)-C(A7) disulfide bond, thereby unfolding proinsulin reduced at the B7/A7 positions. In truth, however, at the present state of knowledge we do not yet know where (or when) on proinsulin might PDI make its covalent linkage to create a mixed disulfide bond. In any case, I have found that there is a relationship between the catalytic activity of PDI and its phenotypic effects to limit the rate of proinsulin egress from the ER. Importantly, PDI overexpression results in similar phenotype to that observed upon ERO1-Beta knockdown, with both decreased proinsulin export and decreased insulin production. This diminution of proinsulin export is linked to the catalytic activity of PDI- especially that contained in the A-domain thioredoxin motif, which appears to be involved in reductase activities of PDI [79].

Preliminary results seem to rule out the intramolecular C(A6)-C(A11) disulfide bond as a potential site for PDI interaction. First, this bond is buried deeply within the globular proinsulin protein [64]. Second, the A6/A11 double mutant proinsulin has the distinction of escaping the ER with normal kinetics [96]. Third, the A6/A11cysteine double mutant proinsulin can also form a structure with the same mobility as native proinsulin by nonreducing Tris-tricine-urea-SDS-PAGE, strongly suggesting that the B19-A20 and B7-A7 disulfide bonds are intact [98]. Fourth, transfecting this A6/A11 double cysteine mutant proinsulin construct into

293 cells and subsequently knocking down PDI results in increased proinsulin secretion (Fig. 4-1). Thus, I believe that ER retention caused by PDI must operate either through the C(B7)-C(A7) or C(B19)-C(A20) disulfide bond — realizing that the former bond is surface exposed and the latter is buried.

Finally, my experiments have yielded results consistent with ERp72 as an oxidoreductase that could be involved in the formation of proinsulin's three disulfide bonds. To determine a direct interaction of proinsulin and ERp72 would further provide evidence to support this finding, and these experiments are currently ongoing. A "direct interaction" of proinsulin and ERp72 has been reported in pancreatic beta cells but to this point, no actual data have been published other than immunofluorescence co-localization [37]. I plan to employ a similar "trap" mutant of ERp72 similar to that used to study PDI interaction with proinsulin. ERp72 has three CHGC thioredoxin domains, and I have "Trap" mutants for all three domains. However there are caveats that are associated with this experiment. By mutating the C-terminal residue of each CXXC motif — based on my understanding of how these motifs operate — this essentially creates a reduced thioredoxin motif. This reduced domain would then attack a disulfide bond in a substrate, mimicking an initial reductase/isomerase step. Although perfect for an oxidoreductase that acts reductase/unfoldase for proinsulin, i.e. PDI, I am unclear whether such an experiment is a suitable mimic for an oxidoreductase that catalytically transfers one or more disulfide bonds to proinsulin. Thus, on the one hand, I have reservations that the experiment may

not be able to isolate ERp72/proinsulin adducts, while on the other am concerned with the interpretation of results even if such adducts are obtained.

My studies do not rule out the possibility that other ER oxidoreductases may participate in the process of proinsulin disulfide bond formation. I have performed a screen of various ER oxidoreductases by siRNA-mediated knockdown; and I find that knockdown of several other gene products can produce phenotypes with similar directionality to those of ERp72-KD or PDI-KD (although at lesser magnitude). Published results in HepG2 cells have already suggested compensation by other ER oxidoreductases when one ER oxidoreductase is knocked down [133]. A degree of functional redundancy of oxidoreductases would thus not be surprising in pancreatic beta cells. Another future question is whether proinsulin disulfide bond formation might occur without ER oxidoreductase-mediated disulfide transfer, i.e., via QSOX, which as pointed out in Chapter 3 can catalyze disulfide bond formation in substrate proteins without going through an ER oxidoreductase intermediate [75].

In summary of Chapter 3, my results suggest that ERp72, rather than PDI, participates in proinsulin disulfide bond formation in pancreatic beta cells. The role of PDI, which I hypothesize is linked to proinsulin unfolding, could be extremely important in the proteasomal degradation of misfolded forms of proinsulin. These findings seem in opposition to some of the work published on PDI-proinsulin interactions in-vitro. However, I believe that the in-vitro conditions

show what is *possible* and may not necessarily recapitulate the biology in the context of the ER of living cells. Indeed, by analogy to what has been described previously for the retrotranslocation of cholera toxin from the ER, where PDI and ERp72 play opposing roles (PDI favors retrotranslocation; ERp72 limits retrotranslocation) [38], the opposing roles of these two major ER oxidoreductases could represent a balance that regulates proinsulin anterograde trafficking.

In conclusion, my overall dissertation research has concentrated on two stages of proinsulin maturation in the secretory pathway. In Chapter 2, I have contributed to a growing understanding that proinsulin endoproteolytic cleavage is likely to be a late evolutionary modification, converting a single-chain ancestral hormone into a cleaved, two-chain ligand. Presumably, insulin and insulin receptors evolved in parallel in the development of signaling more specific to metabolic control. I have found however that it is still possible to activate modern day insulin receptors with single-chain insulin ligands to bring about favorable metabolic effects such as glucose uptake into fat cells and suppression of hepatocyte gluconeogenic enzymes. In Chapter 3, I have contributed to a growing understanding that the making of the three evolutionarily conserved proinsulin disulfide bonds does not occur “merely by accident”. The notion of spontaneous disulfide bond formation is too simplistic for a compartment as complex as the lumen of the endoplasmic reticulum. I have found that, in pancreatic beta cells, specialized ER oxidoreductases both promote, and retard,

proinsulin disulfide bond formation and its subsequent trafficking through the secretory pathway for insulin production.

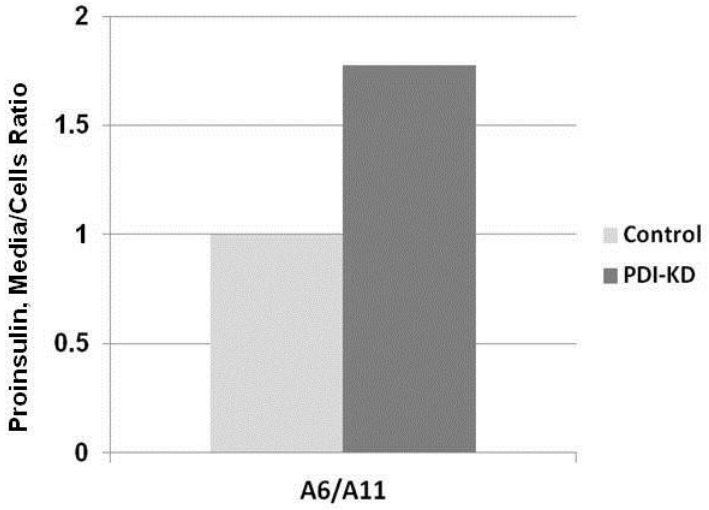

Figure 4-1. PDI-KD increases secretion of mutant A6/A11 proinsulin.

Mutant A6/A11 was transfected into 293 cells, and then transfected with scrambled or PDI siRNA duplexes. After 48 h post-transfection with either scrambled (*light bars*) or PDI siRNA duplexes (*dark bars*), the media bathing 293 cells was changed and fresh media collected between 48 - 72 h. At that time the cells were lysed and proinsulin in both cell lysates and media was measured by RIA. For purposes of quantification, the amount of proinsulin recovered in the media was divided by the amount recovered in the cells. The control value was arbitrarily set to one. (See Chapter 3 Methods for more detail).

REFERENCES

[1] http://annualreport2008.novonordisk.com/how-we-perform/responsible-business-practices/bioethics/gene-technology.asp
[2] http://pi.lilly.com/us/humulin-r-ppi.pdf
[3] Effect of rosiglitazone on the frequency of diabetes in patients with impaired glucose tolerance or impaired fasting glucose: a randomised controlled trial. The Lancet. 2006;368:1096-105.
[4] Alleva DG, Crowe PD, Jin L, Kwok WW, Ling N, Gottschalk M, et al. A disease-associated cellular immune response in type 1 diabetics to an immunodominant epitope of insulin. Journal of Clinical Investigation. 2001;107:173-80.
[5] Appenzeller-Herzog C. Glutathione- and non-glutathione-based oxidant control in the endoplasmic reticulum. Journal of cell science. 2011;124:847-55.
[6] Appenzeller-Herzog C, Riemer J, Zito E, Chin KT, Ron D, Spiess M, et al. Disulphide production by Ero1alpha-PDI relay is rapid and effectively regulated. The EMBO journal. 2010;29:3318-29.
[7] Araki K, Nagata K. Functional in Vitro Analysis of the ERO1 Protein and Protein-disulfide Isomerase Pathway. Journal of Biological Chemistry. 2011;286:32705-12.
[8] Arcelloni C, Falqui L, Martinenghi S, Stabilini A, Pontiroli AE, Paroni R. Processing and release of human proinsulin-cleavage products into culture media by different engineered non-endocrine cells: a specific assessment by capillary electrophoresis. Journal of Endocrinology. 2000;166:437-45.
[9] Arolas JL, Aviles FX, Chang J-Y, Ventura S. Folding of small disulfide-rich proteins: clarifying the puzzle. Trends in biochemical sciences. 2006;31:292-301.
[10] Arvan P. Secretory protein trafficking: genetic and biochemical analysis. Cell biochemistry and biophysics. 2004;40:169-78.
[11] Back SH, Scheuner D, Han J, Song B, Ribick M, Wang J, et al. Translation attenuation through eIF2alpha phosphorylation prevents oxidative stress and maintains the differentiated state in beta cells. Cell Metab. 2009;10:13-26.
[12] Bardwell JCA, McGovern K, Beckwith J. Identification of a protein required for disulfide bond formation in vivo. Cell. 1991;67:581-9.
[13] Bertoli G, Simmen T, Anelli T, Molteni SN, Fesce R, Sitia R. Two conserved cysteine triads in human Ero1alpha cooperate for efficient disulfide bond formation in the endoplasmic reticulum. The Journal of biological chemistry. 2004;279:30047-52.
[14] Bonora E, Zavaroni I, Coscelli C, Butturini U. Decreased hepatic insulin extraction in subjects with mild glucose intolerance. Metabolism: clinical and experimental. 1983;32:438-46.

[15] Bot A, Smith D, Bot S, Hughes A, Wolfe T, Wang L, et al. Plasmid vaccination with insulin B chain prevents autoimmune diabetes in nonobese diabetic mice. Journal of Immunology. 2001;167:2950-5.
[16] Brady MJ, Kartha PM, Aysola AA, Saltiel AR. The role of glucose metabolites in the activation and translocation of glycogen synthase by insulin in 3T3-L1 adipocytes. Journal of Biological Chemistry. 1999;274:27497-504.
[17] Bulleid NJ, Ellgaard L. Multiple ways to make disulfides. Trends in biochemical sciences. 2011.
[18] Butler AE, Janson J, Bonner-Weir S, Ritzel R, Rizza RA, Butler PC. β-Cell Deficit and Increased β-Cell Apoptosis in Humans With Type 2 Diabetes. Diabetes. 2003;52:102-10.
[19] Cara JF, Mirmira RG, Nakagawa SH, Tager HS. An insulin-like growth factor I/insulin hybrid exhibiting high potency for interaction with the type I insulin-like growth factor and insulin receptors of placental plasma membranes. Journal of Biological Chemistry. 1990;265:17820-5.
[20] Chakravarthi S, Jessop CE, Willer M, Stirling CJ, Bulleid NJ. Intracellular catalysis of disulfide bond formation by the human sulfhydryl oxidase, QSOX1. The Biochemical journal. 2007;404:403-11.
[21] Chakravarthi S, Jessop CE, Willer M, Stirling CJ, Bulleid NJ. Intracellular catalysis of disulfide bond formation by the human sulfhydryl oxidase, QSOX1. The Biochemical journal. 2007;404:403-11.
[22] Chang SG, Kim DY, Choi KD, Shin JM, Shin HC. Human insulin production from a novel mini-proinsulin which has high receptor-binding activity. Biochemical Journal. 1998;329:631-5.
[23] Chang Y, Yap S, Ge X, Piganelli J, Bertera S, Giannokakis N, et al. DNA vaccination with an insulin construct and a chimeric protein binding to both CTLA4 and CD40 ameliorates type 1 diabetes in NOD mice. Gene therapy. 2005;12:1679-85.
[24] Cnop M, Welsh N, Jonas J-C, Jörns A, Lenzen S, Eizirik DL. Mechanisms of Pancreatic β-Cell Death in Type 1 and Type 2 Diabetes. Diabetes. 2005;54:S97-S107.
[25] Creemers JW, Jackson RS, Hutton JC. Molecular and cellular regulation of prohormone processing. Seminars in Cell and Developmental Biology. 1998;9:3-10.
[26] Creighton TE, Darby NJ, Kemmink J. The roles of partly folded intermediates in protein folding. Faseb J. 1996;10:110-8.
[27] Deng X, Cagen LM, Wilcox HG, Park EA, Raghow R, Elam MB. Regulation of the rat SREBP-1c promoter in primary rat hepatocytes. Biochemical and biophysical research communications. 2002;290:256-62.
[28] Denley A, Bonython ER, Booker GW, Cosgrove LJ, Forbes BE, Ward CW, et al. Structural determinants for high-affinity binding of insulin-like growth factor II to insulin receptor (IR)-A, the exon 11 minus isoform of the IR. Molecular Endocrinology. 2004;18:2502-12.

[29] Derewenda U, Derewenda Z, Dodson EJ, Dodson GG, Bing X, Markussen J. X-ray analysis of the single chain B29-A1 peptide-linked insulin molecule. A completely inactive analogue. Journal of Molecular Biology. 1991;220:425-33.
[30] Derewenda U, Derewenda Z, Dodson EJ, Dodson GG, Bing X, Markussen J. X-ray analysis of the single chain B29-A1 peptide-linked insulin molecule: A completely inactive analogue. Journal of molecular biology. 1991;220:425-33.
[31] Desilva MG, Lu J, Donadel G, Modi WS, Xie H, Notkins AL, et al. Characterization and chromosomal localization of a new protein disulfide isomerase, PDIp, highly expressed in human pancreas. DNA Cell Biol. 1996;15:9-16.
[32] Dong M, Bridges JP, Apsley K, Xu Y, Weaver TE. ERdj4 and ERdj5 are required for endoplasmic reticulum-associated protein degradation of misfolded surfactant protein C. Molecular biology of the cell. 2008;19:2620-30.
[33] Drews G, Krippeit-Drews P, Düfer M. Oxidative stress and beta-cell dysfunction. Pflügers Archiv European Journal of Physiology. 2010;460:703-18.
[34] Duttaroy A, Kanakaraj P, Osborn BL, Schneider H, Pickeral OK, Chen C, et al. Development of a long-acting insulin analog using albumin fusion technology. Diabetes. 2005;54:251-8.
[35] Edghill EL, Flanagan SE, Patch A-M, Boustred C, Parrish A, Shields B, et al. Insulin Mutation Screening in 1,044 Patients With Diabetes. Diabetes. 2008;57:1034-42.
[36] Every AL, Kramer DR, Mannering SI, Lew AM, Harrison LC. Intranasal vaccination with proinsulin DNA induces regulatory CD4+ T cells that prevent experimental autoimmune diabetes. Journal of Immunology. 2006;176:4608-15.
[37] Feng D, Wei J, Gupta S, McGrath BC, Cavener DR. Acute ablation of PERK results in ER dysfunctions followed by reduced insulin secretion and cell proliferation. BMC cell biology. 2009;10:61.
[38] Forster ML, Sivick K, Park YN, Arvan P, Lencer WI, Tsai B. Protein disulfide isomerase-like proteins play opposing roles during retrotranslocation. The Journal of cell biology. 2006;173:853-9.
[39] Frand AR, Kaiser CA. The ERO1 gene of yeast is required for oxidation of protein dithiols in the endoplasmic reticulum. Molecular cell. 1998;1:161-70.
[40] Frand AR, Kaiser CA. Ero1p oxidizes protein disulfide isomerase in a pathway for disulfide bond formation in the endoplasmic reticulum. Molecular cell. 1999;4:469-77.
[41] Freedman RB, Ganea PJ, Hawkins HC, Hlodan R, McLaughlin SH, Parry JWL. Experimental and Theoretical Analyses of the Domain Architecture of Mammalian Protein Disulphide-Isomerase. Biological Chemistry. 1998;379:321-8.
[42] Gallagher EJ, LeRoith D. Minireview: IGF, Insulin, and Cancer. Endocrinology. 2011;152:2546-51.
[43] Garbi N, Tanaka S, Momburg F, Hammerling GJ. Impaired assembly of the major histocompatibility complex class I peptide-loading complex in mice deficient in the oxidoreductase ERp57. Nature immunology. 2006;7:93-102.

[44] Goldberger RF, Epstein CJ, Anfinsen CB. Acceleration of reactivation of reduced bovine pancreatic ribonuclease by a microsomal system from rat liver. The Journal of biological chemistry. 1963;238:628-35.
[45] Goodge KA, Hutton JC. Translational regulation of proinsulin biosynthesis and proinsulin conversion in the pancreaticβ-cell. Seminars in Cell & Developmental Biology. 2000;11:235-42.
[46] Hartman MG, Lu D, Kim M-L, Kociba GJ, Shukri T, Buteau J, et al. Role for Activating Transcription Factor 3 in Stress-Induced {beta}-Cell Apoptosis. Mol Cell Biol. 2004;24:5721-32.
[47] Hatahet F, Ruddock LW. Substrate recognition by the protein disulfide isomerases. The FEBS journal. 2007;274:5223-34.
[48] Hatahet F, Ruddock LW. Protein disulfide isomerase: a critical evaluation of its function in disulfide bond formation. Antioxidants & redox signaling. 2009;11:2807-50.
[49] Heckler EJ, Rancy PC, Kodali VK, Thorpe C. Generating disulfides with the Quiescin-sulfhydryl oxidases. Biochimica et biophysica acta. 2008;1783:567-77.
[50] Henry RR, Brechtel G, Griver K. Secretion and hepatic extraction of insulin after weight loss in obese noninsulin-dependent diabetes mellitus. Journal of Clinical Endocrinology and Metabolism. 1988;66:979-86.
[51] Hills CE, Brunskill NJ. Cellular and physiological effects of C-peptide. Clin Sci (Lond). 2009;116:565-74.
[52] Hirsch IB. Insulin Analogues. New England Journal of Medicine. 2005;352:174-83.
[53] Hoober KL, Sheasley SL, Gilbert HF, Thorpe C. Sulfhydryl Oxidase from Egg White. Journal of Biological Chemistry. 1999;274:22147-50.
[54] Hosoi T, Ozawa K. Endoplasmic reticulum stress in disease: mechanisms and therapeutic opportunities. Clin Sci (Lond). 2010;118:19-29.
[55] Hou JC, Min L, Pessin JE. Chapter 16 Insulin Granule Biogenesis, Trafficking and Exocytosis. In: Gerald L, editor. Vitamins & Hormones: Academic Press; 2009. p. 473-506.
[56] Howey DC, Bowsher RR, Brunelle RL, Woodworth JR. [Lys(B28), Pro(B29)]-human insulin. A rapidly absorbed analogue of human insulin. Diabetes. 1994;43:396-402.
[57] Hua QX, Gozani SN, Chance RE, Hoffmann JA, Frank BH, Weiss MA. Structure of a protein in a kinetic trap. Nature structural biology. 1995;2:129-38.
[58] Hua QX, Nakagawa SH, Jia W, Hu SQ, Chu YC, Katsoyannis PG, et al. Hierarchical protein folding: asymmetric unfolding of an insulin analogue lacking the A7-B7 interchain disulfide bridge. Biochemistry. 2001;40:12299-311.
[59] Hua QX, Nakagawa SH, Jia W, Huang K, Phillips NB, Hu S, et al. Design of an active ultra-stable single-chain insulin analog. Synthesis, structure, and therapeutic implications. Journal of Biological Chemistry. 2008;10.1074/jbc.M800313200:in press.

[60] Hua QX, Nakagawa SH, Jia W, Huang K, Phillips NB, Hu SQ, et al. Design of an active ultrastable single-chain insulin analog: synthesis, structure, and therapeutic implications. The Journal of biological chemistry. 2008;283:14703-16.
[61] Huang C-j, Lin C-y, Haataja L, Gurlo T, Butler AE, Rizza RA, et al. High Expression Rates of Human Islet Amyloid Polypeptide Induce Endoplasmic Reticulum Stress–Mediated β-Cell Apoptosis, a Characteristic of Humans With Type 2 but Not Type 1 Diabetes. Diabetes. 2007;56:2016-27.
[62] Huang XF, Arvan P. Formation of the insulin-containing secretory granule core occurs within immature β-granules. Journal of Biological Chemistry. 1994;269:20838-44.
[63] Huang XF, Arvan P. Intracellular transport of proinsulin in pancreatic β-cells: structural maturation probed by disulfide accessibility. Journal of Biological Chemistry. 1995;270:20417-23.
[64] Huang XF, Arvan P. Intracellular transport of proinsulin in pancreatic beta-cells. Structural maturation probed by disulfide accessibility. The Journal of biological chemistry. 1995;270:20417-23.
[65] Inaba K, Murakami S, Suzuki M, Nakagawa A, Yamashita E, Okada K, et al. Crystal Structure of the DsbB-DsbA Complex Reveals a Mechanism of Disulfide Bond Generation. Cell. 2006;127:789-801.
[66] Jessop CE, Tavender TJ, Watkins RH, Chambers JE, Bulleid NJ. Substrate specificity of the oxidoreductase ERp57 is determined primarily by its interaction with calnexin and calreticulin. The Journal of biological chemistry. 2009;284:2194-202.
[67] Jessop CE, Watkins RH, Simmons JJ, Tasab M, Bulleid NJ. Protein disulphide isomerase family members show distinct substrate specificity: P5 is targeted to BiP client proteins. Journal of cell science. 2009;122:4287-95.
[68] Kahn CR, Vicent D, Doria A. Genetics of non-insulin-dependent (type-II) diabetes mellitus. Annual review of medicine. 1996;47:509-31.
[69] Kato H, Faria TN, Stannard B, Roberts CT, Jr., LeRoith D. Role of tyrosine kinase activity in signal transduction by the insulin-like growth factor-I (IGF-I) receptor. Characterization of kinase-deficient IGF-I receptors and the action of an IGF-I-mimetic antibody (alpha IR-3). Journal of Biological Chemistry. 1993;268:2655-61.
[70] Khoo C, Yang J, Rajpal G, Wang Y, Liu J, Arvan P, et al. Endoplasmic reticulum oxidoreductin-1-like beta (ERO1lbeta) regulates susceptibility to endoplasmic reticulum stress and is induced by insulin flux in beta-cells. Endocrinology. 2011;152:2599-608.
[71] Kitiphongspattana K, Mathews CE, Leiter EH, Gaskins HR. Proteasome Inhibition Alters Glucose-stimulated (Pro)insulin Secretion and Turnover in Pancreatic β-Cells. Journal of Biological Chemistry. 2005;280:15727-34.
[72] Kjeldsen T, Ludvigsen S, Diers I, Balschmidt P, Sorensen AR, Kaarsholm NC. Engineering-enhanced protein secretory expression in yeast with application to insulin. The Journal of biological chemistry. 2002;277:18245-8.
[73] Klappa P, Ruddock LW, Darby NJ, Freedman RB. The b[prime] domain provides the principal peptide-binding site of protein disulfide isomerase but all

domains contribute to binding of misfolded proteins. The EMBO journal. 1998;17:927-35.
[74] Kobayashi M, Sasaoka T, Sugibayashi M, Iwanishi M, Shigeta Y. Receptor binding and biologic activity of biosynthetic human insulin and mini-proinsulin produced by recombinant gene technology. Diabetes research and clinical practice. 1989;7:25-8.
[75] Kodali VK, Thorpe C. Oxidative protein folding and the Quiescin-sulfhydryl oxidase family of flavoproteins. Antioxidants & redox signaling. 2010;13:1217-30.
[76] Kozlov G, Maattanen P, Schrag JD, Pollock S, Cygler M, Nagar B, et al. Crystal Structure of the bb′ Domains of the Protein Disulfide Isomerase ERp57. Structure. 2006;14:1331-9.
[77] Kozlov G, Maattanen P, Thomas DY, Gehring K. A structural overview of the PDI family of proteins. The FEBS journal. 2010;277:3924-36.
[78] Kuliawat R, Arvan P. Protein targeting via the "constitutive-like" secretory pathway in isolated pancreatic islets: passive sorting in the immature granule compartment. Journal of Cell Biology. 1992;118:521-9.
[79] Kulp MS, Frickel EM, Ellgaard L, Weissman JS. Domain architecture of protein-disulfide isomerase facilitates its dual role as an oxidase and an isomerase in Ero1p-mediated disulfide formation. The Journal of biological chemistry. 2006;281:876-84.
[80] Lagueux M, Lwoff L, Meister M, GoltzenÉ F, Hoffmann JA. cDNAs from neurosecretory cells of brains of Locusta migratoria (Insecta, Orthoptera) encoding a novel member of the superfamily of insulins. European Journal of Biochemistry. 1990;187:249-54.
[81] LaMantia M, Lennarz WJ. The essential function of yeast protein disulfide isomerase does not reside in its isomerase activity. Cell. 1993;74:899-908.
[82] Laybutt D, Preston A, Åkerfeldt M, Kench J, Busch A, Biankin A, et al. Endoplasmic reticulum stress contributes to beta cell apoptosis in type 2 diabetes. Diabetologia. 2007;50:752-63.
[83] Leahy JL, Hirsch IB, Peterson KA, Schneider D. Targeting β-Cell Function Early in the Course of Therapy for Type 2 Diabetes Mellitus. Journal of Clinical Endocrinology & Metabolism. 2010;95:4206-16.
[84] Lee HC, Kim SJ, Kim KS, Shin HC, Yoon JW. Remission in models of type 1 diabetes by gene therapy using a single-chain insulin analogue. Nature. 2000;408:483-8.
[85] Lee HC, Kim SJ, Kim KS, Shin HC, Yoon JW. Remission in models of type 1 diabetes by gene therapy using a single-chain insulin analogue. Nature. 2000;408:483-8.
[86] Lee KH, Wucherpfennig KW, Wiley DC. Structure of a human insulin peptide-HLA-DQ8 complex and susceptibility to type 1 diabetes. Nature immunology. 2001;2:501-7.
[87] Lehuen A, Diana J, Zaccone P, Cooke A. Immune cell crosstalk in type 1 diabetes. Nat Rev Immunol. 2010;10:501-13.

[88] Leibiger IB, Brismar K, Berggren P-O. Novel aspects on pancreatic beta-cell signal-transduction. Biochemical and biophysical research communications. 2010;396:111-5.
[89] Lenzen S, Drinkgern J, Tiedge M. Low antioxidant enzyme gene expression in pancreatic islets compared with various other mouse tissues. Free Radical Biology and Medicine. 1996;20:463-6.
[90] LeRoith D, Roberts CT. Insulin-like Growth Factors. Annals of the New York Academy of Sciences. 1993;692:1-9.
[91] Lesniak M, Gliemann J, Roth J, Easter BR, Sutton DA, Drewes SE. Receptor binding studies on A1-(2-nitro-4-trimethylammoniophenyl)insulin. Hoppe-Seyler's Zeitschrift fur physiologische Chemie. 1979;360:467-71.
[92] Levy JR, Olefsky JM. The trafficking and processing of insulin and insulin receptors in cultured rat hepatocytes. Endocrinology. 1987;121:2075-86.
[93] Levy JR, Ullrich A, Olefsky JM. Endocytotic uptake, processing, and retroendocytosis of human biosynthetic proinsulin by rat fibroblasts transfected with the human insulin receptor gene. Journal of Clinical Investigation. 1988;81:1370-7.
[94] Lindsay DG, Shall S. The acetylation of insulin. Biochemical Journal. 1971;121:737-45.
[95] Lipkind G, Steiner DF. Predicted structural alterations in proinsulin during its interactions with prohormone convertases. Biochemistry. 1999;38:890-6.
[96] Liu M, Haataja L, Wright J, Wickramasinghe NP, Hua QX, Phillips NF, et al. Mutant INS-gene induced diabetes of youth: proinsulin cysteine residues impose dominant-negative inhibition on wild-type proinsulin transport. PloS one. 2010;5:e13333.
[97] Liu M, Hodish I, Haataja L, Lara-Lemus R, Rajpal G, Wright J, et al. Proinsulin misfolding and diabetes: mutant INS gene-induced diabetes of youth. Trends in endocrinology and metabolism: TEM. 2010;21:652-9.
[98] Liu M, Li Y, Cavener D, Arvan P. Proinsulin disulfide maturation and misfolding in the endoplasmic reticulum. The Journal of biological chemistry. 2005;280:13209-12.
[99] Liu M, Ramos-Castaneda J, Arvan P. Role of the connecting peptide in insulin biosynthesis. The Journal of biological chemistry. 2003;278:14798-805.
[100] Liu M, Ramos-Castañeda J, Arvan P. Role of the connecting peptide in insulin biosynthesis. Journal of Biological Chemistry. 2003;278:14798-805.
[101] Lundstrom-Ljung J, Birnbach U, Rupp K, Soling HD, Holmgren A. Two resident ER-proteins, CaBP1 and CaBP2, with thioredoxin domains, are substrates for thioredoxin reductase: comparison with protein disulfide isomerase. FEBS letters. 1995;357:305-8.
[102] Ma L, Robinson LN, Towle HC. ChREBP*Mlx is the principal mediator of glucose-induced gene expression in the liver. Journal of Biological Chemistry. 2006;281:28721-30.
[103] Mamathambika BS, Bardwell JC. Disulfide-linked protein folding pathways. Annual review of cell and developmental biology. 2008;24:211-35.

[104] Marchetti P, Bugliani M, Lupi R, Marselli L, Masini M, Boggi U, et al. The endoplasmic reticulum in pancreatic beta cells of type 2 diabetes patients. Diabetologia. 2007;50:2486-94.
[105] Matsuzawa A, Nishitoh H, Tobiume K, Takeda K, Ichijo H. Physiological Roles of ASK1-Mediated Signal Transduction in Oxidative Stress- and Endoplasmic Reticulum Stress-Induced Apoptosis: Advanced Findings from ASK1 Knockout Mice. Antioxidants & redox signaling. 2002;4:415-25.
[106] Meur G, Simon A, Harun N, Virally M, Dechaume A, Bonnefond A, et al. Insulin Gene Mutations Resulting in Early-Onset Diabetes: Marked Differences in Clinical Presentation, Metabolic Status, and Pathogenic Effect Through Endoplasmic Reticulum Retention. Diabetes. 2010;59:653-61.
[107] Missiakas D, Schwager F, Raina S. Identification and characterization of a new disulfide isomerase-like protein (DsbD) in Escherichia coli. The EMBO journal. 1995;14:3415-24.
[108] Mittelman SD, Van Citters GW, Kim SP, Davis DA, Dea MK, Hamilton-Wessler M, et al. Longitudinal compensation for fat-induced insulin resistance includes reduced insulin clearance and enhanced beta-cell response. Diabetes. 2000;49:2116-25.
[109] Molven A, Njølstad PR. Role of molecular genetics in transforming diagnosis of diabetes mellitus. Expert Review of Molecular Diagnostics. 2011;11:313-20.
[110] Molven A, Ringdal M, Nordbø AM, Ræder H, Støy J, Lipkind GM, et al. Mutations in the Insulin Gene Can Cause MODY and Autoantibody-Negative Type 1 Diabetes. Diabetes. 2008;57:1131-5.
[111] Moore P, Bernardi KM, Tsai B. The Ero1alpha-PDI redox cycle regulates retro-translocation of cholera toxin. Molecular biology of the cell. 2010;21:1305-13.
[112] Morales J. Defining the Role of Insulin Detemir in Basal Insulin Therapy. Drugs. 2007;67:2557-84.
[113] Mori K. Tripartite management of unfolded proteins in the endoplasmic reticulum. Cell. 2000;101:451-4.
[114] Nakagawa SH, Tager HS. Role of the COOH-terminal B-chain domain in insulin-receptor interactions. Identification of perturbations involving the insulin mainchain. Journal of Biological Chemistry. 1987;262:12054-8.
[115] Nakagawa SH, Tager HS. Perturbation of insulin-receptor interactions by intramolecular hormone cross-linking. Analysis of relative movement among residues A1, B1, and B29. Journal of Biological Chemistry. 1989;264:272-9.
[116] Nakatani Y, Kaneto H, Kawamori D, Yoshiuchi K, Hatazaki M, Matsuoka TA, et al. Involvement of endoplasmic reticulum stress in insulin resistance and diabetes. The Journal of biological chemistry. 2005;280:847-51.
[117] Nakayama M, Abiru N, Moriyama H, Babaya N, Liu E, Miao D, et al. Prime role for an insulin epitope in the development of type 1 diabetes in NOD mice. Nature. 2005;435:220-3.

[118] Nakayama M, Beilke JN, Jasinski JM, Kobayashi M, Miao D, Li M, et al. Priming and effector dependence on insulin B:9-23 peptide in NOD islet autoimmunity. Journal of Clinical Investigation. 2007;117:1835-43.
[119] Nguyen VD, Saaranen MJ, Karala A-R, Lappi A-K, Wang L, Raykhel IB, et al. Two Endoplasmic Reticulum PDI Peroxidases Increase the Efficiency of the Use of Peroxide during Disulfide Bond Formation. Journal of molecular biology. 2011;406:503-15.
[120] Nolan CJ, Damm P, Prentki M. Type 2 diabetes across generations: from pathophysiology to prevention and management. The Lancet. 2011;378:169-81.
[121] Pace CN, Grimsley GR, Thomson JA, Barnett BJ. CONFORMATIONAL STABILITY AND ACTIVITY OF RIBONUCLEASE-T1 WITH ZERO, ONE, AND 2 INTACT DISULFIDE BONDS. Journal of Biological Chemistry. 1988;263:11820-5.
[122] Pirneskoski A, Klappa P, Lobell M, Williamson RA, Byrne L, Alanen HI, et al. Molecular Characterization of the Principal Substrate Binding Site of the Ubiquitous Folding Catalyst Protein Disulfide Isomerase. Journal of Biological Chemistry. 2004;279:10374-81.
[123] Podlecki DA, Frank BH, Olefsky JM. In vitro characterization of biosynthetic human proinsulin. Diabetes. 1984;33:111-8.
[124] Pullen RA, Lindsay DG, Wood SP, Tickle IJ, Blundell TL, Wollmer A, et al. Receptor-binding region of insulin. Nature. 1976;259:369-73.
[125] Qiao Z-S, Min C-Y, Hua Q-X, Weiss MA, Feng Y-M. In Vitro Refolding of Human Proinsulin. Journal of Biological Chemistry. 2003;278:17800-9.
[126] Ramiya VK, Shang XZ, Pharis PG, Wasserfall CH, Stabler TV, Muir AB, et al. Antigen based therapies to prevent diabetes in NOD mice. Journal of autoimmunity. 1996;9:349-56.
[127] Rancy PC, Thorpe C. Oxidative Protein Folding in Vitro: A Study of the Cooperation between Quiescin-Sulfhydryl Oxidase and Protein Disulfide Isomerase†. Biochemistry. 2008;47:12047-56.
[128] Riemer J, Hansen HG, Appenzeller-Herzog C, Johansson L, Ellgaard L. Identification of the PDI-Family Member ERp90 as an Interaction Partner of ERFAD. PloS one. 2011;6:e17037.
[129] Rietsch A, Belin D, Martin N, Beckwith J. An in vivo pathway for disulfide bond isomerization in Escherichia coli. Proceedings of the National Academy of Sciences of the United States of America. 1996;93:13048-53.
[130] Robertson DA, Singh BM, Hale PJ, Jensen I, Nattrass M. Metabolic effects of monomeric insulin analogues of different receptor affinity. Diabetic Medicine. 1992;9:240-6.
[131] Rosenstock J, Zinman B, Murphy LJ, Clement SC, Moore P, Bowering CK, et al. Inhaled insulin improves glycemic control when substituted for or added to oral combination therapy in type 2 diabetes: a randomized, controlled trial. Annals of internal medicine. 2005;143:549-58.
[132] Rupp K, Birnbach U, Lundstrom J, Van PN, Soling HD. Effects of CaBP2, the rat analog of ERp72, and of CaBP1 on the refolding of denatured reduced

proteins. Comparison with protein disulfide isomerase. The Journal of biological chemistry. 1994;269:2501-7.
[133] Rutkevich LA, Cohen-Doyle MF, Brockmeier U, Williams DB. Functional relationship between protein disulfide isomerase family members during the oxidative folding of human secretory proteins. Molecular biology of the cell. 2010;21:3093-105.
[134] Sakuraba H, Mizukami H, Yagihashi N, Wada R, Hanyu C, Yagihashi S. Reduced beta-cell mass and expression of oxidative stress-related DNA damage in the islet of Japanese Type II diabetic patients. Diabetologia. 2002;45:85-96.
[135] Saltiel AR, Pessin JE. Insulin signaling pathways in time and space. Trends in cell biology. 2002;12:65-71.
[136] Sargsyan E, Baryshev M, Szekely L, Sharipo A, Mkrtchian S. Identification of ERp29, an endoplasmic reticulum lumenal protein, as a new member of the thyroglobulin folding complex. The Journal of biological chemistry. 2002;277:17009-15.
[137] Satoh M, Shimada A, Keino H, Kashiwai A, Nagai N, Saga S, et al. Functional characterization of 3 thioredoxin homology domains of ERp72. Cell stress & chaperones. 2005;10:278-84.
[138] Scheraga HA, Wedemeyer WJ, Welker E. Bovine pancreatic ribonuclease A: oxidative and conformational folding studies. Methods in enzymology. 2001;341:189-221.
[139] Scheuner D, Kaufman RJ. The Unfolded Protein Response: A Pathway That Links Insulin Demand with β-Cell Failure and Diabetes. Endocrine reviews. 2008;29:317-33.
[140] Scheuner D, Vander Mierde D, Song B, Flamez D, Creemers JW, Tsukamoto K, et al. Control of mRNA translation preserves endoplasmic reticulum function in beta cells and maintains glucose homeostasis. Nat Med. 2005;11:757-64.
[141] Schulman S, Wang B, Li W, Rapoport TA. Vitamin K epoxide reductase prefers ER membrane-anchored thioredoxin-like redox partners. Proceedings of the National Academy of Sciences of the United States of America. 2010;107:15027-32.
[142] Sevier CS, Kaiser CA. Ero1 and redox homeostasis in the endoplasmic reticulum. Biochimica et biophysica acta. 2008;1783:549-56.
[143] Shaw JA, Delday MI, Hart AW, Docherty HM, Maltin CA, Docherty K. Secretion of bioactive human insulin following plasmid-mediated gene transfer to non-neuroendocrine cell lines, primary cultures and rat skeletal muscle in vivo. Journal of Endocrinology. 2002;172:653-72.
[144] Shimizu Y, Hendershot LM. Oxidative folding: cellular strategies for dealing with the resultant equimolar production of reactive oxygen species. Antioxidants & redox signaling. 2009;11:2317-31.
[145] Simmons D. Diabetes and obesity in pregnancy. Best practice & research Clinical obstetrics & gynaecology. 2011;25:25-36.

[146] Smit AB, Spijker S, Van Minnen J, Burke JF, De Winter F, Van Elk R, et al. Expression and characterization of molluscan insulin-related peptide VII from the molluscLymnaea stagnalis. Neuroscience. 1996;70:589-96.
[147] Song B, Scheuner D, Ron D, Pennathur S, Kaufman RJ. Chop deletion reduces oxidative stress, improves beta cell function, and promotes cell survival in multiple mouse models of diabetes. The Journal of clinical investigation. 2008;118:3378-89.
[148] Steiner DF. The proprotein convertases. Current opinion in chemical biology. 1998;2:31-9.
[149] Steiner DF. The proinsulin C-peptide--a multirole model. Exp Diabesity Res. 2004;5:7-14.
[150] Striffler JS. Insulin clearance and microsomal glutathione-insulin transhydrogenase in perfused livers of fed and fasted rats. Diabetes and Metabolism. 1987;13:582-90.
[151] Thomas CG, Spyrou G. ERdj5 sensitizes neuroblastoma cells to endoplasmic reticulum stress-induced apoptosis. The Journal of biological chemistry. 2009;284:6282-90.
[152] Tian G, Xiang S, Noiva R, Lennarz WJ, Schindelin H. The Crystal Structure of Yeast Protein Disulfide Isomerase Suggests Cooperativity between Its Active Sites. Cell. 2006;124:61-73.
[153] Tsai B, Rodighiero C, Lencer WI, Rapoport TA. Protein disulfide isomerase acts as a redox-dependent chaperone to unfold cholera toxin. Cell. 2001;104:937-48.
[154] Ushioda R, Hoseki J, Araki K, Jansen G, Thomas DY, Nagata K. ERdj5 is required as a disulfide reductase for degradation of misfolded proteins in the ER. Science. 2008;321:569-72.
[155] Vajo Z, Fawcett J, Duckworth WC. Recombinant DNA technology in the treatment of diabetes: insulin analogs. Endocrine reviews. 2001;22:706-17.
[156] van Lith M, Hartigan N, Hatch J, Benham AM. PDILT, a Divergent Testis-specific Protein Disulfide Isomerase with a Non-classical SXXC Motif That Engages in Disulfide-dependent Interactions in the Endoplasmic Reticulum. Journal of Biological Chemistry. 2005;280:1376-83.
[157] Van PN, Rupp K, Lampen A, Soling HD. CaBP2 is a rat homolog of ERp72 with proteindisulfide isomerase activity. European journal of biochemistry / FEBS. 1993;213:789-95.
[158] Wajih N, Hutson SM, Wallin R. Disulfide-dependent protein folding is linked to operation of the vitamin K cycle in the endoplasmic reticulum. A protein disulfide isomerase-VKORC1 redox enzyme complex appears to be responsible for vitamin K1 2,3-epoxide reduction. The Journal of biological chemistry. 2007;282:2626-35.
[159] Wang C, Tsou C. Protein disulfide isomerase is both an enzyme and a chaperone. The FASEB Journal. 1993;7:1515-7.
[160] Wang F, Carabino JM, Vergara CM. Insulin glargine: A systematic review of a long-acting insulin analogue. Clinical Therapeutics. 2003;25:1541-77.

[161] Wang J, Takeuchi T, Tanaka S, Kubo SK, Kayo T, Lu D, et al. A mutation in the insulin 2 gene induces diabetes with severe pancreatic beta-cell dysfunction in the Mody mouse. The Journal of clinical investigation. 1999;103:27-37.
[162] Wang Z-H, Liu Y, Ji J-G, Tang J-G. Effects of Deletion and Shift of the A20–B19 Disulfide Bond on the Structure, Activity, and Refolding of Proinsulin. Journal of biochemistry. 2004;135:25-31.
[163] Wedemeyer WJ, Welker E, Narayan M, Scheraga HA. Disulfide Bonds and Protein Folding†. Biochemistry. 2000;39:4207-16.
[164] Weir GC, Bonner-Weir S. Five Stages of Evolving Beta-Cell Dysfunction During Progression to Diabetes. Diabetes. 2004;53:S16-S21.
[165] Weir GC, Marselli L, Marchetti P, Katsuta H, Jung MH, Bonner-Weir S. Towards better understanding of the contributions of overwork and glucotoxicity to the β-cell inadequacy of type 2 diabetes. Diabetes, Obesity and Metabolism. 2009;11:82-90.
[166] Winter J, Klappa P, Freedman RB, Lilie H, Rudolph R. Catalytic activity and chaperone function of human protein-disulfide isomerase are required for the efficient refolding of proinsulin. The Journal of biological chemistry. 2002;277:310-7.
[167] Yamashita H, Takenoshita M, Sakurai M, Bruick RK, Henzel WJ, Shillinglaw W, et al. A glucose-responsive transcription factor that regulates carbohydrate metabolism in the liver. Proceedings of the National Academy of Sciences. 2001;98:9116-21.
[168] Yanagita M, Hoshino H, Nakayama K, Takeuchi T. Processing of mutated proinsulin with tetrabasic cleavage sites to mature insulin reflects the expression of furin in nonendocrine cell lines. Endocrinology. 1993;133:639-44.
[169] Yoshinaga T, Nakatome K, Nozaki J-i, Naitoh M, Hoseki J, Kubota H, et al. Proinsulin lacking the A7-B7 disulfide bond, Ins2Akita, tends to aggregate due to the exposed hydrophobic surface. Biological Chemistry. 2005;386:1077-85.
[170] Zeggini E, Scott LJ, Saxena R, Voight BF, Marchini JL, Hu T, et al. Meta-analysis of genome-wide association data and large-scale replication identifies additional susceptibility loci for type 2 diabetes. Nature genetics. 2008;40:638-45.
[171] Zhang L, Lai E, Teodoro T, Volchuk A. GRP78, but Not Protein-disulfide Isomerase, Partially Reverses Hyperglycemia-induced Inhibition of Insulin Synthesis and Secretion in Pancreatic {beta}-Cells. The Journal of biological chemistry. 2009;284:5289-98.
[172] Zhang L, Nakayama M, Eisenbarth GS. Insulin as an autoantigen in NOD/human diabetes. Current opinion in immunology. 2008;20:111-8.
[173] Zhang Y, Baig E, Williams DB. Functions of ERp57 in the folding and assembly of major histocompatibility complex class I molecules. The Journal of biological chemistry. 2006;281:14622-31.
[174] Zhu X, Orci L, Carroll R, Norrbom C, Ravazzola M, Steiner DF. Severe block in processing of proinsulin to insulin accompanied by elevation of des-64,65 proinsulin intermediates in islets of mice lacking prohormone convertase

1/3. Proceedings of the National Academy of Sciences of the United States of America. 2002;99:10299-304.
[175] Zito E, Chin KT, Blais J, Harding HP, Ron D. ERO1-beta, a pancreas-specific disulfide oxidase, promotes insulin biogenesis and glucose homeostasis. The Journal of cell biology. 2010;188:821-32.
[176] Zito E, Melo EP, Yang Y, Wahlander A, Neubert TA, Ron D. Oxidative protein folding by an endoplasmic reticulum-localized peroxiredoxin. Molecular cell. 2010;40:787-97.